

Marquette University

e-Publications@Marquette

Dissertations (1934 -)

Dissertations, Theses, and Professional
Projects

Mechanisms of Impaired Motor Unit Firing Behavior in the Vastus Lateralis Muscle after Stroke

Spencer Murphy
Marquette University

Follow this and additional works at: https://epublications.marquette.edu/dissertations_mu



Part of the [Engineering Commons](#)

Recommended Citation

Murphy, Spencer, "Mechanisms of Impaired Motor Unit Firing Behavior in the Vastus Lateralis Muscle after Stroke" (2018). *Dissertations (1934 -)*. 1010.

https://epublications.marquette.edu/dissertations_mu/1010

MECHANISMS OF IMPAIRED MOTOR UNIT FIRING BEHAVIOR IN THE
VASTUS LATERALIS MUSCLE AFTER STROKE

by

Spencer A. Murphy, B.S.

A Dissertation submitted to the Faculty of the Graduate School,
Marquette University,
in Partial Fulfillment of the Requirements for
the Degree of Doctor of Philosophy

Milwaukee, Wisconsin

December 2018

ABSTRACT

MECHANISMS OF IMPAIRED MOTOR UNIT FIRING BEHAVIOR IN THE VASTUS LATERALIS MUSCLE AFTER STROKE

Spencer A. Murphy, B.S.

Marquette University, 2018

The purpose of this dissertation research project was to examine the role of impaired motor unit firing behavior on force generation after a stroke. We studied the relationship between intrinsic motoneuron properties and inhibitory sensory pathways to deficient motoneuron activity in the vastus lateralis muscle after a stroke. Individuals with stroke often have deficits with force generation and volitional relaxation. Current models of impaired force output after a stroke focus primarily on the pathology within the corticospinal pathway because of decreased descending drive. Though this is an important aspect of deficient motoneuron output, it is incomplete because motoneurons receive other inputs that can shape motor output. Because the motoneuron is the last site of signal integration for muscle contractions, using methods that study motor unit activity can provide a window to the activity in the spinal circuitry.

This research study utilized a novel algorithm that decomposed electromyography (EMG) signals into the contributions of the individual motor units. This provided the individual firing instances for a large number of concurrently active motor units during isometric contractions of the knee extensors. In the first aim, the association between the hyperemic response and motor unit firing rate modulation to intermittent, fatiguing contractions was investigated. It was found that the magnitude of blood flow was lower for individuals with stroke compared to healthy controls, but both groups increased blood flow similarly in response to fatiguing contractions. This did not relate to changes in muscle fiber contractibility for the participants with stroke; rather, participants better able to increase blood flow showed greater modulation in motor unit firing rates. To further investigate how ischemic conditions impact motor unit output, the second aim used a blood pressure cuff to completely occlude blood flow through the femoral artery with the intent of activating inhibitory afferent pathways. We found that ischemic conditions had a greater inhibitory impact on motor unit output for individuals with stroke compared to healthy controls, possibly because of hyper-excitability group III/IV afferent pathways. The final aim investigated how stroke related changes in the intrinsic excitability of the motoneurons impacted prolonged motor unit firing during voluntary relaxation. A serotonin reuptake inhibitor was administered to quantify motoneuron sensitivity to neuromodulatory inputs. This study found that the serotonin reuptake inhibitor increased muscle relaxation and may have reduced persistent inward current contributions to prolonged motor unit firing. In conclusion, while damage to the corticospinal tract is a major component to poor functionality, the intrinsic properties of the motoneuron and sensory pathways to the motoneuron pool are essential for understanding deficient motor control after a stroke.

ACKNOWLEDGEMENTS

Spencer A. Murphy, B.S.

I am honored and thankful for the contributions to this work from my dissertation committee members, Dr. Brian Schmit, Dr. Sandra Hunter, Dr. Scott Beardsley, Dr. Francesco Negro, and Dr. Allison Hyingstrom. I have learned from each of you, and for that, I am truly grateful.

A special thanks to Dr. Brian Schmit for giving me the opportunity within the Integrative Neural Engineering and Rehabilitation Laboratory (INERL) and to pursue this degree.

I would also like to thank everyone within the INERL for all of the assistance, feedback, and input into these studies.

A special thanks to:

Dr. Matthew Durand for his ultrasound data collection, processing of the blood flow data, and his input to the results of these studies; Dr. Francesco Negro for his assistance and training in the utilization of the high-density surface arrays and the decomposition algorithm; Dr. Revian Berrios Barillas for her hours of data collection for chapter 4; Dr. Andrew Nelson as the PI for the study presented in chapter 4 and administering the drug to the participants.

To my advisor, Dr. Allison Hyingstrom, thank you for all of your input and assistance throughout these past years. You are the essence of a true scientist. I am extremely grateful for your mentorship.

A very special thanks to all of my friends and family.

Thank you to the Janicek family for all of your past and continued support to Ally and me.

To my brothers and sisters, thank you for always having my back.

I could never thank my parents enough for everything they have done for me.

FF Ally Murphy, thank you for all your love and care.

A portion of this project was supported by the National Center for Advancing Translational Sciences, National Institute of Health, Award Number TL1TR001437.

TABLE OF CONTENTS

ACKNOWLEDGEMENTS	i
LIST OF TABLES	vi
LIST OF FIGURES	vii
CHAPTER 1: INTRODUCTION AND BACKGROUND	1
1.1 MOTOR UNIT RECRUITMENT AND DISCHARGE PATTERNS IN PARETIC MUSCLES OF STROKE SURVIVORS	2
1.2 DECOMPOSITION OF INDIVIDUAL MOTOR UNIT FIRING INSTANCES FROM HIGH-DENSITY SURFACE EMG	4
1.3 STROKE-RELATED CHANGES TO NEUROMUSCULAR FATIGUE AND MOTOR CONTROL	8
1.4 IMPACT OF POST-STROKE MOTOR CORTEX CHANGES ON VOLUNTARY ACTIVATION	10
1.5 DECREASED MUSCLE BLOOD FLOW AND HYPER-EXCITABLE SMALL DIAMETER AFFERENT ACTIVITY POST-STROKE	12
1.6 NEUROMODULATORY CONTROL OF SPINAL CORD FUNCTION POST-STROKE	14
1.7 ESTIMATING PICS IN HUMANS	16
1.8 SUMMARY AND CONTRIBUTION TO CURRENT LITERATURE.....	17
1.9 SPECIFIC AIMS	18
CHAPTER 2: DEFICIENT HYPEREMIA AND IMPAIRED MOTOR UNIT FIRING BEHAVIOR AFTER A STROKE.....	20
2.1 INTRODUCTION	20
2.2 MATERIALS AND METHODS.....	23
2.2.1 Participants	23
2.2.2 Torque Measurements	24
2.2.3 Voluntary Activation and Resting Twitch Response	25
2.2.4 Blood Flow Measurements	26
2.2.5 Surface EMG Recordings	27
2.2.6 Motor Unit Decomposition	28
2.2.7 Body Composition and Clinical Measures	30
2.2.8 Experimental Protocol	30
2.2.9 Statistical Analysis	32

2.3 RESULTS	34
2.3.1 MVC Torque and Task Duration Measurements	34
2.3.2 Voluntary Activation	34
2.3.3 Resting Twitch Torque	35
2.3.4 Femoral Artery Blood Flow	36
2.3.5 Motor Unit Firing Rates	39
2.3.6 EMG RMS	40
2.3.7 EMG Mean Frequency	41
2.3.8 Correlations of Relative Changes in Blood Flow and Motor Unit Firing Rates	41
2.4 DISCUSSION	42
2.4.1 Post-stroke Differences in Hyperemia	43
2.4.2 Post-Stroke Blood Flow Deficits do not Relate to Metrics of Peripheral Fatigue or Task Duration	44
2.4.3 Motor Unit Firing Rates Track with Blood Flow Changes	46
2.4.4 Implications for Motor Performance	48
2.4.5 Conclusion	49
CHAPTER 3: STROKE INCREASES ISCHEMIA-RELATED DECREASES IN MOTOR UNIT DISCHARGE RATES	51
3.1 INTRODUCTION	51
3.2 MATERIALS AND METHODS	54
3.2.1 Participants	54
3.2.2 Torque Measurements	55
3.2.3 Surface EMG Recordings	55
3.2.4 Near-infrared Spectroscopy Measurements	56
3.2.5 Experimental Protocol	56
3.2.6 Data Processing	58
3.2.7 Statistical Analysis	61
3.3 RESULTS	61
3.3.1 Mean Firing Rates	61
3.3.2 Recruitment Threshold	64
3.3.3 Recruitment Firing Rates	65
3.3.4 Derecruitment Threshold	66

3.3.5 Derecruitment Firing Rates	66
3.3.6 Local Muscle Oxygen Saturation	67
3.3.7 Maximum Voluntary Contractions	70
3.3.8 Resting Twitch	71
3.3.9 Global Surface EMG	71
3.4 DISCUSSION	72
3.4.1 Transient Group III/IV Muscle Afferent Feedback Inhibits Paretic MU Discharge	72
3.4.2 Implications for Motor Performance	76
3.4.3 Conclusion	77
CHAPTER 4: A SEROTONIN RECEPTOR ANTAGONIST DECREASES PROLONGED MOTOR UNIT FIRING DURING VOLUNTARY RELAXATION POST-STROKE.....	78
4.1 INTRODUCTION	78
4.2 MATERIALS AND METHODS.....	82
4.2.1 Participants	82
4.2.2 Drug Administration	83
4.2.3 Torque Measurements	84
4.2.4 Resting Twitch Torque	84
4.2.5 Patellar Tendon Taps	85
4.2.6 Surface EMG Recordings	85
4.2.7 Motor Unit Decomposition	86
4.2.8 Experimental Protocol	87
4.2.9 Data Processing	89
4.2.10 Paired Motor Unit Analysis (ΔF)	91
4.2.11 Statistical Analysis	93
4.3 RESULTS	94
4.3.1 Torque Measurements	94
4.3.2 Paired Motor Unit Recordings (ΔF)	96
4.3.3 Mean Motor Unit Firing Rates	97
4.3.4 Recruitment Threshold	98
4.3.5 Derecruitment Threshold	98
4.3.6 Slope of Motor Unit Firing Rates During Contraction	98

4.3.7 Slope of Motor Unit Firing Rates During Relaxation.....	99
4.4 DISCUSSION	100
4.4.1 Validity of PIC Estimation Using ΔF via High-Density Surface EMG.....	101
4.4.2 Evidence for Enhanced PICs in the Chronic Stroke Group Using Paired Motor Unit Recordings (ΔF)	102
4.4.3 Cyproheptadine Decreased ΔF Values and Increased Motor Unit Relaxation Rates	105
4.4.4 Cyproheptadine Reduced Motor Unit Gain	105
4.4.5 Implications for Motor Performance	106
4.4.6 Conclusion	107
CHAPTER 5: CONCLUSION	108
5.1 BRIEF SUMMARY	108
5.2 INFLUENCE OF HYPER-EXCITABLE AFFERENT INPUTS AND ENHANCED INTRINSIC EXCITABILITY OF THE MOTONEURON.....	109
5.3 INTERCONNECTION OF THE RETICULAR SYSTEM, GROUP III/IV PATHWAYS, AND MOTOR UNIT FIRING BEHAVIOR AFTER STROKE	110
5.4 POTENTIAL NEW INSIGHTS INTO MOTOR UNIT FIRING BEHAVIOR AND MOTOR CONTROL AFTER A STROKE	112
5.5 FUTURE INVESTIGATIONS.....	113
BIBLIOGRAPHY	114

LIST OF TABLES

Table 2.1: Participant Characteristics	24
Table 3.1: Participant Characteristics	55
Table 4.1: Participant Characteristics	83

LIST OF FIGURES

Figure 2.1: Experimental protocol	31
Figure 2.2: Single participant examples.....	32
Figure 2.3: Voluntary activation	35
Figure 2.4: Resting twitch torque.....	36
Figure 2.5: Blood flow through the femoral artery	37
Figure 2.6: Changes in blood flow and task duration correlations	38
Figure 2.7: MVC and blood flow after the first cycle	39
Figure 2.8: Mean motor unit firing rates.....	40
Figure 2.9: Changes in motor unit firing rates and blood flow correlations	42
Figure 3.1: Experimental protocol	58
Figure 3.2: Single participant example	63
Figure 3.3: Mean firing rates during the occlusion protocol	63
Figure 3.4: Local oxygen saturation during occlusion.....	68
Figure 3.5: Mean time constant for the exponential decay of oxygen saturation	68
Figure 3.6: Linear regressions of each motor unit firing rate during occlusion	69
Figure 3.7: Average slope values of linear regression lines for MU firing rates and oxygen saturation	70
Figure 3.8: Group mean motor unit firing rates and mean % O ₂ saturation at each contraction	70
Figure 4.1: Experimental protocol	88
Figure 4.2: Single participant examples.....	90
Figure 4.3: Paired motor unit technique	91
Figure 4.4: Hysteresis of motor unit firing rates.....	92
Figure 4.5: Mean ΔF values.....	97
Figure 4.6: Mean motor unit relaxation rates	100

CHAPTER 1: INTRODUCTION AND BACKGROUND

Sir Charles Sherrington coined the phrase ‘the final common pathway’ to refer to the motoneuron as the last site of signal integration for supraspinal and spinal inputs that shape muscle contractions and force output. Voluntary movement is contingent on the ability to control the generation of muscle force. Optimal motor performance relies on the synaptic inputs from descending cortical and sub-cortical centers, sensory afferent input, and post synaptic electrical properties of the motoneuron. However, after a stroke, damage to motor centers limits descending inputs to motoneuron pools. In addition, there may be secondary changes in excitability in sub-cortical pathways and motoneuron properties due to loss of regulation from the cortex. Damage to any of these components likely impairs force regulation post stroke. Because muscle fibers contract in a 1:1 ratio with the firing of the motoneuron that innervates them, changes in the neural drive to the motoneuron and electrical properties of the motoneurons can be detected through measurement of the motor unit action potentials within the muscle fibers. This provides a window to the activity of the spinal circuitry. A goal of these studies is to delineate neural mechanisms that may contribute to force impairment post stroke and to discern novel insight into altered motor unit output; therefore, the objective of this dissertation is to 1) determine the relationship between peripheral blood flow and motor unit firing rates during fatiguing isometric contractions; 2) quantify the inhibiting effect of group III/IV afferent input to paretic motoneurons; and 3) examine the intrinsic properties of paretic motoneurons by quantifying the effects of a serotonin receptor antagonist on motor unit firing behavior. The purpose of this dissertation is to provide information about cortical

and subcortical contributions, including intrinsic properties of the motoneuron, to motor unit firing deficiencies within the knee extensor muscles after a stroke.

1.1 Motor Unit Recruitment and Discharge Patterns in the Paretic Muscles of Stroke Survivors

The neuromuscular system has two general strategies to grade force: 1) Rate-coding – modulation of the rate of action potentials driving the motor units, and 2) recruitment/de-recruitment of motor units (Enoka and Duchateau 2017). One of the underlying behaviors of motor unit recruitment is the Henneman Size Principle – motor units are recruited in an orderly sequence, from those that produce the smallest force to those that produce the largest force (HENNEMAN 1957). It is displayed in the positive relationship between twitch force and recruitment threshold. The orderly recruitment of motor units is mainly due to differences in motoneuron size in that the smallest motoneurons require the least amount of current to reach voltage threshold (Heckman and Enoka 2004). Earlier recruited motor units discharge at a higher rate than later recruited motor units, and this forms a layered shape known as the “onion-skin” firing pattern (De Luca and Contessa 2012; De Luca and Hostage 2010). The modulation of the recruited motor units occurs in unison because of common excitation to the motoneuron pool, known as common drive (De Luca et al. 1982). To increase the amount of force produced by the muscle, the neuromuscular system would use two means of force production to apply three possible strategies: 1) Increase the motor unit firing rate, 2) recruit inactive motor units, or 3) a simultaneous combination of both. These strategies provide the Central Nervous System (CNS) with a means of controlling activation of the motor unit pool without having to control each motor unit separately.

There is evidence in chronic stroke for alterations in rate coding and recruitment in paretic motor units that likely contributes to impaired force generation. Though reductions in descending neural drive and muscle atrophy are contributing factors, there is also evidence of a reduction in motor unit firing rates for a given level of force in the paretic muscles (Chou et al. 2013; Gemperline et al. 1995; Hu et al. 2016; McManus et al. 2017; McNulty et al. 2014; Miller et al. 2014). In contrast to firing behavior in healthy individuals, the voluntarily activated, paretic motor unit has limited ability for rate modulation (Chou et al. 2013; Mottram et al. 2014), compressed recruitment thresholds (Chou et al. 2013; Hu et al. 2015), and lower motor unit number estimation (Kouzi et al. 2014). In neurologically intact individuals, there is a linear, inverse correlation between recruitment threshold and mean firing rate (onion-skin); however, onion skin correlations from stroke survivors are disrupted in the paretic motor units of the upper limb (Hu et al. 2016). The disruption of the size principle may reflect a shift to a higher proportion of type I (Lukács et al. 2008) or type II (Hafer-Macko et al. 2008) muscle fibers after a stroke. Contrary to chronic stroke, acute stroke showed evidence in the upper limbs of ordered motor unit firing behavior, which may provide insight into chronic changes within the motor unit post-stroke (Hu et al. 2015; Sauvage et al. 2006). There is also evidence of prolonged motor unit firing following voluntary and reflex muscle activation, causing an impaired control of motor unit firing at rest and consciously attempting to relax the muscle (Mottram et al. 2010; Murphy et al. 2015). The evidence is still incomplete and mainly comes from the upper extremity; however, these observations show that stroke survivors have a decreased ability for both recruitment and rate coding – two essential strategies neurologically intact individuals use for effective force

production. Understanding individual motor unit behavior post-stroke will help to categorize the functional impairment resulting from the inability to control force output. These studies will examine how cortical and subcortical inputs affect rate coding, recruitment, and whole muscle activation during fatiguing and non-fatiguing contractions.

1.2 Decomposition of Individual Motor Unit Firing Instances from High-Density Surface EMG

Within the spinal cord, alpha motor neurons process the combination of inputs from afferent feedback and supraspinal centers into the neural drive that activates the muscle. Recordings of the muscle fiber action potentials provides access to motor unit information because the neuromuscular junction is a highly reliable synaptic connection (Farina et al. 2008a). Because of this reliability, there is a one-to-one relationship between the discharge of the motoneuron and the motor unit action potential detected over and within the muscle fibers, providing a window to the inputs of the spinal circuitry. With this knowledge, the cumulative summation of the discharge of the active motoneurons have been assessed by decomposing EMG recordings into the individual firing instances of the motor units generating the EMG signal. These studies will specifically investigate how motor unit firing behavior differs for individuals with stroke compared to healthy controls. Individual motor units will be acquired from the decomposition of high-density surface EMG (HDsEMG).

Historically, in the laboratory and the clinic, motor unit discharges have been identified from invasive wire or needle electrodes that acquire intramuscular EMG (Merletti and Farina 2009). Though intramuscular EMG has been relevant and reliable, it

provides a small number of motor units and is only applicable at low contraction levels because of interference of many overlapping sources (Farina and Negro 2015; Farina et al. 2008b). Recently, multi-channel (high-density, 64 channels in these studies) surface EMG decomposition algorithms using latent component approaches have been developed and validated to non-invasively identify a large number of concurrently active motor units (Holobar et al. 2010; Holobar and Zazul 2007; Negro et al. 2016).

Decomposition of surface EMG aims at reversing the convolutive mixture of the motor unit action potentials (MUAPs). During isometric contractions (as opposed to dynamic contractions), variations to the detected MUAP shapes from changes in muscle geometry and length are eliminated and the MUAP shapes are assumed stationary; therefore, the model is described as a linear time-invariant convolutive mixture of a series of delta functions (MUAPs) that represent the discharges of the individual motor units (sources) during isometric contractions (Holobar et al. 2010; Holobar and Zazul 2007; Negro et al. 2016):

$$x_i(k) = \sum_{l=0}^{L-1} \sum_{j=1}^n h_{ij}(l) s_j(k-l) + n_i(k), \quad i = 1, \dots, m, k = 0, \dots, D_R$$

$x_i(k)$ is the i th EMG channel, k is discrete time, D_R is the duration of the recording, $h_{ij}(l)$ is the action potential of the j th motor unit recorded from channel i , $s_j(k)$ is the spike train of the j th motor unit, $n_i(k)$ is the additive noise at channel i , L is the duration of the action potentials, n is the number of active motor units, and m is the number of channels.

Though multiple decomposition techniques are available, the algorithm utilized in these studies builds on the mathematical model of the EMG mixing process just

described (i.e. latent component analysis). The main objective of latent component analysis is to estimate the mixing matrix (sources that mix to create the EMG signals) directly from the observations (individual EMG channels) without prior information about the mixing process or motor unit discharges. The framework and pseudocode has been described and validated in a previous study (Negro et al. 2016). Briefly, the decomposition algorithm combines approaches based on convolutive blind source separation to iteratively extract the sources (similar to Independent Component Analysis) (Hyvärinen 1999), and then estimates the motor unit spike train using a peak detection algorithm applied to the square of the sources and K-mean classification of the identified peaks. The sources are considered acceptable quality using a silhouette measure (SIL) that provides a normalized index of reliability (0 to 1) similar to signal to noise ratio and is an estimate of the quality of the extracted source.

The utility of decomposition of high-density surface EMG lies in the direct measurement of individual motor unit firing behavior. Not only is it non-invasive, but previous surface EMG metrics provided only indirect and broad measures of neural drive, such as EMG RMS. For instance, a large number of motor units allows for analysis into the relationships of recruitment threshold and firing rate (onion skin property) (De Luca and Contessa 2015; 2012) or a larger number of paired motor unit recordings for studying contribution of persistent inward currents (Powers and Heckman 2015). Recently, surface EMG techniques to extract motor unit firing behavior has been applied to studying the stroke population (Hu et al. 2016; 2015; McManus et al. 2017; Murphy et al. 2015). The large number of motor units acquired and directly measuring from individual motor units

makes this novel technique a valuable resource when studying motor control in both healthy and stroke populations.

A main limitation in this blind source separation technique is that it is limited to isometric contractions (Farina et al. 2008a; Negro et al. 2016). This provides no insight into motor unit behavior during dynamic contractions; therefore, these studies were limited to isometric contractions. Another issue is the inter-participant differences in body composition. The sources are separated from the recording electrodes by tissues that act as a volume conductor. The volume conductor properties determine the features for the detected signals and the frequency content. As each individual is different, the difference between the source and the recording electrodes becomes a relevant issue. The biological tissues act as spatial and temporal low-pass filters, and participants with less muscle mass and more subcutaneous fat will have important effects on the signal (Blok et al. 2002). Also, for participants with large amounts of force and low subcutaneous fat, crosstalk between sources may reduce the selectivity of the decomposition algorithm (Roeleveld et al. 1997). A final limitation discussed here, is that the muscle fibers must run parallel to the skin compared to pennate muscle fibers. The representation of the MUAP that are parallel to the recording electrodes allows for more accurate estimation of the action potentials from the high-density surface EMG (Gallina et al. 2013). The muscle used in these studies (vastus lateralis) allows for the muscle fibers and electrodes to be oriented in parallel planes (Lieber and Fridén 2000) for the most accurate estimation of MUAPs within the quadriceps muscle group.

1.3 Stroke-related Changes to Neuromuscular Fatigue and Motor Control

Neuromuscular fatigue has been defined as any exercise induced reduction in the ability of a muscle to generate force and can be quantified through the reduction in maximal muscle force capability (Bigland-Ritchie and Woods 1984; Enoka and Duchateau 2008). Reduction in force production is determined by central factors, such as voluntarily activating the muscle through descending commands, and peripheral factors, such as adequate blood flow to meet the metabolic demands of the contracting muscle. Failure of either central or peripheral factors, or both, can cause reductions in force generation (Gandevia 2001). Lesions in the motor cortex caused by a stroke results in the loss of excitatory drive from the descending motor pathways (Jang et al. 2017; Murase et al. 2004; Peters et al. 2017; Schwerin et al. 2008). Consistent with increased neuromuscular fatigability, individuals with stroke demonstrated altered kinematics after short bouts of walking and even decreased distance walked during the 6-minute walk test compared with healthy controls (Chen and Patten 2008; Dean et al. 2001; Jonkers et al. 2009; Nadeau et al. 1999). Currently, models of motor impairment attribute post-stroke force generating deficits to muscle atrophy and baseline reductions in cortical commands; however, these models do not consider stroke-related changes to subcortical and other spinal levels that contribute to sub-optimal activation of the muscle and increased fatigability.

In healthy controls, peripheral mechanisms (muscular) dominate task failure, especially during sustained, ischemic contractions. Evidence for peripheral fatigue is the reduction in force production independent of the central nervous system, including changes within the muscle fibers. Peripheral fatigue has been evaluated using the

compression of the surface EMG power spectrum (Merletti et al. 1990; Riley and Bilodeau 2002; Svantesson et al. 1999) and changes in maximal twitch torque (Knorr et al. 2011). Decreases in mean or median frequency of the power spectrum indicates a reduction in muscle fiber conduction velocity and decreases in maximal twitch torque is likely due to decreases in excitation-contraction coupling of the muscle fibers. In both cases, the decline is related to metabolic accumulation (De Luca 1984; Fitts 2011a). The buildup of muscle ischemia contributes to the buildup of metabolites, making it essential to provide adequate blood flow to the exercising muscle as greater perfusion results in reduced metabolic accumulation. Currently, there are no studies available that investigate the contributions of blood flow to neuromuscular fatigue between stroke and control participants; however, for healthy controls, it is agreed that most declines in force generation during fatiguing contractions is ascribed predominantly to acute changes in muscle contractile properties. Essentially, changes beyond the motoneuron determine fatigue for intact controls.

Previous studies indicate that neural factors contribute predominantly to neuromuscular fatigue in individuals with stroke (Bowden et al. 2014; Hyngstrom et al. 2012; Klein et al. 2010; Knorr et al. 2011; Kuhnen et al. 2015; McManus et al. 2017; Riley and Bilodeau 2002; Rybar et al. 2014b). Alterations post-stroke due to the disruptions in corticomotor pathways result in deficient neural excitation of the muscle during exercise or sustained activity. Central fatigue encompasses motoneuron intrinsic properties and inputs to the motoneuron, such as decreases in motor commands through the corticospinal tract, increases in inhibitory afferent input, and decreases/increases in excitatory afferent input (Enoka and Duchateau 2008; Knorr et al. 2011; Lewek et al.

2006). A lack of neural excitation of the paretic muscle over the course of activity causes premature reductions in force compared with muscular mechanisms; furthermore, reductions in central activation may limit motor unit firing rates and modulation necessary for sufficient force output (Gemperline et al. 1995; Mottram et al. 2014). Insufficient neural command affects the ability to appropriately modulate motor unit firing rates, and consequently, the ability to properly generate force. Attention to post-stroke changes to neural factors is important because vulnerability to central fatigue may contribute to impaired activities of daily living.

Increased paretic neuromuscular fatigability would impact a person's functional strength. Though it has been shown that lower extremity (hip flexor muscles) fatiguing contractions results in faster task failure compared to controls (Hyngstrom et al. 2012), limited information currently exists on the force generating deficits of the knee extensor muscles and the implications on motor performance post-stroke. Furthermore, fewer studies have specifically investigated post-stroke changes to spinal factors such as changes to motor unit firing behavior, afferent input, and intrinsic properties of the motoneuron.

1.4 Impact of post-stroke motor cortex changes on voluntary activation

Ultimately, post-stroke force impairment during maximal efforts arise from the nervous system's inability to volitionally activate the affected muscle due to a compromised corticospinal tract. Hemiparesis – so called because of muscle weakness on one side of the body – is a common clinical outcome after stroke because of the damage to one side of the cortex (Twitchell 1951). As voluntary movement is reliant on the

ability to transmit commands from the cortex to the motoneuron pools via the descending tracts, much of the literature focuses on the reduction in descending cortical drive to the paretic motoneuron pools and impaired paretic muscle activation (Bowden et al. 2014; Horstman et al. 2008; Jones 2017; Knorr et al. 2011; Newham and Hsiao 2001). Though the exact mechanisms of deficient muscle activation after a stroke lesion are not completely understood, reductions in descending pathway connections is a significant contributor to changes in the neural drive to the motoneuron pools (Delvaux et al. 2003; Murase et al. 2004). In response to decreased descending drive, spinal motoneurons lose their controlling input (Young and Mayer 1982). Activation and modulation of paretic motoneurons decreases without appropriate cortical control; therefore, paretic muscles cannot modulate force to sufficiently control or complete functional tasks. It was important in the current studies looking at subcortical changes post-stroke to not neglect the importance of cortical deficits to voluntarily control the muscle.

The twitch interpolation technique is a method commonly used to measure the degree of voluntary activation. In these studies, voluntary activation refers to the completeness of skeletal muscle activation during voluntary muscle contractions; therefore, maximum voluntary activation relies on the ability to recruit all available motor units at maximal firing rate (Allen et al. 1995; Herbert and Gandevia 1999). In the interpolated twitch technique, an electrical stimulus evokes a muscle twitch at maximum voluntary contraction (superimposed twitch) and then again when the muscle is completely relaxed (resting twitch). If the superimposed stimulus at maximum force evokes additional torque, maximum activation of the motoneuron pool is not acquired. Though even healthy, intact controls struggle for 100% voluntary activation

using this technique, multiple studies have shown significant reductions in voluntary activation after a stroke (Bowden et al. 2014; Hoffmann et al. 2016; Knorr et al. 2011; Riley and Bilodeau 2002), with voluntary activation levels as low as 55.8 ± 26.8 % during isometric, maximal voluntary contractions of the knee extensor muscles after a stroke (Horstman et al. 2008). This is an important technique for motor control investigations because voluntary activation is a measure of the neural command, including afferent input, to the motoneuron pool during voluntary effort, and it is a non-invasive method that has the potential of identifying impairments in neural drive.

1.5 Decreased Muscle Blood Flow and Hyper-Excitable Small Diameter Afferent Activity Post-Stroke

Motor unit firing rates may decline during sustained isometric contractions or ischemic conditions because of metabolic accumulation in response to blood flow occlusion. Group III (thinly myelinated) and group IV (unmyelinated) afferents, which project to motoneurons via inhibitory interneurons, mediate exercise through their inhibitory effect on the output of spinal motoneurons. Contraction induced mechanical and chemical stimuli activates the molecular receptors of group III/IV afferents with the onset of exercise, increasing the discharge of these muscle afferents (Amann 2012; Taylor et al. 2016). As group III/IV firing increases, the development of central fatigue is facilitated through their inhibitory effect on the output from spinal motoneurons, causing a reduction in muscle activation (Amann et al. 2008). Following a stroke, in which certain descending motor tracks are interrupted, the gain of these inhibitory interneurons is likely to be altered. There is evidence that reflexes associated with group III/IV muscle afferents may be hyper-excitable following stroke (Hidler and Schmit 2004; Sangani et

al. 2009; 2007). Reduced blood flow in the paretic leg of participants with stroke may cause a decrease in motoneuron firing rates because of the activation of group III and IV afferents. It has been shown that at rest (Billinger et al. 2009), and during isometric contractions of the knee extensors at varying intensities, blood flow in the paretic leg is dampened compared to control legs (Durand et al. 2015). With a reduced hyperemic response and an increase in metabolic accumulation in the exercising muscle post-stroke, in combination with increased excitability of small diameter afferents, it is feasible that group III and IV afferents will inhibit motoneurons and further decrease firing rates, reduce motor unit recruitment, and lower the magnitude of muscle activation during contractions compared to controls.

Group III/IV afferents may also impact the development of peripheral fatigue and the hemodynamic response to exercise. The role of group III/IV afferents to peripheral fatigue manifests in the contributions to cardiovascular output. Previous experiments in the intact population showed that exercising humans with attenuated feedback of group III/IV pathways causes a reduced blood flow delivery and an accelerated rate of peripheral fatigue of up to 60% faster compared to intact group III/IV pathways (Amann 2012; Amann et al. 2011; Amann and Secher 2010; Amann et al. 2014). The arterial baroreflex has been suggested to decrease the impact of group III/IV afferents because of the interaction within the brainstem, buffering group III/IV mediated reflexes (Kim et al. 2005; Sheriff et al. 1990). In stroke, it is believed that the brainstem may be hyperactive because of the loss of inhibition from a damaged motor cortex (Dewald et al. 1999; Kline et al. 2007; Matsuyama et al. 2004; McPherson et al. 2008; Sukal et al. 2007); therefore, not only may group III/IV pathways be hyperexcitable and inhibit motoneuron output

after stroke, increased blood flow observed after group III/IV activation may be attenuated because of excitability from the brainstem. This would likely impact both peripheral and central metrics of fatigue after stroke. For these reasons, the hyperemic response to intermittent fatiguing contractions, as well as motor unit firing behavior during ischemic conditions, will be investigated in these studies.

1.6 Neuromodulatory Control of Spinal Cord Function Post Stroke

In the intact state, the descending monoaminergic input from the brainstem regulates intrinsic excitability of motoneurons causing amplification of ionotropic synaptic input. Spinal motoneurons are participant to particularly strong neuromodulation by monoamines serotonin (5-HT) and norepinephrine (NE) which increase persistent inward currents (PICs) (Lee and Heckman 2000). PIC amplitudes are regulated by the levels of monoamines. Motoneurons exhibit a dendritic PIC that amplifies synaptic input. For a given input in healthy humans, this is evident through greater firing rates (possibly sustained firing) and a decrease in recruitment threshold (Gorassini et al. 2002a). Firing patterns in human participants initially increase steeply but then plateau as the PIC is fully active (Heckmann et al. 2005). Levels of monoamines such as serotonin and norepinephrine are regulated by the cortex through tonic inhibition and vary with the force demands of the task. In normal motor behavior, PICs produce effects on motoneuron firing that are unique and play an important functional role.

A key regulator of PIC amplitude is monoaminergic drive from the reticular formation in the brainstem. Spinal motoneurons receive dense contacts from monoaminergic axons, which release the neuromodulators serotonin and norepinephrine.

5-HT and NE bind to metabotropic receptors that ultimately alter the cell's intrinsic excitability by changing ion channel behavior (Rekling et al. 2000). Self-sustained firing related to the monoaminergic input occurs in motor units responsible for low force contractions (Heckman et al. 2003; Lee and Heckman 1998) needed for performing many activities of daily living. An important source of PIC inhibition is from sensory inputs often activated by movement (Heckman et al. 2008; Hyngstrom et al. 2007).

Monoaminergic brainstem nuclei are believed to be tonically active, regulated primarily by supraspinal inhibition depending on the needs of the task (Aston-Jones et al. 2000; Hyngstrom et al. 2007; Jacobs and Fornal 1999; 1997). The stroke lesion likely disrupts cortical inhibition of brainstem monoaminergic centers, which would result in an increase in descending monoaminergic drive.

Stroke-related damage to the cortex may, thus, result in an increased monoaminergic drive to spinal motoneuron pools. This was observed in the decerebrate cat as motoneuron firing behavior consistent with PICs were dependent on continuous activity of descending monoaminergic input to the spinal cord. A significant drop in intrinsic excitability of the motoneurons was observed after spinalization eliminated the brainstem projections of the monoamines to the spinal cord (Hounsgaard et al. 1988). This disinhibition increases the excitatory neuromodulatory drive from the reticular formation to the spinal cord and there is some indirect evidence for this in participants with stroke (Dewald et al. 1999; Kline et al. 2007; Matsuyama et al. 2004; McPherson et al. 2008; Sukal et al. 2007). It is feasible that enhanced motoneuron PICs after a stroke may be caused by disinhibition to monoaminergic brainstem input to the spinal cord previously suppressed through inhibition from the cortex. This would be especially

detrimental during the relaxation phase of voluntary contractions (Lewek et al. 2007). The origins of the disrupted rate modulation post stroke may result from limitations in descending drive, inhibitory afferent input, and intrinsic changes to the motoneuron properties such as PICs.

1.7 Estimating PICs in Humans

Because intracellular recordings from human motor neurons is not possible, a technique using paired motor units (referred to as paired motor unit analysis or ΔF) has been used to estimate PIC magnitude in humans (Gorassini et al. 2002a; b; Gorassini et al. 2004; Mottram et al. 2009; Vandenberg and Kalmar 2014). This method compares firing rates at recruitment and de-recruitment to estimate intrinsic excitability of the motoneurons. The technique requires a pair of motor unit firing rates: 1) an earlier recruited, lower threshold (reporter) unit and 2) a later recruited, higher threshold (test) unit. The reporter unit is used to help control for firing rate changes due to changes in excitatory synaptic inputs to the motoneuron. The difference in firing rate (ΔF) of the reporter unit from when the test unit is recruited to when it is de-recruited is thought to reflect the magnitude of the PIC contribution to the total excitatory drive of the test unit. The ΔF value provides a metric to the hysteresis in firing behavior caused by PICs. The hysteresis of the motor unit firing rates is assumed to be maintained by an added depolarization produced from the sustained activation of the PICs (Gorassini et al. 2002a). A more positive ΔF has been found to be consistent with larger PICs (Powers et al. 2008). This technique has garnered attention within spastic populations, such as stroke

(Mottram et al. 2014) and spinal cord injury (Gorassini et al. 2004), because it is believed PICs play a role in muscle spasms.

Because this is an estimation of PIC contribution and not a direct measure, it is possible that other motoneuron properties contribute to the hysteresis of the motor unit firing behavior. A simulation study suggested that positive ΔF measurements could be susceptible to spike threshold accommodation or spike frequency adaptation in the absence of PIC contribution (Revill and Fuglevand 2011). However, another simulation study suggested that although ΔF measurements can be affected by other factors, values greater than 1 Hz require a significant level of PIC generation (Powers and Heckman 2015). The different factors that contribute to positive ΔF values will be considered in these studies.

There are four key assumptions when using this technique to estimate PICs in humans (Gorassini et al. 2002a; Gorassini et al. 2004) but are briefly summarized here: 1) Due to its dendritic origin, motoneuron PICs are activated before or at recruitment and the PIC provides a depolarizing current that helps sustain motoneuron firing. 2) The firing rate varies with synaptic input and is used to estimate input to the cell. 3) The reporter and test motor units process synaptic inputs similarly. 4) Because of common drive to the paired motor units, the reporter motor unit provides an estimate of synaptic drive to the test unit.

1.8 Summary and Contribution to Current Literature

Quantifying the contributions of cortical and subcortical inputs to the motoneuron pool, along with intrinsic properties of the motoneuron, after suffering a stroke is critical

to the development of targeted rehabilitation strategies. Previous studies relied on broad measurements of central factors such as mean frequency and EMG RMS. Currently, only a few studies examined post-stroke motor unit firing rates from a large number of simultaneously active motor units (Hu et al. 2016; 2015; Li et al. 2014; McManus et al. 2017), and only one study (from this laboratory) examined motor unit firing rates decomposed from high-density surface EMG from the knee extensor muscles (Murphy et al. 2015). This dissertation provides three new studies that examined the post-stroke activity of a large number of simultaneously active motor units concerning central (voluntary activation) and peripheral blood flow contributions to neuromuscular fatigue (chapter 2), inhibitory afferent input to the motoneuron pool during occlusion of blood flow (chapter 3), and intrinsic properties of the motoneurons assessed using a serotonin reuptake inhibitor (chapter 4). To date, no other studies exist concerning these topics in the knee extensor muscles after a stroke. As a whole, these studies investigated central contributions to deficient muscle activation from the cortex, afferent input, and the intrinsic properties of the motoneuron. This dissertation provides critical information, not previously investigated, that benefits our understanding of abnormal motor control post-stroke using activity directly from paretic motor units.

1.9 Specific Aims

AIM 1: Determine the relationship between the hyperemic response to exercise and motor unit firing behavior during an intermittent, fatiguing task of the knee extensor muscles after a stroke.

In the first aim, we will determine whether motor unit firing behavior of the vastus lateralis muscle tracks with the hyperemic response through the femoral artery

during a submaximal, intermittent task. Hypothesis: The hyperemic response and modulation of motor unit firing rates to fatiguing contractions will be blunted in the paretic limb of individuals with stroke.

AIM 2: Quantify the post-stroke inhibitory effects of ischemia on motor unit firing rates and recruitment during submaximal contractions.

In the second aim, mean paretic motor unit firing rates will be compared with healthy control motor units in response to complete blood flow occlusion to the paretic leg. Hypothesis: In response to occlusion, the paretic leg will show a greater decrease in motor unit firing rates compared to controls.

AIM 3: Quantify stroke-related sensitivity of motor unit firing behavior to the neuromodulator serotonin during submaximal knee extensor contractions.

In the third aim, we will quantify the effects of a serotonin receptor antagonist on motor unit firing behavior during volitional relaxation of the vastus lateralis muscle.

Hypothesis: The serotonin receptor antagonist will reduce prolonged firing and increase motor unit rate of relaxation during volitional relaxation and reduce the magnitude of PIC contribution to the motoneuron.

CHAPTER 2: THE RELATIONSHIP BETWEEN BLOOD FLOW AND MOTOR UNIT FIRING RATES IN RESPONSE TO FATIGUING EXERCISE POST-STROKE

2.1 INTRODUCTION

In addition to baseline weakness, individuals with stroke can have decreased ability to generate on-going sub-maximal forces during activities, such as walking, that require repeated activation of muscles and this can limit function. For example, individuals with stroke have decreased walking endurance (Dean et al. 2001; Iosa et al. 2012; Lloyd-Jones et al. 2009), and have changes in walking kinematics and kinetics over short distances (Chen and Patten 2008; Jonkers et al. 2009). In addition, slow walking speeds in people with stroke are associated with greater fatigability of lower limb muscles (Rybar et al. 2014b). Despite the functional implications, mechanisms of neuromuscular fatigue (the acute, exercise-induced reduction in the ability to generate force) post stroke are not well studied.

In healthy individuals and people with stroke, fatigability of muscles can be quantified as a reduction in maximal strength or power or the inability to maintain a submaximal force during ongoing contractions (Enoka and Duchateau 2008). Fatigability of muscles can originate from factors which limit the nervous system's ability to excite muscle tissue (central fatigue) or from factors at the level of the muscle which interfere with muscle contractile properties (peripheral fatigue) (Enoka and Duchateau 2008; Gandevia 2001; Hunter 2018). Central fatigue is often quantified through estimates of voluntary activation using the superimposed twitch technique (Allen et al. 1995; Shield and Zhou 2004). In response to fatigue there is an increase in the amplitude of a

superimposed twitch (SIT) force during a maximal effort contraction (e.g. the increase in the SIT force after a fatiguing task compared with before the task). At baseline (Horstman et al. 2008) and after fatigue (Bowden et al. 2014; Knorr et al. 2011), individuals with stroke have decreased ability to voluntarily activate musculature fully even with maximal efforts. Electrophysiological studies using transcranial magnetic stimulation have shown this may be due to a loss of excitatory descending drive most likely caused by the stroke-related lesions to the motor cortex (Foltys et al. 2003b; Jang et al. 2017; Peters et al. 2017). Based on studies showing decreased excitability in descending motor pathways, it is not surprising that recent evidence suggests that in people with stroke, central fatigue is a more significant contributor to fatigability of the paretic limb muscles than for the non-paretic limbs and healthy controls (Bowden et al. 2014; Hu et al. 2006; Hyngstrom et al. 2012; Klein et al. 2010; Knorr et al. 2011; Kuhnen et al. 2015; McManus et al. 2017; Riley and Bilodeau 2002; Rybar et al. 2014b). These studies attribute force generating deficits to baseline reductions in cortical commands, but they do not consider stroke-related changes to corticoreticular pathways or afferent input to spinal motoneurons from the build-up of metabolic by-products that could contribute to increased neuromuscular fatigability.

Peripheral fatigue refers to neuromuscular fatigue that is due to reductions in muscle contractile function. For example, excessive accumulation of metabolic by-products that occurs with muscle contractions interferes with the excitation-contraction coupling (Kent-Braun et al. 2012). Accumulation of metabolic byproducts can result from inadequate perfusion of the muscle. Following stroke, this may impact contractile properties as blood flow to the muscles of the paretic limb is decreased at rest (Billinger

et al. 2009; Durand et al. 2015; Ivey et al. 2004) and during brief, submaximal contractions (Durand et al. 2015) compared with healthy controls. Moreover, limitations in the hyperemic response to exercise is related to strength and other measures of function (Durand et al. 2015). In individuals with stroke, the contribution of inadequate blood flow to decreased muscle contractile properties and neuromuscular fatigue is not known.

Inadequate muscle perfusion and accumulation of metabolites within the muscle can also affect neural activation of the muscle via activation of chemo-sensitive group III and IV afferent endings in the muscle (Matthews 1972). Excitation of group III/IV pathways has been shown to increase central fatigue through inhibition of spinal motoneurons and the motor cortex (Gandevia 2001; Gandevia et al. 1996; Martin et al. 2008; Matthews 1972). This inhibition at the spinal and cortical level ultimately reduces force output. Importantly, there is indirect evidence that individuals with stroke have hyperexcitable group III/IV pathways which may result in increased sensitivity to inadequate perfusion (Hidler and Schmit 2004; Li 2017). Thus, if accumulation of metabolites inhibits motoneuron firing rates via group III/IV afferent inhibition (Kaufman et al. 1983), individuals post stroke who have decreased muscle perfusion during exercise may experience a greater decrease in motor unit firing rates compared to those with adequate perfusion; however, because of common inputs from the premotor/motor cortex to the reticular system and the corticospinal system that may be disrupted after stroke, a systemic disruption in the autonomic control of vessel constriction and motor unit firing behavior is possible. Understanding the effect of blood perfusion to exercising

muscles and motor unit firing is important because cooperation between the two systems may provide a method for recovery.

The association between blood flow and individual motor unit firing behavior during intermittent fatiguing contractions post-stroke has not been studied but may provide important insight for impaired force generation and task endurance in chronic stroke. The purpose of this study was to 1) identify reductions in the hyperemic response to intermittent, sub-maximal isometric fatiguing knee extension contractions in individuals with stroke compared with those without stroke and 2) determine the relationship between the change in blood flow with metrics of fatigue and motor unit firing behavior. We *hypothesized* that 1) if the hyperemic response of people with stroke was lower than healthy controls for non-fatiguing exercise, then it would also be lower during fatiguing exercise; and 2) if lower blood flow results in greater muscle fatigue (peripheral fatigue) and lower motor unit firing rates (central fatigue), then the lower hyperemic response during fatiguing exercise would be associated with reductions in the electrically evoked force response (twitch) and motor unit rate modulation.

2.2 MATERIALS AND METHODS

2.2.1 Participants

All participants gave informed consent before participation in this study, and the procedures were approved by the Medical College of Wisconsin Institutional Review Board (PRO190103). Ten participants with chronic, hemiparetic stroke (6 male, 4 female, 60 ± 6 yrs) and nine neurologically intact participants (6 male, 3 female, 63 ± 7 yrs)

participated in the study. Stroke participant general inclusion criteria were: single, unilateral stroke (obtained through verbal communication from the physician and consistent with neurological physical examination); able to ambulate at least 30 feet (with or without an assistive device); ≥ 6 months post stroke; at least 18 years old; and able to give informed consent. Stroke participant general exclusion criteria included: brainstem stroke; any uncontrolled medical condition; contractures of any lower extremity joints; inability to follow 2-3 step commands; substance abuse; people unable to walk more than 10 feet without physical assistance; narrow angle glaucoma; chronic liver or kidney disorders; major psychiatric disorders; neurodegenerative disorders. Table 1 reports the participant characteristics.

Subject Characteristics		
	Control (n=9)	Stroke (n=10)
Sex, Male	6	6
Age (yr)	60 \pm 6	63 \pm 7
Height (cm)	173.2 \pm 14.7	172.1 \pm 11.7
Weight (kg)	80.3 \pm 14.6	85.9 \pm 19.7
Leg Muscle Mass (kg)	8.79 \pm 2.63	7.30 \pm 1.78
Total Body Fat (%)	35.8 \pm 6.5	39.8 \pm 4.5
Fugl-Meyer Score	NA	23 \pm 7

Table 2.1. Participant Characteristics.

2.2.2 Torque Measurements

Participants were seated upright on a Biodex System 3 (Biodex Medical Systems, Shirley, NY) with the test leg hip and knee angles at 90 degrees of flexion. Isometric knee extension torque measurements were made using a JR3 E-series load cell (JR3, Inc., Woodland, CA) mounted to the dynamometer spindle by means of a custom aluminum

coupling. A quarter inch aluminum arm extended from the axis of the load cell to a bracket that secured either left or right ankle attachments. The ankle attachments were secured to the test leg two inches above the lateral malleolus. The torque was acquired by an EMG-USB2+ amplifier (256-channel regular plus 16-auxiliary channels, OT Bioelettronica, Turin, Italy), low-pass filtered at 500 Hz, sampled at 2048 Hz, and recorded using the OT Biolab software. The data was then zero phased, low-pass filtered at 15 Hz using a 4th order Butterworth filter prior to analysis.

2.2.3 Voluntary Activation and Resting Twitch Response

The knee extensor muscles were electrically stimulated using a constant current generator (DS7A, Digitimer, Welwyn, Wales) that delivered a rectangular pulse of 100 μ s duration over the quadriceps muscle group. The stimulation intensity (range 200 mA to 500 mA) was set at 20% above the level required to produce a maximal resting twitch amplitude that caused a supramaximal stimulation. The stimulation occurred at the peak torque (visually determined when the torque reached a steady plateau) of a maximum voluntary contraction (MVC) and is referred to as the “superimposed twitch.” Once the knee extension torque returned to 0 Nm, a second stimulation was provided to elicit the resting twitch response. The maximal torque generated by the knee extensors in response to the electrical stimulation was acquired. The superimposed twitch was calculated as the magnitude of the increase provoked by the electrical stimulus during the MVC (i.e. peak of superimposed twitch minus the peak of the MVC contraction) (Allen et al. 1995). The resting twitch was the torque magnitude generated from the electrically evoked contraction of the relaxed muscle (i.e. the magnitude of the torque produced at rest). The

voluntary activation was defined here as the completeness of motor unit recruitment and firing rate during a maximum voluntary contraction and was calculated using an interpolated twitch technique (Klass et al. 2007; Shield and Zhou 2004):

$$\text{Voluntary Activation (\%)} = \left(1 - \frac{\text{superimposed twitch}}{\text{resting twitch}}\right) * 100\%$$

2.2.4 Blood Flow Measurements

The participants rested upright in the Biodex seat for a minimum of 15 minutes prior to assessments of blood flow. Diameter, blood flow velocity, and volume of blood flow through the superficial femoral artery were obtained with a Doppler angle of insonation fixed at 60 degrees using a linear array 4.0-12.0 MHz transducer designed for vascular imaging and equipped to a Vivid e ultrasound machine (General Electric, Fairfield, CT). Sonography makes it possible to estimate the volume blood flow ($\frac{mL}{min} = \left(\frac{cm^3}{min}\right) = \text{velocity} \left(\frac{cm}{min}\right) \times \text{area} (cm^2)$) by careful measurement of the area, via the image, and the velocity distribution using the Doppler trace ($\text{velocity} = \text{frequency} \times \text{wavelength}$) (Walter et al. 1986). Five independent measurements at rest consisting of 3 complete cardiac cycles per measurement were averaged prior to beginning the experimental protocol to establish the resting values. Blood flow measurements during the fatigue protocol were taken immediately after each fatigue cycle (1 cycle = 5 isometric contractions at 40% MVC held for 10s and separated by a 4s rest) while the participant remained seated upright and still for a 10s video capture of the superficial femoral artery. The same portion of the artery was able to be visualized following all fatigue cycles because the participants were secured to the chair with a lap

belt and the isometric contractions did not result in movement of the lower limb. Only measurements obtained during the first three complete cardiac cycles following each fatigue cycle were included for analysis because local blood flow is a tightly coupled metabolic demand. Blood flow measurements were normalized to lean muscle mass of the whole lower limb determined by the dual-energy absorptiometry (Lunar iDXA, General Electric, Fairfield, CT) analysis. Normalized blood flow was not available for one of the control participants and one of the individuals with stroke because the participants declined body composition analysis.

2.2.5 Surface EMG Recordings

High-density surface electromyograms (HDsEMG) were obtained using a 64 channel 2-D electrode array with 8 mm interelectrode distance (ELSCH064R3s - 13 rows, 5 columns, OT Bioelettronica, Turin, Italy). A double-sided adhesive sticker designed for and compatible with the array was placed over the array. The holes within the adhesive sticker were filled with a conductive electrode paste (Ten20, Weaver and Company, Aurora, Co). The participant's skin was sterilized with an alcohol swab and rubbed to remove superficial dead skin. The array was placed over the belly of the vastus lateralis, midway between the patella and the greater trochanter. A reference electrode was placed over the ipsilateral lateral malleolus. Signals for each channel were differentially amplified between 1000 and 5000 V/V (participant dependent) and band-pass filtered (10-500 Hz) using the EMG-USB2+ amplifier. The signals were sampled at 2048 Hz, A/D converted to 12 bits, and acquired using the OT Biolab software throughout the duration of the fatigue protocol.

Prior to analysis, a 2nd order bandpass filter (10-500 Hz) and a notch filter (60 Hz) were applied to each channel of the HDsEMG array. The EMG root mean square (RMS) for each channel was calculated for the five consecutive, ten second isometric contraction

($RMS = \sqrt{\frac{1}{N} \sum_{n=1}^N x_n^2}$, $n = \text{data point}$, $N = \text{total data points}$) for the first and last

cycle of the fatigue protocol (described below). For a spectral descriptor, the mean

frequency of the EMG was also calculated: $f_{mean} = \frac{\int_0^{\frac{f_s}{2}} f S(f) df}{\int_0^{\frac{f_s}{2}} S(f) df}$, where $S(f)$ is the Power

Spectral Density (PSD) of the signal and f_s is the sampling frequency. The EMG signal, $x(t)$, has a Fourier transform, $X(f)$, and a power spectral density $S(f) = |X(f)|^2$. The RMS and mean frequency values of all channels were averaged together for each fatigue cycle to provide an average RMS and mean frequency of the entire high-density surface array.

2.2.6 Motor Unit Decomposition

The 63 differentially amplified sEMG channels were visually examined to exclude channels that did not show EMG activity. The remaining channels were decomposed to attain instances of single motor unit action potentials by implementing a multichannel convolutive blind source separation algorithm described and validated by Negro et al (2016). In summary, the decomposition algorithm discriminates between individual motor unit action potentials from multi-unit signals. The general framework for HDsEMG decomposition uses the approaches based on convolutive blind source separation by convolutive kernel compensation (Holobar and Zazul 2007), and the spike trains are estimated using a peak detection algorithm and K-means classification. To

provide a normalized index of reliability similar to the pulse to noise ratio, a silhouette measure (SIL) was computed on each estimated source, and the source was considered of acceptable quality if SIL was greater than 0.85. SIL provides a measure of the quality of the extracted motor unit spike trains based on the relative amplitude of the deconvolved spikes compared to the baseline noise. Motor units were identified by applying the decomposition algorithm separately to the first and last cycles of the fatigue protocol. Under the assumption that motor unit action potential shape may change with endurance, motor units were not matched between the first and last cycles; however, under the assumption of stable motor unit action potential properties, this configuration provided the possibility to identify reliably the same motor units within the same cycle (Martinez-Valdes et al. 2017a).

Before calculating the discharge rates of the inter-spike intervals (ISI), abnormally long (>250 ms, 4 Hz) or short (<20 ms, 50 Hz) ISI values were excluded. The instantaneous firing rates of individual motor units were calculated as the inverse of the inter-spike interval (Hz, PPS, $\frac{1}{ISI}$). The motor unit action potential instances were time-locked with the torque trace. The mean firing rates were determined as the average firing rates during all five 10s holds at 40% MVC for one fatigue cycle (i.e. First and Last Cycles, see figures 2.1 and 2.2). Therefore, the firing rate of the first fatigue cycle consists of the average firing rate for the first five contractions of the fatigue protocol, and the firing rate of the last fatigue cycle consists of the average firing rate for the last five contractions of the fatigue protocol.

2.2.7 Body Composition and Clinical Measurements

Anthropomorphic measurements were performed by a licensed bionutritionist. Body composition analysis was conducted using an iDXA (GE Lunar Medical System, Madison, WI) to determine the estimated visceral fat percentage, total lower limb mass, lean muscle mass of the limbs, and percent fat composition of each limb. A Lower Extremity Fugl-Meyer (assessment of motor impairment) was performed by a licensed physical therapist.

2.2.8 Experimental Protocol

The paretic leg and the right leg of the control participants were tested. Figure 2.1 illustrates the timeline of the experimental protocol, and Figure 2.2 illustrates single participant examples for a control and an individual with stroke. Participants began by performing at least five baseline isometric maximum voluntary contractions (MVC) of the knee extensor muscles with one minute of rest between trials. Visual feedback and verbal cueing were provided to the participant. The peak torque of all the trials was used as the MVC. Voluntary activation and resting twitch measures were made following the final MVC trial. A rest period of at least 5 minutes was provided following the final voluntary activation trial. Participants then performed the fatigue protocol. One cycle of the fatigue protocol consisted of five consecutive isometric contractions at 40% MVC and each contraction lasted for 10s with a 4s rest provided between each contraction. Visual feedback of the torque trace and target torque was provided using a custom written LabVIEW (National Instruments, Austin, TX) program. Immediately after each fatigue cycle, a vascular measurement of blood flow was taken. An additional 15 seconds of rest

was applied after each cycle to allow ample time for the vascular measurements. A participant repeated the fatigue protocol until the individual was unable to hold the torque trace within 10% of the target torque for 5s continuously or until the participant had at least 3 deviations of greater than 10% of the target torque within a 10s contraction. Final vascular, voluntary activation and resting twitch measurements were made immediately (within 10s) following task failure. Surface EMG using the high-density electrode array was recorded throughout the duration of the fatigue protocol.

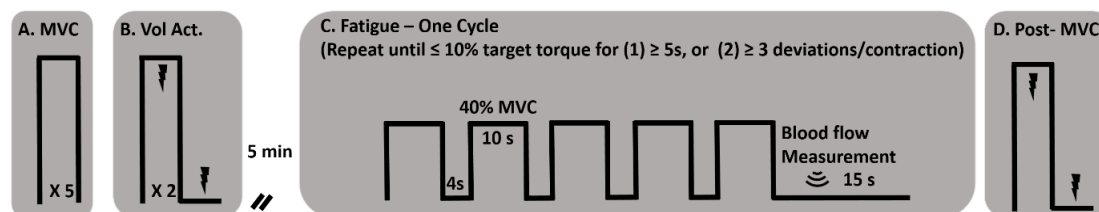


Figure 2.1. Experimental Protocol. A) MVCs of the knee extensor muscles with a one-minute rest between trials. B) An interpolated twitch procedure was performed for a measure of voluntary activation and resting twitch torque. C) A single cycle for the fatigue protocol consisted of 5 consecutive 10 second isometric contractions, separated by a 4 second rest, at 40% MVC. A blood flow measurement was performed over the femoral artery of the test leg using an ultrasound machine. The fatigue cycle was repeated until the participant could not hold the isometric contraction within 10% of the target torque for more than 3 deviations per isometric contraction or for greater than 5 consecutive seconds. D) A post-MVC including the interpolated twitch procedure was performed immediately after the final blood flow measurement.

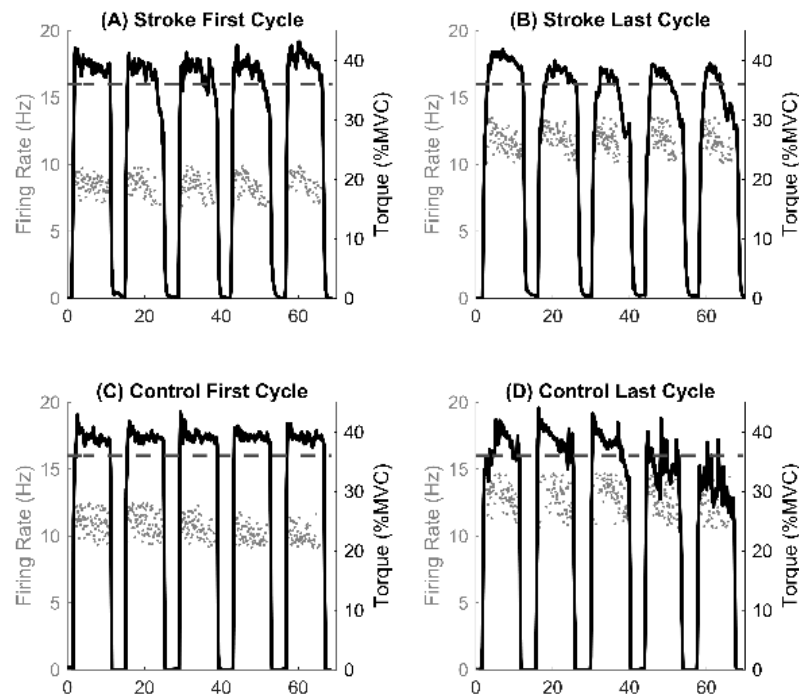


Figure 2.2. Single participant example. The motor unit firing instantaneous discharges (grey dots) and the corresponding torque generated (black trace) for the first (left) and last (right) fatigue cycles. The dashed line represents the point of task failure if the torque was not maintained above that value. Note the inability to maintain the torque above the task failure line in the last cycle compared to the first cycle.

2.2.9 Statistical Analysis

Data processing was performed in Matlab R2017b (Mathworks, Natick, MA), and statistical tests were performed using IBM SPSS Statistics 24 (IBM, Armonk, NY). Data are reported as the mean \pm standard deviation. For one of the control participants and one of the individuals with stroke, body composition analysis was declined; therefore, those participants could not have blood flow normalized to lean muscle mass and were not included in that part of the analysis. The motor units for three control participants did not fulfill the SIL criteria ($SIL > 0.90$); therefore, only the motor units from 6 control participants are considered.

Separate repeated measures, mixed model ANOVAs were performed to detect statistical differences between the tested GROUP (stroke, control) and fatigue CYCLE (first and last) in: 1) normalized blood flow; 2) absolute blood flow; 3) motor unit firing rates by participant mean; 3) voluntary activation; 4) resting twitch amplitude; 5) mean EMG RMS; and 6) EMG mean frequency. The between group variable was GROUP. CYCLE was the within group comparison. A multifactorial ANOVA was used to compare the individual motor unit firing rates (main factors: 1) CYCLE (first and last fatigue cycles), and GROUP (Stroke, Control). A repeated measures ANOVA was not used for the individual motor units because detection of the same motor units at the first and last fatigue cycles could not be determined. A Bonferroni correction was used in all post hoc testing.

Separate one-way analysis of variances (ANOVAs) were used to test for relative change [$\Delta = \left(\frac{\text{variable}_{\text{lastcycle}}}{\text{variable}_{\text{firstcycle}}} - 1 \right) * 100\%$] in: 1) mean MVC; 2) mean EMG RMS; 3) EMG mean frequency; 4) motor unit firing rate by participant average; 5) mean blood flow 6) voluntary activation; and 7) resting twitch torque. A one-way ANOVA was also used to test for differences in task duration in terms of number of fatigue cycles completed.

Using the least squares estimates method for linear regression models, coefficient of determinations and model parameters were calculated for the following correlations: 1) Δ blood flow and task duration; 2) Δ blood flow and Δ MVC; 3) Δ blood flow and Δ motor unit firing rate; 4) absolute blood flow and MVC torque. ANOVAs were performed to test the significance of the correlations using the F-statistic. A runs test for detecting randomness was used to determine whether the linear regression fits the data.

The linear regression models were included if the residuals showed a random, non-systematic pattern.

2.3 RESULTS

2.3.1 MVC Torque and Task Duration Measurements

At baseline, controls had a greater knee extension MVC compared to individuals with stroke (129.80 ± 53.16 Nm vs 76.41 ± 29.45 Nm, $p = 0.003$). The relative decline in MVC was similar for both groups ($-39.822 \pm 10.07\%$ vs $-34.30 \pm 12.66\%$, $p = 0.311$). There was no difference in the number of fatigue protocol cycles completed (11.91 ± 10.28 cycles vs 15.72 ± 8.23 cycles, $p = 0.383$).

2.3.2 Voluntary Activation

A significant interaction effect was observed in the voluntary activation measurement between the control and stroke groups, $F(1,17) = 24.973$, $p < 0.001$, as the individuals with stroke had a larger decrease in the voluntary activation from the first cycle to the last cycle of the fatigue protocol ($93.63 \pm 4.48\%$ to 75.38 ± 10.47 , $p < 0.001$) (Figure 2.3A). There was no significant difference in voluntary activation of the control participants ($97.42 \pm 2.43\%$ to $95.64 \pm 4.46\%$, $p = 0.465$) with fatigue. A main effect of fatigue cycle was observed, $F(1,17) = 37.000$, $p < 0.001$, as there was a decrease in voluntary activation with fatigue. There was also a main effect of group $F(1,17) = 24.829$, $p < 0.001$, where voluntary activation in the stroke group was less than controls. Relative change in voluntary activation showed a significantly greater decrease in the stroke group

compared to the controls ($p < 0.001$) (Figure 2.3B). In summary, the individuals with stroke had a greater decrease in voluntary activation with the fatigue protocol, as well as a lower baseline voluntary activation.

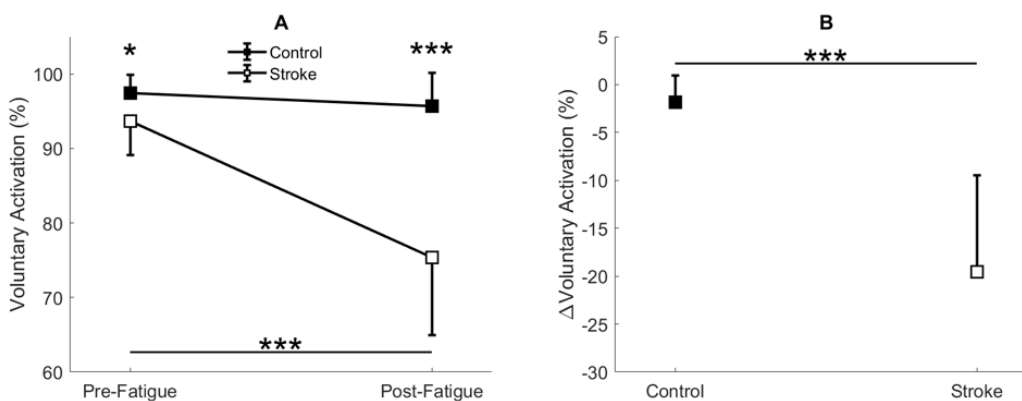


Figure 2.3. Voluntary activation. Voluntary activation assessed using the twitch interpolation technique comparing the first and last cycle (A) and the relative change before and after the fatigue protocol (B). A significant interaction effect ($p < 0.001$) was observed as individuals with stroke significantly decrease voluntary activation with fatigue. Voluntary activation was significantly lower for the stroke participants at pre-fatigue ($p < 0.05$) and post-fatigue ($p < 0.001$), and significantly decreased with fatigue for the stroke participants ($p < 0.001$) but not the controls (A). A significantly greater normalized decrease in voluntary activation was observed for the stroke participants ($p < 0.001$) compared to controls (B).

2.3.3 Resting Twitch Torque

A significant interaction effect was observed in the resting twitch torque between the control and stroke limbs, $F(1,17) = 7.391$, $p = 0.015$, as there was a greater decline in resting twitch torque response in controls (41.50 ± 17.17 Nm to 18.58 ± 11.14 Nm, $p < 0.001$) compared to individuals with stroke (33.79 ± 17.20 Nm to 22.69 ± 13.01 Nm, $p = 0.002$) (Figure 2.4). There was also a main effect of cycle, $F(1,17) = 61.312$, $p < 0.001$, but not a main effect of group, $F(1,17) = 0.077$, $p = 0.785$. Relative change in resting twitch torque showed a significantly greater decrease for the control group compared to

the stroke group ($p = 0.005$) (Figure 2.4B). In summary, the control participants had a greater decrease in muscle contractile properties (resting twitch torque) in response to the fatigue protocol.

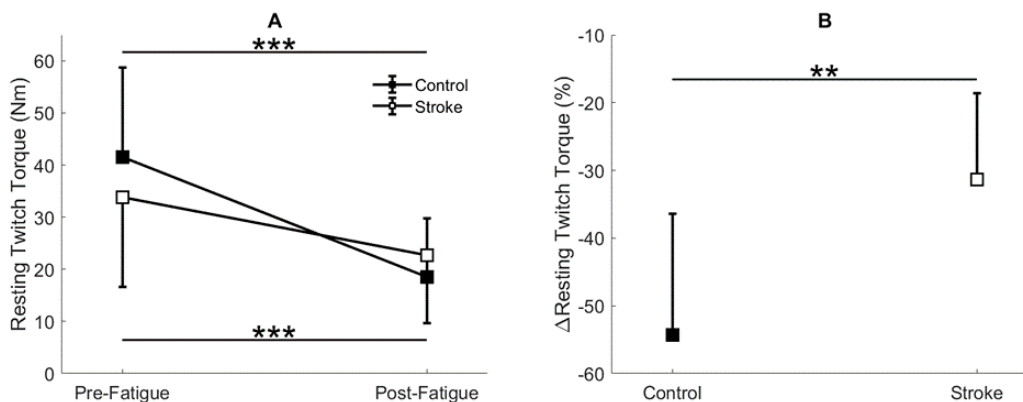


Figure 2.4. Resting twitch torque. Resting twitch torque amplitude elicited from electrical stimulation to the rectus femoris comparing the first and last cycle (A) and the relative change before and after the fatigue protocol (B). A significant interaction effect ($p = 0.015$) was observed as control participants significantly decreased resting twitch amplitude with fatigue. Resting twitch torque significantly decreased for both the stroke participants ($p < 0.01$) and controls ($p < 0.001$) (A). Controls had a significantly greater normalized decrease ($p < 0.01$) in resting twitch torque compared to the stroke participants (B).

2.3.4 Femoral Artery Blood Flow

There was a significant main effect of normalized blood flow with fatigue cycle, $F(1,15) = 24.385$, $p < 0.001$, as blood flow increased in both groups with fatigue (Figure 2.5). There was also a significant main effect of group, $F(1,15) = 40.086$, $p < 0.001$, as blood flow through the femoral artery was greater for the control limb compared to the paretic limb. No significant interaction effect (group*cycle) was observed, $F(1,15) =$

1.739, $p = 0.207$. Overall lower levels of normalized blood flow were observed in the stroke group, but blood flow increased with fatigue regardless of group.

Because the normalized blood flow only applied to 17 of the participants (one control and one individual with stroke did not partake in body composition analysis), the absolute magnitude (non-normalized) was also calculated so that all participants are included (Figure 2.5). Similar results were obtained for the absolute blood flow through the femoral artery in comparison to the normalized blood flow. A significant main effect of fatigue cycle, $F(1,17) = 11.570$, $p = 0.003$, and group, $F(1,17) = 11.385$, $p = 0.004$, was observed. There was no interaction effect, $F(1,17) = 1.060$, $p = 0.318$. The data shows that regardless of group there was an increase in blood flow, but the blood flow response magnitude was greater for controls.

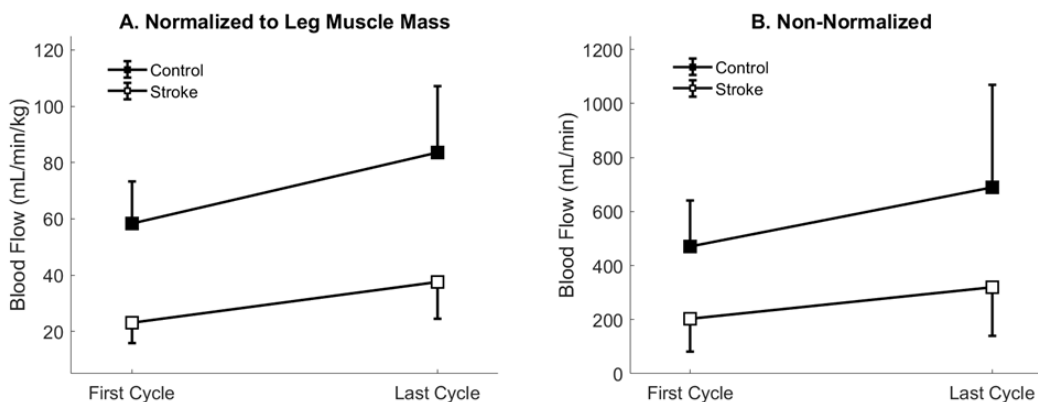


Figure 2.5. Blood Flow through the femoral artery. Blood flow normalized to leg muscle mass (left) and absolute magnitude (right) comparing the first and last cycles. Main effects of limb and fatigue cyler were observed in both cases as both groups significantly increased blood flow with fatigue and the control participants had a greater magnitude of blood flow than the individuals with stroke.

Regression analysis showed that changes in blood flow significantly correlated with task duration for the control group ($r^2 = 0.574$, $F(1,7) = 9.450$, $p = 0.018$, $\beta = 0.141$) as greater increases in blood flow related to longer task duration (Figure 2.6). Blood flow and task duration did not correlate for the stroke group ($r^2 = 0.010$, $F(1,8) = 0.079$, $p = 0.786$, $\beta = 0.031$).

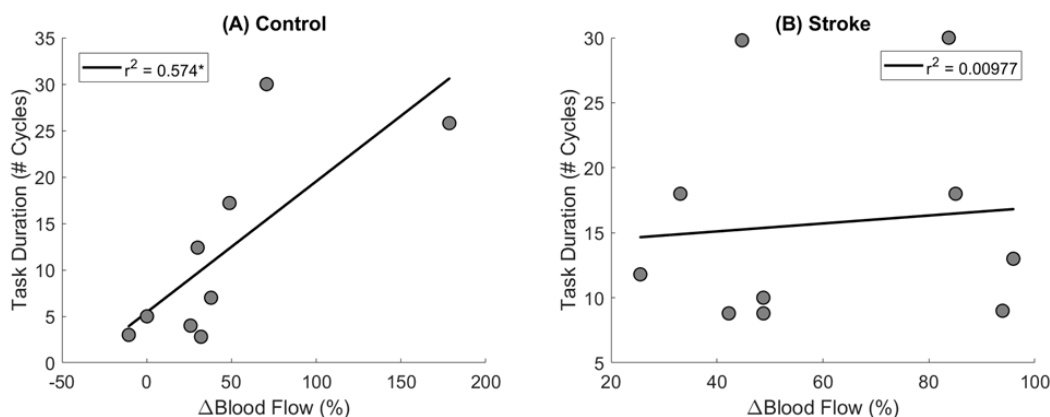


Figure 2.6. Changes in blood flow and task duration. Changes in blood flow significantly correlated with task duration for the control group ($p = 0.018$) (A) but not the stroke group ($p = 0.786$) (B).

Blood flow after the first fatigue cycle and MVC torque generation significantly correlated together for both control ($r^2 = 0.506$, $F(1,7) = 7.170$, $p = 0.030$, $\beta = 2.300$) and stroke participants ($r^2 = 0.782$, $F(1,8) = 28.600$, $p < 0.001$, $\beta = 3.375$) (Figure 2.7), showing that stronger individuals produced larger post-contraction blood flow responses. Changes in blood flow were not significantly correlated with changes in MVC torque generation for stroke ($r^2 = 0.003$, $F(1,8) = 0.020$, $p = 0.890$, $\beta = -0.020$) or control groups ($r^2 = 0.035$, $F(1,7) = 0.257$, $p = 0.628$, $\beta = 0.034$).

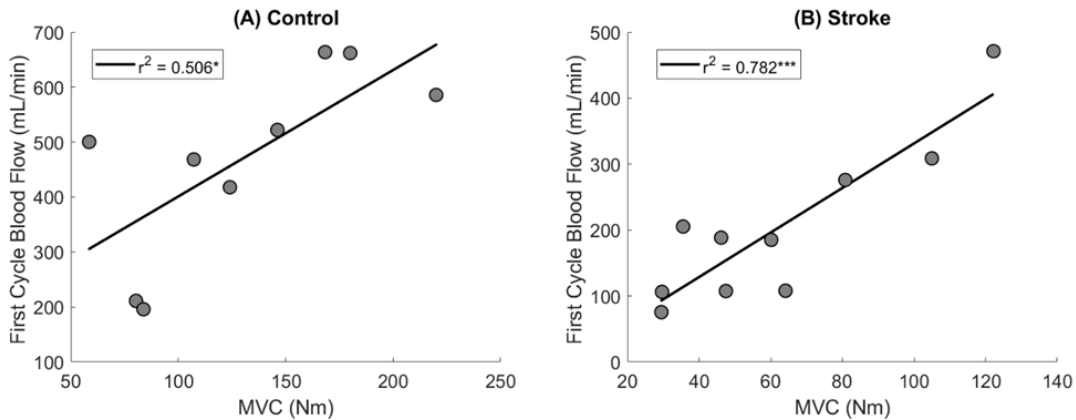


Figure 2.7. MVC and Blood Flow after the First Cycle. Higher magnitudes of blood flow were observed for stronger individuals in both control ($p = 0.030$) (A) and stroke groups ($p < 0.001$) (B).

2.3.5 Motor Unit Firing Rates

A total of 186 motor units for the control limb (102 First Cycle, 84 Last Cycle), and 145 motor units for the participants with stroke (86 First Cycle, 59 Last Cycle) were accepted for data processing (totaling 331 motor units). When comparing the mean motor unit firing rates for the individual participants, a significant interaction effect occurred (group*cycle), $F(1,14) = 10.336$, $p = 0.006$, as there was a greater increase in firing rates for the controls as compared to stroke (Figure 2.8). Main effects of group, $F(1,14) = 10.10958$, $p = 0.005$, and cycle, $F(1,14) = 13.487$, $p = 0.003$, were also observed. The mean firing rates of the individual motor units for each group and cycle were: control = 13.29 ± 3.03 Hz; stroke = 10.49 ± 2.69 Hz; first cycle = 11.53 ± 3.18 Hz; last cycle = 12.77 ± 3.11 Hz. Comparisons of the mean motor unit firing rate for the first fatigue cycle showed control motor unit firing rates were significantly greater ($p = 0.039$) than the participants with stroke. The relative change in firing rate was greater for control participants ($14.97 \pm 3.78\%$) compared to the individuals with stroke ($1.99 \pm 11.90\%$), $F(1,14) = 6.572$, $p = 0.023$. In summary, the control limb had higher motor unit firing

rates and greater motor unit rate modulation with fatigue compared to the individuals with stroke.

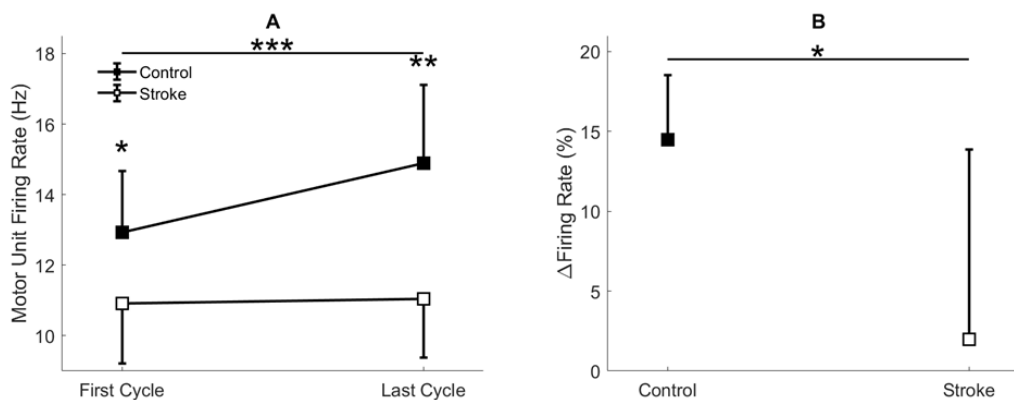


Figure 2.8. Motor unit firing rate. A significant interaction effect was observed ($p = 0.006$) as the control participants significantly increased motor unit firing rates with fatigue cycle. Stroke participants had significantly lower firing rates at the first ($p < 0.05$) and last ($p < 0.01$) fatigue cycles, and only the control group significantly increased firing rates with fatigue ($p < 0.001$) (A). Control participants had a significantly greater increase in normalized firing rates compared to the stroke group ($p < 0.05$) (B).

2.3.6 EMG Root Mean Square (RMS)

There was a significant interaction effect (cycle*group) observed, $F(1,17) = 10.544$, $p = 0.005$, as there was a greater increase in the RMS magnitude in the control participants ($435.32 \pm 302.33 \mu\text{V}$ to $551.95 \pm 353.86 \mu\text{V}$) as compared to individuals with stroke ($244.40 \pm 161.12 \mu\text{V}$ to $279.45 \pm 161.12 \mu\text{V}$). A main effect of fatigue cycle, $F(1,17) = 36.453$, $p < 0.001$, was observed, but there was not a main effect of group, $F(1,17) = 3.887$, $p = 0.065$. The relative increase in EMG RMS was greater in the controls compared to individuals with stroke ($32.42 \pm 17.67\%$ vs $15.97 \pm 9.41\%$), $F(1,17) = 6.609$, $p = 0.020$. In summary, the magnitude and relative change in RMS was greater for the control participants compared to the participants with stroke.

2.3.7 EMG Mean Frequency

There was a main effect of fatigue cycle, $F(1,17) = 45.597$, $p = 0.016$, as the mean frequency decreased (73.32 ± 14.75 Hz to 67.12 ± 14.64 Hz) from the first cycle to last cycle. There was not a main effect of limb, $F(1,17) = 0.331$, $p = 0.573$, but the interaction effect (cycle*group) approached significance, $F(1,17) = 4.267$, $p = 0.054$. There was a significantly greater relative decrease in EMG mean frequency in control compared to individuals with stroke ($-14.87 \pm 11.94\%$ vs $-1.14 \pm 15.61\%$), $F(1,17) = 14.558$, $p = 0.048$. In summary, the decrease in relative change and magnitude in mean EMG frequency was greater for the control participants.

2.3.8 Correlations of Relative Changes in Blood Flow and Motor Unit Firing Rates

Correlations were performed to test if changes in motor unit firing rates track with changes in blood flow from the first fatigue cycle to the last fatigue cycle (Figure 2.9). There was a positive correlation between change in blood flow and change in motor unit firing rates ($r^2 = 0.654$, $F(1,8) = 15.10$, $p = 0.004$, $\beta = 0.362$) for the individuals with stroke, but not for the control group ($r^2 = 0.00242$, $F(1,4) = 0.099$, $p = 0.768$, $\beta = 0.009$). In summary, changes in blood flow had a significant positive correlation for changes in firing rate for the participants with stroke but not for controls, showing that motor unit firing rates tracked with blood flow only for the individuals with stroke.

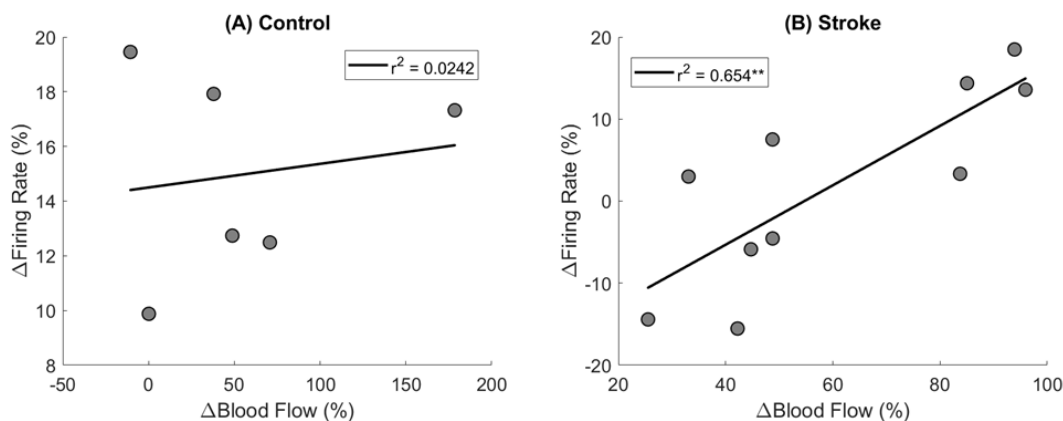


Figure 2.9. Changes in motor unit firing rates and blood flow. Change in motor unit firing rate correlated with changes in blood flow from the first fatigue cycle to the last fatigue cycle for the participants with stroke ($p < 0.01$) (B) but not for controls (A).

2.4 DISCUSSION

To understand the role of muscle perfusion during fatiguing contractions after a stroke, we compared the hyperemic response of healthy controls to individuals with stroke and associated this with differences in motor unit firing rates. The novel findings in this study were: 1) the net magnitude of the blood flow through the femoral artery was blunted for people with stroke during intermittent, fatiguing contractions (Figure 2.5); 2) greater increases in blood flow related to longer task duration for the control group but not the stroke group (Figure 2.6); and 3) changes in motor unit firing rates correlated with changes in blood flow for people with stroke (Figure 2.9). The individuals with stroke did have a lower magnitude of blood flow through the femoral artery, but this did not have as great of impact on peripheral metrics, such as resting twitch torque, compared to controls; furthermore, the positive correlation among changes in motor unit firing rates and blood flow suggests a connection between muscle perfusion and neural inputs to the motoneuron. Thus, despite a decreased hyperemic response in the stroke group, blood flow appears to have a greater impact on peripheral fatigue and task duration for the

control group; however, the association between corticospinal and corticoreticular systems may have a greater influence on blood flow and motor unit firing rates for the stroke group compared to the control group.

2.4.1 Post-stroke differences in hyperemia

Post-contraction hyperemia was greater for controls compared to participants with stroke (Figure 2.5). In addition, stronger torque production resulted in greater hyperemia for both control and stroke groups (Figure 2.7). As was previously shown, an increased blood flow response in the paretic limb positively correlated with limb strength (Durand et al. 2015). Stronger individuals typically have a greater blood flow response, likely because of strength-associated differences in the intramuscular pressure and mechanical compression of the vessels (Barnes 1980; Durand et al. 2015; Hunter et al. 2009). Therefore, it is likely that differences in blood flow magnitude are partially due to strength differences between and within the control and stroke groups.

It is also possible that autonomic dysregulation contributed to the blunted magnitude of the blood flow response in the individuals with stroke. After a stroke, a simultaneous increase in parasympathetic activity and decrease in sympathetic activity has been observed during Ewing's battery assessment and during continuous monitoring of heart rate variability, blood pressure, and respiration (Dütsch et al. 2007; Xiong et al. 2014). This may increase peripheral vasoconstriction, lowering the blood flow magnitude in the stroke group compared to the control group.

2.4.2 Post-stroke blood flow deficits do not relate to metrics of peripheral fatigue or task duration

Healthy individuals and people with stroke had similar relative declines in MVC torque and similar time to task failure, indicating that both groups reached a similar degree of neuromuscular fatigue at task failure; however, differences in the degree of central fatigue for the stroke group compared to the degree of peripheral fatigue for the control group showed different mechanisms of neuromuscular fatigue. The control group had greater changes within the muscle fibers (peripheral fatigue) as indicated by greater decreases in resting twitch torque (Figure 2.4) and greater compression of the EMG spectrum compared to the stroke group (De Luca 1984; Knorr et al. 2011; Merletti et al. 1990; Riley and Bilodeau 2002). Individuals with stroke, however, showed greater decreases in voluntary activation (Figure 2.3), less increase in EMG RMS, and less motor unit rate modulation (Figure 2.8) compared to the controls. These metrics indicate some combination of decreases from descending motor command and excitatory afferent inputs, as well as increases from inhibitory afferent inputs, to the motoneuron (Bowden et al. 2014; Gandevia 2001; Knorr et al. 2011; McManus et al. 2017; Riley and Bilodeau 2002). We also observed that greater increases in blood flow correlated with longer task duration only for the control group (Figure 2.6). Thus, the differences in metrics of central and peripheral fatigue may explain why blood flow did not have a greater disturbance to muscle contractile properties for the participants with stroke.

Controls had a much greater reduction in metrics of peripheral fatigue regardless of the much greater magnitude of post-contraction blood flow. Although blood flow increased for both groups, changes in blood flow related to task duration only for the control group. The accumulation of metabolic byproducts, such as extracellular K^+/Ca^{2+}

from a slowed sarcoplasmic reticulum uptake and H^+ from lactic acid (Fitts 2011b; Kent-Braun et al. 2012), has a debilitating effect on muscle contractile properties and conduction velocity (Kupa et al. 1995; Tesch et al. 1983). This was reflected in lower post-fatigue twitch amplitudes (Kent-Braun et al. 2012) and compression of the EMG power spectrum (De Luca 1984) for the control group but not the stroke group. This aligned with previous fatigue studies that involved sustained contractions; however, those studies did not associate these metrics with metabolite accumulation and perfusion (Bowden et al. 2014; Fimland et al. 2011; Knorr et al. 2011; McComas et al. 1973; McManus et al. 2017; Riley and Bilodeau 2002). We were able to study the effects of blood flow on muscle fiber properties because the intermittent task (as opposed to a sustained task) involves a perfusion-dependent mechanism – greater perfusion results in reduced metabolic accumulation (Sadamoto et al. 1983). This was evident for the controls as participants with greater blood flow had longer task duration. Regression analysis showed that greater blood flow did not correlate with task duration for the stroke group. The differing effects of blood flow on metrics of peripheral fatigue and task duration suggest that the influence of post-contraction hyperemia was not the same for controls and participants with stroke.

It appears the individuals with stroke were inhibited by central fatigue before blood flow was a factor in muscle force generation. One might expect the greater perfusion to result in a greater clearance of metabolites (Sadamoto et al. 1983) and greater fatigue resistance; however, that was not the case for the stroke group in this study (Figure 2.6). Even with an expected exercise-induced metabolic buildup (Landin et al. 1977) and the much lower hyperemic response for the stroke group, lack of blood flow

does not cause the fatigue. Like previous studies, voluntary activation was significantly reduced at task failure (Figure 2.3) (Bowden et al. 2014; Knorr et al. 2011; Newham et al. 1995; Riley and Bilodeau 2002). The decreased voluntary activation assumes a decreased neural drive to the muscle (Allen et al. 1995; Shield and Zhou 2004). This is likely facilitated by a loss of excitatory drive from the descending motor pathways after the stroke lesion (Jang et al. 2017; Murase et al. 2004). The reduced voluntary activation not only reflects a reduction in the integrity of the corticospinal tract, but also explains a portion of the post-stroke impairments in the firing rate magnitude and rate modulation (Figure 2.8) manifested in the reduced EMG (Gemperline et al. 1995). It is likely that the effects of deficient blood flow on muscle fiber properties and task duration were not observed because of the dominant central factors contributing to neuromuscular fatigue.

2.4.3 Motor unit firing rates correlated with blood flow changes after stroke

We saw that changes in blood flow correlated with motor unit firing rate modulation in the stroke group. Motor unit firing rates increased in all control participants with fatigue; however, motor unit firing rates decreased in magnitude in 4/10 stroke participants. These 4 individuals also had lower changes in blood flow compared to those with greater rate modulation (Figure 2.9B). A possible explanation for the positive correlations observed for the stroke group but not the control group may be that the stroke lesion disrupted the common drive to the corticospinal and corticoreticular tracts (Brownstone and Chopek 2018; Buford and Davidson 2004; Herbert et al. 2015). Because corticoreticular projections originate from common areas as the corticospinal projections (primarily from the primary motor cortex and premotor cortical areas),

disruptions of these common areas after a stroke likely have implications on autonomic control of blood flow from the reticular system and activation of the motoneuron pools through the corticospinal system. In animal models with decerebration or ischemic cortical lesions, inhibitory inputs from corticobulbar pathways to the reticular formation are lost, causing a greater relative increase in reticulospinal influence and a concurrent relative decrease in corticospinal influence (Herbert et al. 2015; Hounsgaard et al. 1988). This is thought to be the case in human stroke as there is evidence of increased activity in the reticulospinal pathways, possibly from the disinhibition of the reticular formation, and a loss of corticospinal input (Foltys et al. 2003b; Jang et al. 2017; Kline et al. 2007; McPherson et al. 2018; McPherson et al. 2008; Murphy et al. 2015). The decreased post-contraction blood flow through the femoral artery in this study may indicate increased autonomic drive, possibly caused by a disinhibited reticular drive providing an excessive sympathetic outflow. The reticular system is known to modulate autonomic outflow and is a source for the vasoconstrictor norepinephrine (Nette et al. 2006; Schwarz et al. 2015). The positive correlation between the hyperemic response and motor unit firing rate modulation is likely a result of the damage to these common pathways – controls and individuals with stroke that had less damage to these common pathways likely had greater modulation of motor unit firing rates and voluntary activation, as well as greater inhibition to the sympathetic outflow from the reticular formation.

An alternative explanation for the positive correlation between blood flow and motor unit modulation (Figure 2.9B) is that the decreased blood flow for the individuals with stroke may have an inhibitory effect on the motoneuron pool. Motor unit firing rates may be associated with blood flow because metabolic accumulation activates group

III/IV afferent pathways, and these pathways are known to have an inhibitory effect on the motoneuron pool during fatiguing exercise (Amann 2012; Amann et al. 2008; Taylor et al. 2016). The inhibitory effects of ischemia on motor unit output may also be enhanced because these pathways may be hyper-excitabile after a stroke (Hidler and Schmit 2004; Li 2017); therefore, not only may group III/IV pathways be hyperexcitable and inhibit motoneuron output after stroke, blood flow may be attenuated because of excitability from the brainstem. The lack of motor unit modulation and inability to significantly increase EMG RMS may partly be due to enhanced inhibitory afferent input from group III/IV pathways. Though it is possible these afferents were activated in the control group, central factors were not significantly affected before peripheral fatigue was a factor. Enhanced group III/IV pathways may also explain why changes in motor unit firing rates significantly correlated with changes in blood flow for the stroke group but not the control group. Thus, it is plausible that the stroke-related deficiencies in the peripheral blood flow to the exercising muscle and a change in the excitability of the group III/IV afferent pathways may enhance the inhibitory response to ischemia, restricting motor unit firing rates and modulation.

2.4.4 Implications for motor performance

This study emphasized some points that should be considered to optimize motor recovery. The intermittent contractions, as opposed to sustained, showed the effects of perfusion on motor performance after a stroke. This provides insight into functional motor performance because many activities of daily living, such as walking, consist of intermittent contractions. Currently, stroke rehabilitation strategies consider

cardiovascular fitness and limb strength as separate issues. This study showed that stronger individuals with stroke also have greater blood flow responses to exercise (Figure 2.7). It seems logical that improving the hyperemic response to exercise would help improve motor performance, but the data from this study would suggest that neural issues are the limiting factor to force generation during fatiguing exercise. It appears that improving neural function should remain the primary focus for rehabilitation strategies; however, inhibitory afferent pathways are activated in response to reduced perfusion. Blood flows indirect contributions to the neural afferent inputs should not be overlooked when evaluating motor performance after a stroke. The evidence of increased reticulospinal influence together with the loss of corticospinal influence suggests that these two systems may be an undeveloped method for recovery. It is also possible that as neural function improves, perfusion to the muscle becomes more important. It has been shown that the hyperemic response to non-fatiguing muscle contractions has a positive relationship to limb function (Durand et al. 2015). This data allows us to speculate that improving the hyperemic response to exercise could optimize motor recovery.

2.4.5 Conclusion

This study quantifies the association between blood flow and motor unit firing behavior that play a role in the inability for participants with stroke to volitionally control the lower limbs. These results align with other studies that central fatigue is a greater limiting factor over peripheral factors for torque generation by the paretic leg of chronic stroke survivors (Bowden et al. 2014; Hu et al. 2006; Hyngstrom et al. 2012; Klein et al. 2010; Knorr et al. 2011; Kuhnen et al. 2015; McManus et al. 2017; Rybar et al. 2014b).

This study was unique in that it examined the effects of the hyperemic response to exercise during intermittent, fatiguing contractions of the knee extensor muscles. A combination of the central factors (decreased voluntary activation, motor unit firing rates, and RMS EMG) may have caused early cessation of the fatigue task before deficient peripheral blood flow played a factor in muscle contractile properties and task duration; however, the loss of common pathways between the reticular system and spinal motoneurons may explain the systemic loss of both blood flow and motor unit rate modulation in some of the stroke participants. It may also be that the lower hyperemic response may have been responsible for ischemic conditions that activated inhibitory afferent input from group III/IV pathways that decreased output from the paretic motoneurons. This study merits further investigation to the effects of ischemia on paretic motor unit firing rates.

CHAPTER 3: STROKE INCREASES ISCHEMIA-RELATED DECREASES IN MOTOR UNIT DISCHARGE RATES

3.1 INTRODUCTION

The purpose of this study was to quantify the inhibitory effects of transient ischemia via whole limb blood flow occlusion on paretic motor units to further understand potential neural mechanisms of force generating impairments during exercise in chronic stroke survivors. The firing behavior of motoneurons resulting in muscle activation is due to a combination of excitatory and inhibitory synaptic inputs and baseline intrinsic excitability of the motoneuron pool (Heckman and Enoka 2012). Following stroke, baseline impairments in the nervous system's ability to activate paretic motoneuron pools and muscles limits force generation. Several studies have documented stroke-related changes in paretic motor unit rate coding and recruitment (Chang et al. 2013; Chou et al. 2013; Gemperline et al. 1995; Li et al. 2014; McNulty et al. 2014; Mottram et al. 2014; Pollock et al. 2014) are the two key neural strategies to grade force. During brief submaximal contractions, paretic motor unit firing rates have a compressed range compared with individuals without stroke, especially at higher force (Chou et al. 2013). In addition, recent studies have shown decreased ability to increase the magnitude of paretic global surface EMG during sub-maximal fatiguing contractions (Rybar et al. 2014a). Not surprisingly, given the primary pathology in the motor cortex, electrophysiological studies using transcranial magnetic stimulation have demonstrated decreased excitability in descending motor pathways post stroke (Foltys et al. 2003a; Jang et al. 2017; Peters et al. 2017; Schwerin et al. 2008). However, motoneurons receive other synaptic inputs that can shape motor output (Heckman and Enoka 2012). For

example, little is known on how inhibitory spinal pathways, such as the group III/IV pathways, may contribute to impaired motor unit firing behavior and muscle activation during exercise post stroke.

Group III/IV receptors are sensitive to muscle ischemia and compression associated with muscle contractions (Matthews 1972). In individuals without stroke and evidence from animal models, the group III/IV pathways are known to have an inhibitory effect on motor output by limiting muscle activation, force generation, and during both single limb and whole body fatiguing exercise potentially decreasing voluntary drive (central fatigue) (Taylor et al. 2016). In other neurological conditions, such as spinal cord injury, this pathway is hyperexcitable, (Schmit et al. 2002; Schmit et al. 2003; Theiss et al. 2011; Wu et al. 2006) presumably due to decreased regulation by supraspinal centers. Understanding how activation of this pathway impacts motor output post stroke is important as it may exacerbate baseline impairments in motor unit firing behavior and muscle activation, thus further limiting force generating capabilities.

The inhibitory effects of ischemia on motor output may be enhanced post stroke due to impaired blood flow to the paretic muscle. Several studies showed that individuals with stroke have impaired peripheral large and small conduit regulation of blood flow. First, resting blood flow in the femoral artery is lower in the paretic leg (Billinger et al. 2009; Sherk et al. 2015) and there is an impaired flow mediated dilation response compared with the non-paretic leg and with individuals without stroke even when normalized to muscle mass and strength (Durand et al. 2015; Ivey et al. 2004). Moreover, during volitional contractions, the hyperemic response to contractions at various load levels is blunted compared to those without stroke (Durand et al. 2015). Important to

function, the paretic leg hyperemic response to volitional contractions has been shown to be positively correlated with clinical measures of function (Durand et al. 2015). In summary, these studies indicate that there is impaired blood flow to resting and exercising muscles in the paretic leg that leads to an increased accumulation of metabolic byproducts and activation of group III/IV pathways compared with individuals without stroke.

In addition to impaired blood flow to exercising paretic muscle, the excitability of the group III/IV pathways may be increased post stroke, as seen with the group Ia afferents and resultant spasticity (Li 2017). Hidler and Schmit demonstrated experimentally and with computational modeling that group III/IV pathways contributed more than group Ib or Ia pathways to reflex force inhibition of the paretic elbow flexors (Hidler and Schmit 2004). Others have shown increased stroke-related reflex responses through cold and pain stimuli and increased central hypersensitivity in pain pathways (Soo Hoo et al. 2013). The inhibitory impact of group III/IV activity on motor output is seen in other patient populations, such as congestive heart failure (Amann et al. 2014), and motor performance is improved in healthy individuals when mechanosensitive group III/IV pathways are pharmacologically blocked (Amann et al. 2011).

Thus, it is plausible that the stroke-related changes in the regulation of peripheral blood flow to exercising muscle and a change in the excitability of the group III/IV spinal pathways may enhance the inhibitory response to ischemia, limiting motor unit firing behavior. Here we quantified the effects of whole leg ischemia on paretic vastus lateralis motor unit firing rates during sub-maximal isometric contractions. We hypothesized that in response to ischemia, knee extensor paretic motor unit firing rates would decrease to a

larger extent than those without stroke. Secondary measures of maximal voluntary contraction and resting twitch responses were made to provide mechanistic insights.

3.2 MATERIALS AND METHODS

3.2.1 Participants

All participants gave informed consent before participation in the study, and procedures were approved by the Medical College of Wisconsin Institutional Review Board (PRO190103). Ten participants with chronic hemiparetic stroke (8 male, 2 female, 58.9 ± 9.4 years) and ten age matched neurologically intact participants (8 male, 2 female, 60.2 ± 9.5 years) participated in the study. Stroke participant inclusion criteria were: single, unilateral stroke (obtained through verbal communication from the physician and consistent with neurological physical examination); able to ambulate at least 30 feet (with or without an assistive device); ≥ 6 months post stroke. Stroke participant exclusion criteria included: brainstem stroke; any uncontrolled medical condition; contractures of any lower extremity joints; inability to follow 2-3 step commands. Table 1 reports the participant characteristics.

Subject	Age	Years Since Stroke	Fugl-Meyer (LE)
1	64	12	18
2	65	11	24
3	68	13	21
4	60	15	25
5	65	17	28
6	58	3	31
7	61	24	34
8	37	12	27
9	52	11	17
10	68	34	22

Table 3.1. Characteristics of all individuals with stroke.

3.2.2 Torque Measurements

Knee extension torque measurements were made using a Biodex dynamometer (Biodex Medical System, Shirley, NY). Participants sat on a Biodex chair with their knee flexed to 90° and the leg securely attached to the Biodex attachment 2 cm above the lateral malleolus. The torque was measured using the Biodex load cell (force-torque transducer), sampled at 2048 Hz, acquired by an EMG-USB2+ amplifier (256-channel regular plus 16-auxiliary channels, OT Bioelettronica, Turin, Italy), and recorded using the OT Biolab software.

3.2.3 Surface EMG Recordings

Surface electromyograms (EMGs) were obtained using a 64 channel 2-D electrode array (13 rows, 5 columns). A double-sided adhesive sticker designed for and compatible with the array was placed over the array. The holes within the adhesive sticker were filled with a conductive electrode paste (Ten20, Weaver and Company, Aurora, Co). The array was placed over the belly of the vastus lateralis, midway between the patella and the greater trochanter, after sterilizing the participant's skin with an

alcohol swab and rubbing to remove superficial dead skin. The signals for each channel were differentially amplified between 1000 and 5000 V/V (participant dependent) and band-pass filtered between 10 and 500 Hz using the EMG-USB2+ amplifier. The signals were sampled at 2048 Hz and acquired with the OT Biolab software throughout the duration of the experimental protocol.

3.2.4 Near-Infrared Spectroscopy Measurements

Near-Infrared Spectroscopy (NIRS) measurements were obtained using a SenSmart Universal Oximetry System (Nonin Medical Inc., Plymouth, MN). Near-infrared-light was used to measure the regional skeletal muscle tissue oxygen saturation (rSO₂). Receiving optodes were placed over the rectus femoris of the test leg. The signals were sampled at 2 Hz and collected by the embedded software of the device. Continuous baseline measurements were taken with the participant sitting still and upright in the Biodex chair for 5 min prior to onset of any experimental procedures. To control for inter-participant variability, the NIRS measurements were normalized to the mean of the baseline period and collected throughout the experimental protocol.

3.2.5 Experimental Protocol

All control participants performed the protocol with their right leg, and all individuals with stroke performed the protocol with the paretic leg. Figure 1 illustrates the timeline of the protocol. First, each participant performed at least five baseline maximum voluntary contractions (MVC) of the knee extensor muscles with 1 min of rest between trials. The peak force of all the trials was used as the MVC. Participants were

given verbal and visual feedback. After at least a 5-min rest period following the final MVC, participants performed a sub-maximal isometric ramp and hold torque tracking protocol. For the ramp and hold protocol, the participants were instructed to trace a trapezoid trajectory displayed on a computer screen by contracting their knee extensor muscles to generate torque. Real-time visual feedback was provided to the participant indicating the torque produced by the knee extensor muscles. The trapezoid was 18 s in duration consisting of a 4s rising phase from rest, a 10s hold phase at 20% MVC, and a 4s decline phase back to rest. For each ramp and hold trial, one trapezoid contraction was repeated six times with a 1-min resting period between trials. After at least a 5-min break, a second protocol of both MVCs and ramp and holds was performed while occluding blood flow. A blood pressure cuff designed for the leg was inflated to 225 mmHg over the upper thigh of the test leg to transiently occlude blood flow to the test leg. The cuff remained inflated throughout the six isometric knee extension contractions (Figure 3.1). We chose to fully occlude blood flow for a brief period of time to elicit a maximal response without injury. During the protocol with repeated MVCs only, after each MVC, a constant current generator (DS7A, Digitimer, Welwyn, Wales) delivered a rectangular pulse of 100 μ s duration with maximum amplitude of 400 V, which was used to percutaneously stimulate the quadriceps muscle. The stimulation intensity (usually 200 mA to 500 mA) was set at 20% above the level required to produce a maximal resting twitch amplitude that caused a supramaximal stimulation.

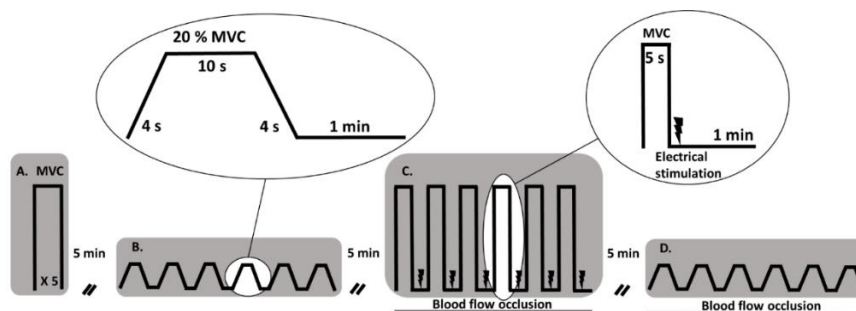


Figure 3.1. Experimental protocol. A) 3-5 baseline maximum voluntary contractions (MVC) with the knee extensors with a one-minute rest between contractions. B) 6 “ramp and hold” isometric knee extensor contractions, at 20% MVC, with a one-minute rest between cycles. C) 6 MVCs with a one-minute rest between MVCs while the test leg was occluded. After each MVC when the muscle was fully relaxed, electrical stimulation was applied to the quadriceps to elicit a resting twitch response. D) The “ramp and hold” protocol during whole leg occlusion. A five-minute break was provided between each separate part of the protocol. NIRS and sEMG of the quadriceps muscle were recorded throughout the experiment.

3.2.6 Data processing

Torque

Torque signals were zero phased low-pass filtered at 15 Hz using a 2nd order Butterworth filter prior to analysis and processed using Matlab (MathWorks, Natick, MA). Peak torque was calculated for each MVC and elicited resting twitch. In addition, time from the peak amplitude of the twitch to a drop in 75% amplitude was determined to quantify relaxation rates for the resting twitches.

Motor Unit Decomposition

The 64 (63 after differential amplification) individual EMG channels were visually examined to remove noisy channels. The remaining channels were decomposed to attain information of single motor unit action potential trains using a multichannel convolutive blind source separation algorithm previously described and validated by Negro et al (2016). To provide a normalized index of reliability similar to the pulse to

noise ratio, a silhouette measure (SIL) was computed on each estimated source, and the source was considered of acceptable quality if SIL was greater than 0.90. SIL provides a measure of the quality of the extracted motor unit spike trains based on the relative amplitude of the deconvolved spikes compared to the baseline noise. Of the units with $SIL > 0.90$, we then calculated the 2D correlation between MUAP shapes of tracked units in different contractions and found cross-correlation values >0.85 . Because we wanted to examine motor units that were likely continuously contributing to force generation, an identified motor unit was excluded for further analysis if its firing rate (pulses per second – pps, Hz) was less than 5 Hz. A total of 75 units were accepted for the control group and 37 for the stroke group. The motor unit action potential timings were time-locked with the torque trace (Figure 3.2). The firing instances for each motor unit were lowpass filtered with a unit area Hanning window of 1-s duration. Motor units were identified applying the decomposition algorithm on six individual ramp and hold trials. The trials were concatenated from the original recordings with a resting segment of four seconds between each ramp and hold trial. Under the assumption of stable motor unit action potential properties, this configuration and similar approaches provided the possibility to reliably identify the same motor units in different trials (Martinez-Valdes et al. 2017b); however, here units were only tracked within a given protocol and not between the occlusion and non-occlusion protocols.

The instantaneous firing rates of individual motor units were calculated as the inverse of the inter-spike interval. The firing rate at recruitment and derecruitment were defined as the mean of the first and last three inter-spike intervals. Motor unit recruitment and derecruitment thresholds were determined as the torque (normalized to MVC) for the

first and last discharge time for each motor unit, respectively. The mean firing rates during the hold phase of the ramp and hold contractions, de/recruitment firing rates, and de/recruitment thresholds, were compared for the first contraction a motor unit continuously fired with the final contraction that a motor unit continuously fired.

Global Surface EMG RMS Measurements

The EMG root mean square (RMS) for each channel of the HDsEMG array was calculated during the 10s hold phase for each contraction

($RMS = \sqrt{\frac{1}{N} \sum_{n=1}^N x_n^2}$, $n = \text{data point}$, $N = \text{total data points}$). The global surface

EMG RMS was calculated as the mean RMS of all channels for each contraction.

Regional muscle oxygen saturation

To determine relative levels of oxygen saturation within the quadriceps muscle, NIRS measurements of local oxygen saturation within the rectus femoris were determined before the beginning of each contraction by averaging the NIRS values during the 2-s interval before the ramp and hold contraction. During the occlusion protocol, the coefficients (with 95% confidence bounds) to model the exponential decay of O₂ saturation were determined using Matlab's Curve Fitting Toolbox. The time constant ($\tau = \frac{1}{\lambda}$) of the exponential decay model ($N = N_0 e^{-\lambda t}$) was determined and the population means for both stroke (N = 10) and control (N = 10) participants were compared.

A linear regression modeled the relation between the change in firing rate and the change in O₂ during the occlusion protocol. This was accomplished using firing rate during the last contraction a motor unit fired as a percent of the first contraction that a motor unit fired versus the change in O₂ saturation over the entire 20% MVC ramp and

hold occlusion protocol. The slope of the regressions was calculated, and the mean of the linear regression slopes was compared between stroke and controls.

3.2.7 Statistical Analysis

We performed separate repeated measures, mixed model ANOVAs on the following dependent variables for the occlusion and non-occlusion conditions: firing rate during the hold phase, recruitment firing rate, derecruitment firing rate, recruitment threshold, derecruitment threshold, and mean global surface EMG. The between group variables were GROUP (paretic and control). CONTRACTION (first contraction and last contraction) was the within group comparison. A Bonferroni correction was used in all post hoc testing and only performed when an interaction effect between CONTRACTION and GROUP was present. Separate two sample t-tests were used to detect the difference between stroke and control participants for the exponential decay time constant and the mean slope value for the linear regression for change in firing rate per change in muscle O₂ saturation. All statistical tests were performed using an alpha level of 0.05 for significance. Data are reported as the mean \pm standard deviation.

3.3 RESULTS

3.3.1 Mean Firing Rates

During the occlusion condition, there was a significant main effect of contraction as firing rates were lower for the final contraction (7.89 ± 1.93 pps) compared to baseline (8.24 ± 1.99 pps, $p < 0.001$). There was also a main effect of GROUP on motor unit firing

rate ($p = 0.02$). Stroke (7.49 ± 2.36 pps) had lower mean firing rates compared with control participants (8.35 ± 1.67 pps, $p = 0.02$). There was a significant interaction effect between contraction and group in which the paretic leg had a larger decrease in firing rates as compared to controls ($p < 0.001$, Figure 3.2 single participant example, Figure 3.3 group). *Post hoc* pairwise comparisons revealed a significant decrease ($p < 0.001$) in stroke motor unit firing rates between the baseline contraction and the final contraction during occlusion, but there was no significant difference ($p = 0.72$) for control motor unit firing rates between baseline and final contractions (Figure 3.3). This equates to an average $12.32 \pm 9.99\%$ decrease in firing rates for stroke (final contraction vs first contraction) and $0.12 \pm 12.42\%$ increase in firing rate for control participants. There was also a significant difference in firing rates between the paretic and control legs in the final contraction ($p < 0.001$), but not for the first contraction ($p = 0.52$) (Figure 3.3). Thus, for sub-maximal contractions with similar relative efforts, both groups had similar firing rates at baseline, but paretic motor unit firing rates decreased to a larger degree compared to the controls with occlusion. Finally, with stroke and control data combined, the percent decline in firing rates was positively correlated with net torque generated ($r^2 = 0.262$, $p = 0.030$). Whereby, weaker individuals had a greater decrease in relative firing rate. There was a trend towards a positive correlation between the change in firing rate and the change in MVC, in the individuals with stroke, but it was not significant ($r^2 = 0.325$, $p = 0.085$).

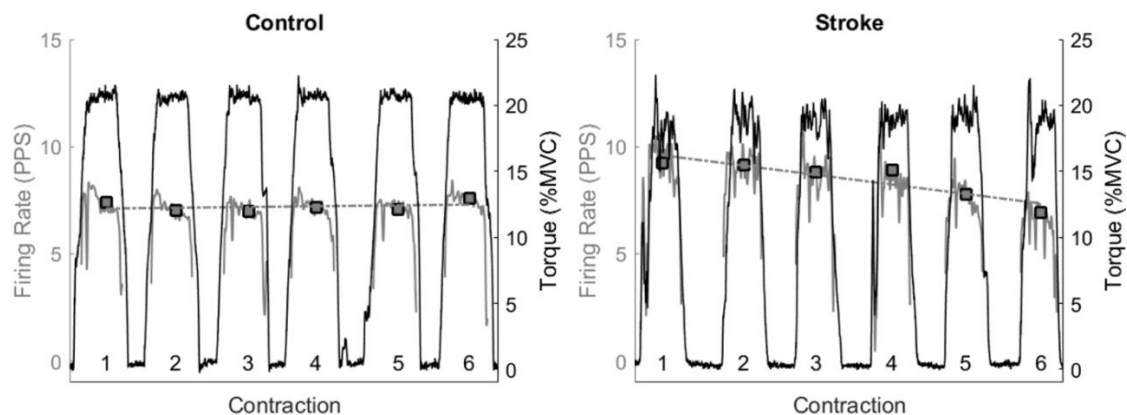


Figure 3.2. Single participant examples of individual motor unit firing rates during the occlusion protocol. The gray trace shows the filtered firing rates using a 1000 ms Hanning window. The bold squares represent the average firing rate of the motor unit for the ramp and hold cycle. A linear fit of the average firing rates for each cycle is represented using the dashed gray line. The black trace represents the torque. Consistent with the group effect, note the greater decline in motor unit firing rates (gray trace) for the individual with stroke as compared to the control example.

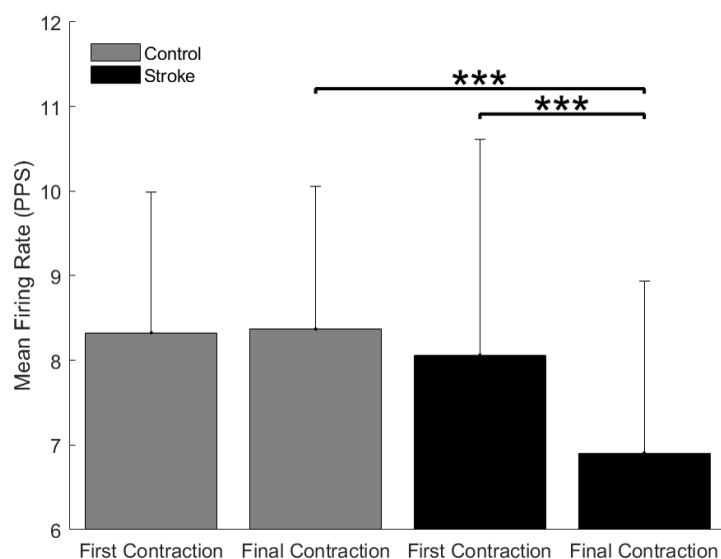


Figure 3.3. Mean firing rates during the 20% ramp and hold occlusion protocol for the stroke and control participants. Individuals with stroke had a larger decline in firing rates as compared to controls (contraction *group effect, $p < 0.001$).

In the condition without occlusion, there was no statistical differences for: group (stroke: 8.24 ± 1.64 pps; control: 8.64 ± 2.09 pps; $p = 0.40$), contraction (baseline: 8.44 ± 2.05 pps; final: 8.55 ± 1.89 pps; $p = 0.24$), and contraction * group interaction ($p = 0.98$). In summary, stroke and control motor unit firing behavior was not statistically different during the no occlusion condition. On an individual level, 7/10 individuals with stroke had lower mean firing rates (<8 pps) compared with 2/8 controls. In addition, 8/10 individuals with stroke had absolute torque recruitment thresholds less than 20 vs 4/8 controls.

3.3.2 Recruitment Threshold

During the occlusion condition, there was no significant contraction effect (baseline = 11.76 ± 5.79 %MVC vs final cycle = 11.04 ± 5.28 %MVC, $p = 0.09$). There was not a significant main effect of group ($p = 0.87$) for motor unit recruitment thresholds (control = 11.44 ± 5.49 % MVC vs. paretic = 11.31 ± 5.69 %MVC. There was also no interaction effect of contraction and group ($p = 0.97$). These results suggest the same pool of units were recruited. In 23/37 units from the stroke group, the recruitment threshold decreased from the first to last contraction and in 13/37 units the recruitment threshold increased. Within the occlusion trials, there appears to be a trend toward an increase in recruitment threshold when comparing the first and last contractions.

In the no occlusion condition, control motor unit recruitment thresholds (11.42 ± 4.35 %MVC) were not statistically different from the paretic (10.83 ± 5.63 % MVC) motor unit recruitment thresholds (main effect of GROUP: $p = 0.87$). There was no main effect of contraction ($p = 0.19$) (Baseline = 10.98 ± 5.33 %MVC vs. Final 11.41 ± 4.37

%MVC) cycles. There was also no significant interaction effect of contraction and group ($p = 0.17$). The range of recruitment thresholds was compressed in individuals with stroke versus control for the first contraction (stroke = 39.99%MVC; control = 57.11%MVC) and the last contraction (stroke = 43.19 %MVC; control = 50.97 %MVC).

3.3.3 Recruitment Firing Rates

During occlusion, there was a significant main effect of contraction for recruitment firing rates as firing rates decreased in the final cycle (6.96 ± 1.85 pps) compared to the baseline cycle (7.45 ± 2.05 pps, $p = 0.001$). There was no main effect of group (stroke = 6.79 ± 2.16 pps vs control 7.40 ± 1.83 pps, $p = 0.08$) and no significant interaction effect between contraction and GROUP ($p = 0.16$).

During the condition without occlusion, there was a significant main effect of group as control recruitment firing rates (7.95 ± 2.09 pps) were higher than individuals with stroke (6.73 ± 1.79 pps, $p = 0.009$), but there was no main effect of contraction ($p = 0.62$) on recruitment firing rates as baseline (7.53 ± 2.20 pps) and final (7.45 ± 1.93 pps) were similar. There was also no significant interaction effect between contraction and group ($p = 0.82$). These results show that when the protocol was performed without occlusion, stroke recruitment firing rates were lower than control motor units, but baseline and final contractions did not affect the recruitment firing for stroke or control motor units.

3.3.4 Derecruitment Threshold

There was no main effect of group between control (13.39 ± 5.06 %MVC) and stroke (13.44 ± 5.56 %MVC, $p = 0.66$) for motor unit derecruitment threshold during occlusion. No main effect of contraction was also observed ($p = 0.57$) because baseline (13.48 ± 5.42 %MVC) was similar to the final (13.34 ± 5.04 %MVC) cycle. There was also no interaction effect of contraction and group ($p = 0.25$).

There was no main effect of group ($p = 0.62$) or contraction ($p = 0.83$) for motor unit derecruitment threshold during the no occlusion condition. Control (13.25 ± 4.09 %MVC) was similar to stroke (13.85 ± 5.05 %MVC) for derecruitment threshold, and derecruitment threshold was similar for baseline (13.69 ± 4.51 %MVC) and final (13.27 ± 4.45 %MVC) cycles. There was also no interaction effect of contraction and group ($p = 0.10$).

3.3.5 Derecruitment Firing Rates

During the occlusion condition, there was a significant main effect of GROUP ($p = 0.004$) where individuals with stroke had lower rates at derecruitment (6.39 ± 2.42 pps) compared to controls (7.10 ± 2.02 pps). There was no significant main effect of contraction ($p = 0.53$) for motor unit derecruitment firing rates where baseline (7.00 ± 2.19 pps) was similar to the final (6.73 ± 2.17 pps) cycle. There was no significant interaction effect of contraction and group ($p = 0.18$).

Likewise, in conditions without occlusion, there was a significant main effect of group ($p = 0.006$) with control (6.98 ± 1.66 pps) derecruitment firing rates higher than stroke (6.56 ± 2.60 pps) derecruitment firing rates. There was not a significant main

effect of contraction ($p = 0.07$) for motor unit derecruitment firing rates (Baseline= 6.65 ± 2.21 pps vs. Final= 6.99 ± 1.90 pps) cycle. There was no significant interaction effect of contraction and group ($p = 0.34$).

3.3.6 Local Muscle Oxygen Saturation

Figure 3.4 shows the fitted exponential decays for each individual participant's local oxygen saturation during occlusion. Individuals with stroke had a greater time constant for exponential decay of local muscle oxygen consumption compared to control participants (22.90 ± 10.26 min vs. 5.46 ± 4.09 min, $p < 0.001$) during ischemia (Figure 3.5). Stroke time constants ranged from 9.2 min to 35.6 min, and control time constants ranged from 0.4 min to 13.3 min. Only two of the control time constants overlapped into the lower range of the stroke time constants. Linear regressions of each motor unit firing rate with the local muscle oxygen saturation yielded an average r^2 value of 0.49 for stroke and 0.41 for control (Figure 3.6); further, the average slope value of the linear regression line was significantly more negative for stroke than for control ($p < 0.001$) (Figure 3.7). At an individual level, the change in firing rate was correlated with the relative change in oxygen saturation ($r^2 = 0.290$, $p = 0.021$). Regression analysis of the group mean firing rate and mean O_2 saturation at each contraction significantly correlated for individuals with stroke ($r^2 = 0.913$, $p = 0.002$, slope = 0.05 PPS/% O_2 sat.) and near significant for controls ($r^2 = 0.587$, $p = 0.076$, slope = 0.01 PPS/% O_2 sat.) (Figure 3.8).

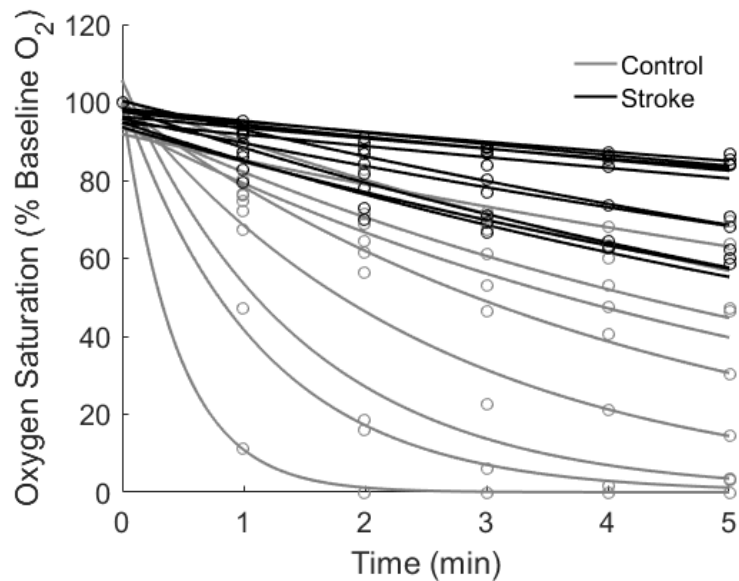


Figure 3.4. Local oxygen saturation of the rectus femoris before the beginning of each ramp and hold contraction at 20% MVC for stroke and control. Minute zero represents the muscle oxygen saturation before the first ramp and hold contraction, and minute five represents the muscle oxygen saturation before the final contraction of the ramp and hold at 20% MVC. A model of exponential decay was fitted to the data.

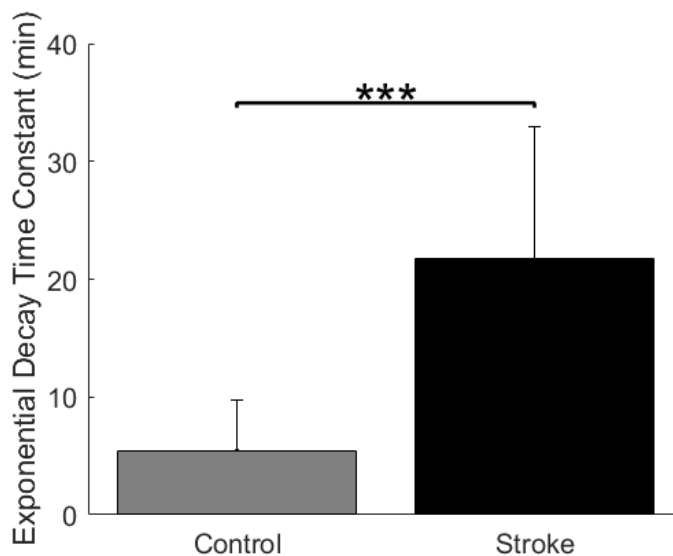


Figure 3.5. Mean time constant for the exponential decay of the local muscle oxygen saturation of the rectus femoris during occlusion at 20% MVC ramp and hold cycle for the stroke and control populations.

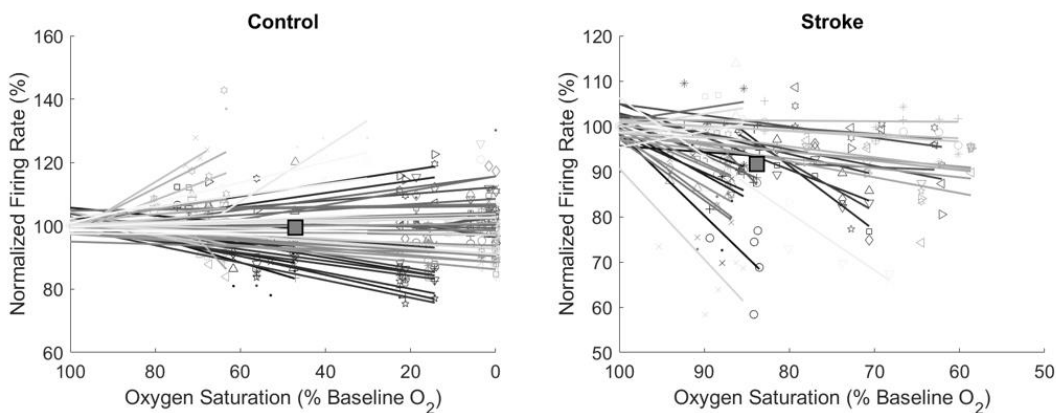


Figure 3.6. Linear regressions of each motor unit firing rate as a percentage of the first contraction it fired versus the local muscle oxygen saturation for all stroke and control recorded motor units during the 20% MVC occlusion protocol. Each shape and color combination represent the firing rate at that local oxygen saturation. Squares are the group mean for the firing rate and local muscle oxygen saturation.

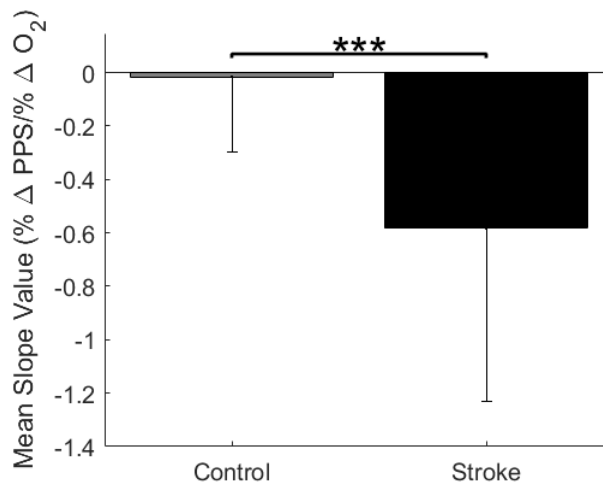


Figure 3.7. The average slope value of the linear regression lines for the motor unit firing rate versus the oxygen saturation between stroke and control during the 20% MVC occlusion protocol.

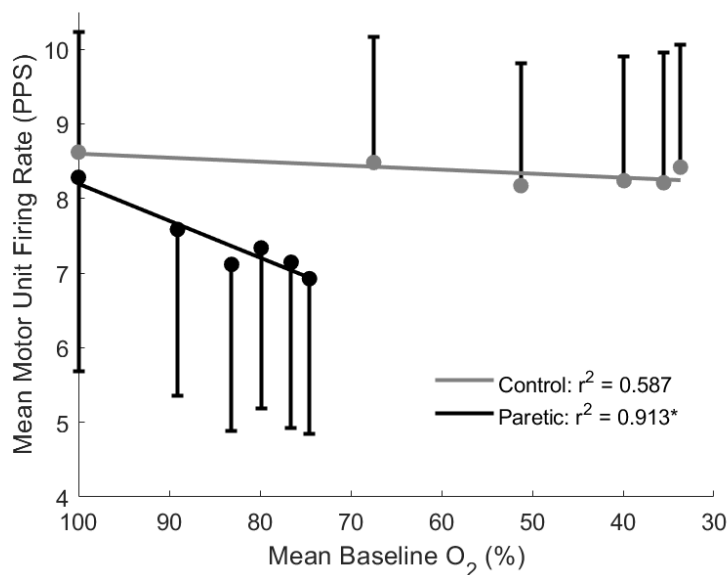


Figure 3.8. Group mean motor unit firing rates and mean % O₂ saturation at each contraction. Mean motor unit firing rates significantly correlated with mean O₂ saturation ($r^2 = 0.913$, $p = 0.002$) for individuals with stroke. The greater slope also suggests O₂ saturation has a greater impact on motor unit firing rates for individuals with stroke compared to controls.

3.3.7 Maximum Voluntary Contractions (MVCs)

Baseline MVCs were significantly lower for stroke compared to controls (123.21 ± 62.32 Nm vs. 179.00 ± 61.20 Nm, $p < 0.049$, see Table 2). During the MVC occlusion, there was a significant main effect of contraction (first contraction = 139.60 ± 64.92 Nm, last contraction = $107.19 \pm$ Nm, $p < 0.001$). There was a significant interaction of contraction and group ($p = 0.015$) whereby the controls had a larger decline in MVC between cycles compared with the participants with stroke (control: first contraction = 164.92 ± 66.75 Nm, last contraction = 116.75 ± 44.35 Nm; stroke: first contraction = 114.21 ± 54.93 Nm, last contraction = 97.62 ± 51.47 Nm). There was no main effect of group (control = 139 ± 64.92 Nm; stroke = 107.19 ± 47.78 Nm, $p = 0.161$).

3.3.8 Resting Twitch

During occlusion, there was a significant main effect of contraction (first contraction = 33.70 ± 10.87 Nm, last contraction = 27.81 ± 8.04 Nm, $p = 0.001$) for the resting twitch amplitude because amplitude decreased for both stroke (28.91 ± 6.49 Nm to 25.65 ± 6.40 Nm) and control (38.80 ± 12.43 Nm to 30.14 ± 9.02 Nm). There was not a significant main effect of group ($p = 0.126$) and no significant interaction effect of contraction and group ($p = 0.085$). Time to 75% relaxation also had a significant main effect of contraction (first contraction = 116.07 ± 40.70 ms, last contraction = 143.16 ± 50.49 ms, $p = 0.010$) as both stroke (125.97 ± 35.61 ms to 165.42 ± 50.54 ms) and control (104.92 ± 43.11 ms to 118.11 ± 36.85 ms) increased in relaxation time. There was also no significant main effect of group ($p = 0.105$) and no interaction effect of contraction and group ($p = 0.163$) for time to 75% relaxation.

3.3.9 Global Surface EMG

Repeated measures ANOVA during the occlusion protocol showed no main effect of contraction ($p = 0.303$) or group ($p = 0.825$), and no interaction effect ($p = 0.116$) for the mean global sEMG. The non-occlusion protocol also showed no main effect of contraction ($p = 0.063$) or group ($p = 0.231$), and no interaction effect ($p = 0.268$) for the mean global sEMG. Paired t-test showed that the stroke group was not significantly different during the non-occlusion and occlusion protocols at the first contraction (95.19 ± 34.00 μ V vs 99.08 ± 28.76 μ V, $p = 0.80$) or the last contraction (99.03 ± 36.52 μ V vs 97.85 ± 46.07 μ V, $p = 0.96$). This was also similar for the control group as the mean

RMS was not significantly different between the non-occlusion and occlusion protocols at the first ($123.06 \pm 65.08 \mu\text{V}$ vs $121.08 \pm 59.62 \mu\text{V}$, $p = 0.95$) or the last contractions ($133.25 \pm 42.83 \mu\text{V}$ vs $126.41 \pm 79.13 \mu\text{V}$, $p = 0.78$). This data shows that the mean RMS was not impacted by the occlusion protocol between groups.

3.4 DISCUSSION

In this study, we demonstrated that paretic motor unit firing behavior is more sensitive to inhibitory effects of transient occlusion compared with responses in individuals without stroke. Occlusion of the paretic leg caused a larger decrease in the average motor unit firing rates during a sub-maximal contraction without substantial changes in muscle contractile properties. Remarkably, the decline in motor unit firing rates occurred despite individuals with stroke having a greater time constant for the rate of change of oxygen saturation and a lower relative change in oxygen saturation compared with the controls. Because group III/IV muscle afferents are sensitive to muscle ischemia and have an inhibitory effect on motor unit firing behavior, our results suggest that group III/IV afferents contribute to altered motor unit firing and may contribute to impaired force generation in chronic stroke during exercise.

3.4.1 Transient Group III/IV muscle afferent feedback inhibits paretic MU discharge

The major finding of this study was that motor unit firing rates decreased when blood flow was transiently occluded to the contracting paretic muscle (Figure 3.3 & 3.8). Potential mechanisms for the larger decrease in paretic motor unit firing during occlusion

compared to the controls include: (1) impaired descending drive to the paretic motoneuron pools with repeated contractions, (2) greater decreases in paretic oxygen saturation during occlusion, and (3) increased excitability in group III/IV spinal pathways. Because on average across the group, there was no detected decrease in firing rates for the stroke or control groups in the no occlusion condition, the decrease in firing rates during occlusion was not likely due to a baseline inability of descending pathways to activate the motor units or rate coding impairments at the level of the motoneuron over multiple contractions across the 5-min condition.

The group findings during the no occlusion condition in this study, contrast with other studies which have shown differences between controls and individuals with stroke in firing rates during sub-maximal contractions (Gemperline et al. 1995; Mottram et al. 2014). On an individual level, most of the participants with stroke did have lower firing rates than the controls (7/10) and in instances where there the torques were similar between a control and participant with stroke, the paretic motor units had lower firing rates than controls. Our results may differ from others due to key differences in the task: (1) relative effort vs matched target torque, (2) muscle groups (upper extremity vs lower extremity muscles) and (3) contraction type (triangle ramp vs ramp and hold). Finally, we could not fully evaluate motor unit firing rate saturation as we did not perform multiple target torque conditions.

Because the occlusion condition was performed after the no occlusion and the occlusion + MVC protocol, it is possible that the decline in firing rates was due to increased fatigability in the stroke survivors (Hyngstrom et al. 2012; Knorr et al. 2011). However, individuals were given at least 5 minutes rest between protocols and the

respective magnitudes of the global surface EMG from the first cycle of the two protocols in people with stroke was similar indicating similar neural drive for a given target torque. In addition, there was no significant change in EMG amplitude within a protocol for both the stroke and control groups. If there was substantial muscle fatigue, the magnitude of EMG would be expected to be greater in order to meet the force demands of the task (Enoka and Stuart 1992; Garland et al. 1994). Because during the occlusion trial, there was a decrease in firing rates but no change in EMG amplitude or force, this suggests that a recruitment vs rate coding strategy was used to maintain force across contractions.

A larger decrease in paretic motor unit firing rates could be attributed to a larger relative decrease in oxygen saturation due to occlusion as compared to controls. However, in our study, individuals with stroke had a decreased rate of change in oxygen saturation in response to occlusion compared to controls. Group differences in the oxygen saturation response due to occlusion are likely due to paretic muscle becoming less oxidative and/or having less mitochondrial content. Both of these changes are known secondary consequences of stroke, primarily due to limb disuse (Billinger et al. 2012; De Deyne et al. 2004; Landin et al. 1977). Because current methodology limits the absolute measurement of oxygen saturation at baseline, future studies will examine absolute levels of oxygen saturation during transient and chronic baseline conditions and the relationship to motor unit firing behavior.

Previous studies in other neurological conditions, such as spinal cord injury, have demonstrated that group III/IV pathways are hyperexcitable. Although these studies focused on the flexor withdrawal and activation of flexor muscles, they demonstrate an exaggerated motor response for a given sensory input (Hornby et al. 2004; Schmit et al.

2002; Schmit et al. 2003). In our study, we show that even though the mechanics of the stimulus was the same (same compression pressure), the inhibitory response was larger (greater decline in mean firing) in people with stroke compared with controls (Figures 3.3 & 3.8). Likewise, in congestive heart failure patients, the same input of muscle contraction and stimulation of group III/IV afferents results in an overexaggerated vascular response (Amann et al. 2014). It is possible, therefore, that altered group III/IV muscle afferent activity in our stroke participants resulted in inhibition of motoneuron output. Here, with respect to controls, we did not find a large inhibitory effect on control motor unit firing rates (Figure 3.3 & 3.8) performing brief knee extension contractions although there was a trend for a shift in recruitment thresholds within the occlusion trial. Certainly, under different exercise conditions, such as whole body and limb exercise in healthy controls, group III/IV pathways have inhibitory effects on motor output (Amann et al. 2011; Taylor et al. 2016). This difference may be because our protocol involved transient ischemia and brief, submaximal contractions in a single muscle group.

Although ischemia can also alter the exercising muscle contractile properties, our data support the idea of a change in central mechanisms. From our data, we demonstrate that twitch amplitude did not differ between stroke and control, suggesting that the observed changes in motor unit firing were not due to changes in muscle contractile properties. It may have been predicted that the inhibition would have affected other motoneuron properties such as a shift in recruitment threshold. However, no systematic shift in recruitment thresholds was detected in this data set. We did however, observe a decrease in firing rates at recruitment for both groups during the occlusion condition which supports an inhibitory effect on motoneuron firing properties. Because the

transient occlusion was performed on the test leg and not remotely, we cannot say whether the effect was a spinal response or more centralized effect. Finally, our study used transient occlusion of blood flow to manipulate the activation of group III/IV afferents. Although transient, the inhibitory response provided insight into what individuals could experience during intense exercise or activity.

3.4.2 Implications for motor performance

In our study, we demonstrate that transient group III/IV feedback mechanisms also play a role in impaired motor unit firing in the paretic muscle. In daily life, many activities of daily living are performed during sub-maximal force conditions in which there is reciprocal activation of muscle groups - this may lessen the ischemia related inhibition. After stroke, there is an impaired ability to generate appropriate forces resulting in functional consequences such as diminished capacity to make accurate movements, increased variability in movement output (Blennerhassett et al. 2008; Chang et al. 2013; Kuhnen et al. 2015; Lodha et al. 2010) and decreased task endurance (Kuhnen et al. 2015). We show that individuals with the largest reductions in motor unit firing rates were also generating smaller target torques - in other words, were weaker at baseline. Indeed, during the condition with no occlusion, we found no decrease in firing rates during a sustained 20% contraction for either group. However, ischemia-related inhibition of paretic motor units might be relevant during sustained high intensity contractions - such as carrying a heavy grocery bag or exercising against a heavy load. Future studies should examine if therapies that increase blood flow during exercise improve motor performance.

3.4.3 Conclusion

Here we show the impact of transient total occlusion on paretic motor unit firing behavior during a sub-maximal task. Our results corroborate previous studies demonstrating impaired motor unit firing and recruitment after stroke (Chou et al. 2013; Gemperline et al. 1995) and extend previous findings by demonstrating how transient sensory inputs can potentially contribute to force generating deficits during contractions. We found that resting twitch relaxation time increased similarly for both the stroke and control groups in response to ischemia, possibly reflecting support of the “muscle wisdom” hypothesis which proposes that prolonged force relaxation of the muscle is a response to decreases in motor unit firing rates so as to maintain force levels (Bigland-Ritchie et al. 1983; Marsden et al. 1983). While relaxation times often increase and the motor unit firing rate typically decreases there is minimal support that the two variables are causally linked to offset fatigue (Fuglevand and Keen 2003). This study further extends the findings of chapter 2 how the absolute magnitude of blood flow to an exercising muscle tracks with motor unit firing behavior in chronic stroke.

CHAPTER 4: A SEROTONIN RECEPTOR ANTAGONIST DECREASES PROLONGED MOTOR UNIT FIRING DURING VOLUNTARY RELAXATION POST-STROKE

4.1 INTRODUCTION

In addition to weakness, individuals with stroke also have difficulty with sub-maximal force regulation. This includes not only an impaired ability to regulate a constant force (Horstman et al. 2008; Kuhnen et al. 2015), but also the ability to volitionally decrease force (i.e. controlled relaxation) (Chae et al. 2006; Chae et al. 2002). Difficulties with decreasing force results in prolonged torque and EMG during volitional relaxation (Mottram et al. 2010; Murphy et al. 2015; Seo et al. 2011). This might be especially detrimental to motor tasks that require alternating contraction-relaxation activity in muscle groups, such as walking (Lewek et al. 2007). Because many activities of daily living involve sub-maximal force regulation, understanding mechanisms of impaired force regulation is important for developing treatment strategies.

Previous work has shown that changes in the magnitude of descending excitatory drive to motoneuron pools contributes to force generating deficits in the paretic arm and leg (Jang et al. 2017; Peters et al. 2017; Schwerin et al. 2008; Wei et al. 2014). Here we examine the possibility that prolonged motor unit firing behavior and force generation during relaxation could be attributed to post synaptic changes in the paretic motoneuron. Several studies have detailed changes in paretic motor unit firing behavior as compared to those without stroke. For example, saturation of firing rates (McNulty et al. 2014; Mottram et al. 2014; Mottram et al. 2009), compression of recruitment thresholds (Hu et

al. 2015), changes in afterhyperpolarization (McManus et al. 2017), and spontaneous motor unit firing (Mottram et al. 2010) has been documented.

Spontaneous paretic motor unit firing behavior occurs after an excitatory synaptic input (e.g. descending command, Ia excitation) has ceased but motor unit firing continues. Spontaneous firing may reflect dysregulation of persistent inward currents (PICs). PICs are voltage sensitive, depolarizing currents (Heckman et al. 2008), and result in plateau potentials which cause firing in the absence of continued synaptic input. Functionally it has been proposed that if properly regulated, self-sustained firing would allow for supraspinal centers to attend to other tasks during a motor task (Heckman et al. 2003). If dysregulated, prolonged firing could interfere with motor commands especially during conditions in which excitatory drive is decreasing (e.g. dysfacilitation) such as during volitional relaxation

A key regulator of PIC amplitude is the magnitude of monoaminergic drive from the reticular formation in the brainstem. Spinal motoneurons receive dense contacts from monoaminergic axons, which release the neuromodulators serotonin (5-HT) and norepinephrine (NE). 5-HT and NE bind to metabotropic receptors that ultimately alter the cell's intrinsic excitability by changing ion channel behavior through second messenger pathways (Rekling et al. 2000). It is believed that the monoaminergic related self-sustained firing occurs in motor units responsible for low force contractions (Heckman et al. 2003; Lee and Heckman 1998) needed for performing many activities of daily living. Monoaminergic brainstem nuclei are believed to be tonically active, regulated primarily by cortical inhibition depending on the needs of the task (Aston-Jones et al. 2000; Jacobs and Fornal 1999; 1997). For example, these brainstem centers are

known to increase drive to spinal centers during repetitive and rhythmic movement (e.g. locomotion), during increased demand of movements (e.g. walking faster) and also in response to an acute stressor (fight or flight response) (Heckman et al. 2003; Heckman et al. 2009). Stroke likely disrupts cortical inhibition of brainstem monoaminergic centers, which would result in an increase in baseline (steady state) descending monoaminergic drive.

During voluntary contractions, single motor unit firing behavior can change in a non-linear fashion in relation to the exerted torque. This creates a hysteresis to the firing behavior in which the motor units fire at a higher rate during the descending (de-recruitment) phase compared to ascending (recruitment) phase (De Luca et al. 1982; Gorassini et al. 2002a; b; Milner-Brown et al. 1973). Because excitatory input cannot be measured directly in humans, the paired motor unit recording technique (ΔF) was developed as an indirect measure of this hysteresis to estimate PIC contribution (Gorassini et al. 2002a). This method uses a lower threshold (reporter) motor unit to estimate excitatory drive of a higher threshold (test) motor unit by comparing the firing rate of the reporter unit at recruitment and de-recruitment of the test unit. It is assumed that a higher firing rate at recruitment (hysteresis) indicates that PIC activation is not fully active in the higher threshold unit. A greater ΔF value reflects a greater PIC contribution to the total current driving the test unit. This method has been used to study PIC contribution in individuals with stroke (Mottram et al. 2014; Mottram et al. 2009) because it is believed that enhanced PICs may contribute to spasticity and prolonged firing.

There is evidence of increased activity in reticulospinal pathways after a stroke. Participants with stroke have shown to have a delay in the termination of contractions (Chae et al. 2006; Chae et al. 2002). The presence of significantly augmented elbow flexion torque and EMG activity in the paretic limb during vibratory input to the biceps brachii suggests that the paretic motoneurons may become hyper-excitabile and invoke PICs following stroke (McPherson et al. 2008). Seo et al (2011) showed that individuals with chronic stroke have a prolonged relaxation time in muscle activity of the hand following a grip task and that a serotonin antagonist (cyproheptadine) reduced the prolonged muscle activation during relaxation. Also in the arm, others have shown increased excitability of auditory startle response, which is consistent with increased activity in reticulospinal pathways (Honeycutt and Perreault 2012; Li 2017; McPherson et al. 2018). It is, thus, feasible that PICs could contribute to prolonged discharge of motor unit firing behavior observed in the paretic muscles of stroke survivors.

The purpose of this study was to quantify the effects of a serotonin receptor antagonist on motor unit firing behavior during controlled isometric relaxation of the vastus lateralis muscle. 5-HT in the spinal cord is likely to be involved in motor output gain control (Jacobs and Fornal 1999; Jacobs et al. 2002; Wei et al. 2014). This study will aim to establish that drugs that suppress the effects of 5-HT will decrease the excitability of the motoneurons and inhibit spinal reflexes (Jacobs and Fornal 1999; Jacobs et al. 2002; Wei et al. 2014). To this date, this is the first study to examine the effects of a serotonin receptor antagonist using a high-density surface EMG array to extract a large number of individual motor unit firing rates during repeated, isometric contractions of the knee extensor muscles. This technology allowed for a large number of acquired pairs for

the ΔF calculations that estimate PIC contribution (Powers and Heckman 2015) as well as direct measures of the motor unit relaxation rate during volitional relaxation. Because neuromodulatory input to the spinal cord may be enhanced after a stroke and serotonin facilitates PICs and prolonged firing, we *hypothesized* that a serotonin receptor antagonist will 1) reduce prolonged motor unit firing and increase muscle relaxation during volitional relaxation and 2) reduce the ΔF metric for estimating magnitude of PIC contribution to the motoneuron.

4.2 MATERIALS AND METHODS

4.2.1 Participants

All participants gave informed consent before participation in this study, and the procedures were approved by the Medical College of Wisconsin Institutional Review Board (PRO190103). Ten participants with chronic, hemiparetic stroke (5 male, 5 female, 63.20 ± 8.90 yrs) and ten age matched, neurologically intact participants (6 male, 4 female, 61.30 ± 8.27 yrs) participated in the study (Table 1). Stroke participant general inclusion criteria were: single, unilateral stroke (obtained through verbal communication from the physician and consistent with neurological physical examination); able to ambulate at least 30 feet (with or without an assistive device); ≥ 6 months post stroke; must be at least 18 years old; cognitively able to give informed consent. Stroke participant general exclusion criteria included: brainstem stroke; any uncontrolled medical condition; contractures of any lower extremity joints; inability to follow 2-3 step commands; substance abuse; people unable to walk more than 10 feet without physical

assistance; taking any medication or supplement that has 5-HT or norepinephrine mechanisms of action; narrow angle glaucoma; chronic liver or kidney disorders; major psychiatric disorders; neurodegenerative disorders.

Subject Characteristics: Stroke						
Subject	sex	age	Time since stroke (years)	Fugl-Meyer (LE)	Walking speed (m/s)	Berg
1	male	55	9.8	29	0.96	45
2	female	66	7.7	17	0.28	38
3	female	62	22.5	30	1.22	47
4	female	57	19.6	14	0.40	46
5	female	76	4.3	30	1.09	48
6	male	67	1.4	11	0.14	24
7	male	48	11.6	21	0.34	43
8	female	79	4.3	27	0.66	49
9	male	55	5.4	22	0.83	42
10	male	67	9.4	19	0.67	48
Average	50% male	63.20	9.60	22.00	0.66	43.00
Subject Characteristics: Control						
1	female	62				
2	male	63				
3	female	72				
4	male	54				
5	male	55				
6	female	51				
7	female	74				
8	male	67				
9	male	49				
10	male	66				
Average	60% male	61.30				

Table 4.1. Participant Characteristics.

4.2.2 Drug Administration

A randomized double-blind crossover design was used. The participants took a placebo in one session and a 5-HT receptor antagonist, cyproheptadine, in the other session. Order of testing was randomized, and the participants and investigators were blinded to the drug used (two-part telescoping capsule). The drug and placebo was prepared at Froedtert Memorial Lutheran Hospital Investigational Drug Service associated with the Medical College of Wisconsin. Sessions occurred on separate days at least one week apart. A single dose of Cyproheptadine consisted of 8 mg and was

administered by a licensed physician. The drug or the placebo was given at least 4 hours prior to protocol measurements to maintain the double-blind study. Participants taking baclofen were asked to skip their morning dose.

4.2.3 Torque Measurements

Participants were seated upright on a Biodex System 3 (Biodex Medical Systems, Shirley, NY) with the test leg hip and knee angles at 90 degrees of flexion. Isometric knee extension torque measurements were made using a JR3 E-series load cell (JR3, Inc., Woodland, CA) mounted to the dynamometer spindle by means of a custom aluminum coupling. A quarter inch aluminum arm extended from the axis of the load cell to a bracket that secured either left or right ankle attachments. The ankle attachments were secured to the test leg 2 inches above the lateral malleolus. The torque was acquired by an EMG-USB2+ amplifier (256-channel regular plus 16-auxiliary channels, OT Bioelettronica, Turin, Italy), low-pass filtered at 500 Hz, sampled at 2048 Hz, and recorded using the OT Biolab software. The data was then zero phased, low-pass filtered at 15 Hz using a 4th order Butterworth filter prior to analysis (Matlab).

4.2.4 Resting Twitch Torque

A constant current generator (DS7A, Digitimer, Welwyn, Wales) delivered a rectangular pulse of 100 μ s duration to percutaneously stimulate the resting rectus femoris muscle. The stimulation intensity (usually 200 mA to 500 mA) was set at 20% above the level required to produce a maximal resting twitch amplitude that caused a

supramaximal stimulation. The torque generated by the knee extensors in response to the electrical stimulation was recorded.

4.2.5 Patellar Tendon Taps

A P series LinMot Linear motor (LinMot Inc, Delavan, WI) administered 5 consecutive taps at 0.5 Hz to the patellar tendon to provoke the stretch reflex of the quadriceps muscle group. The “tendon tapper” was controlled by the LinMot E1010 servo controller for voltage sensitive velocity output. A custom-written LabView program controlled the administration of the taps and recorded the torque response. A 2.0V, 50ms, input to the servo controller generated a tap velocity of ~1.28 m/s. The tendon tapper was mounted on an adjustable, aluminum stand and positioned ~1 inch from the surface of a 1x1 inch rubber eraser centered over the patellar tendon to displace the force across the tendon.

4.2.6 Surface EMG Recordings

High-density surface electromyograms (HDsEMG) were obtained using a 64 channel 2-D electrode array with 8 mm interelectrode distance (ELSCH064R3s - 13 rows, 5 columns, OT Bioelettronica, Turin, Italy). A double-sided adhesive sticker designed for and compatible with the array was placed over the array. The holes within the adhesive sticker were filled with a conductive electrode paste (Ten20, Weaver and Company, Aurora, Co). The participant’s skin was sterilized with an alcohol swab and rubbed to remove superficial dead skin. The array was placed over the belly of the vastus lateralis, midway between the patella and the greater trochanter. A reference electrode

was placed over the lateral malleolus. Signals for each channel were differentially amplified between 1000 and 5000 V/V (participant dependent) and band-pass filtered (20-500 Hz) using the EMG-USB2+ amplifier. The signals were sampled at 2048 Hz, A/D converted to 12 bits, and acquired using the OT Biolab software throughout the duration of the protocol. Prior to analysis, a 2nd order bandpass filter (20-500 Hz) and a notch filter (60 Hz) were applied to each acquired EMG channel.

4.2.7 Motor Unit Decomposition

The 63 differentially amplified sEMG channels were decomposed to attain instances of single motor unit action potentials via implementation of a multichannel convolutive blind source separation algorithm described and validated by a previous study (Negro et al. 2016). In summary, the decomposition algorithm discriminates between individual motor unit action potentials from multi-unit (EMG) signals. The general framework for HDsEMG decomposition uses the approaches based on convolutive blind source separation by convolutive kernel compensation (Holobar and Zazul 2007), and the spike trains are estimated using a peak detection algorithm and K-means classification. To provide a normalized index of reliability similar to the pulse to noise ratio, a silhouette measure (SIL) was computed on each estimated source. SIL provides a measure of the quality of the extracted motor unit spike trains based on the relative amplitude of the deconvolved spikes compared to the baseline noise. The source was considered of acceptable quality if SIL was greater than 0.85 (SIL ranges between 0 and 1). Motor units were identified by applying the decomposition algorithm to the ramp and hold protocol. Under the assumption of stable motor unit action potential properties,

this configuration provided the possibility to identify reliably the same motor units throughout one protocol (Martinez-Valdes et al. 2017a).

4.2.8 Experimental Protocol

Control participants performed the protocol with the right leg and the individuals with stroke performed the protocol on the paretic leg. Figure 4.1 illustrates the timeline of the experimental protocol. At least four hours prior to data collection the placebo or cyproheptadine was administered to the participant. All participants were sat upright in the Biodex chair. Data acquisition and visual feedback of the torque trace and target torque was provided using a custom written LabVIEW program and DAQ card (National Instruments, Austin, TX). Participants began by performing at least five baseline isometric maximum voluntary contractions (MVC) of the knee extensor muscles with one minute of rest between trials. Visual feedback and a verbal cue were provided to the participant to begin the isometric contraction. An electrical stimulation was provided to the quadriceps muscle group as soon as the knee extensor torque returned to zero from the MVC to obtain a resting twitch torque. The peak torque of all the MVC trials was used as the MVC. A rest period of at least 5 minutes was provided following the final MVC trial. A tendon tap protocol was performed to obtain the reflex response of the knee extensor muscle group. Another break of at least 5 minutes was given before the submaximal, isometric ramp and hold protocol was performed. This consisted of five continuous ramp and hold isometric contractions in which the target torque trace increased from 5% MVC to 20% MVC over a 4s period (slope = 3.75 %MVC/s) (isometric ramp). After a plateau phase (isometric hold) at 20% MVC for 4s, the target

torque trace declined back down to 5% MVC over another 4s interval. The participant then held the contraction at 5% MVC for 4s before beginning the ramp and hold contraction again. Participants were instructed not to relax to zero knee extension torque between ramp and hold contractions to optimize continuous firing of individual motor units across ramp and hold contractions. Thus, participants completed 5 consecutive ramp and hold contractions before completely relaxing. Surface EMG using the high-density electrode array was recorded throughout the duration of the experimental protocol.

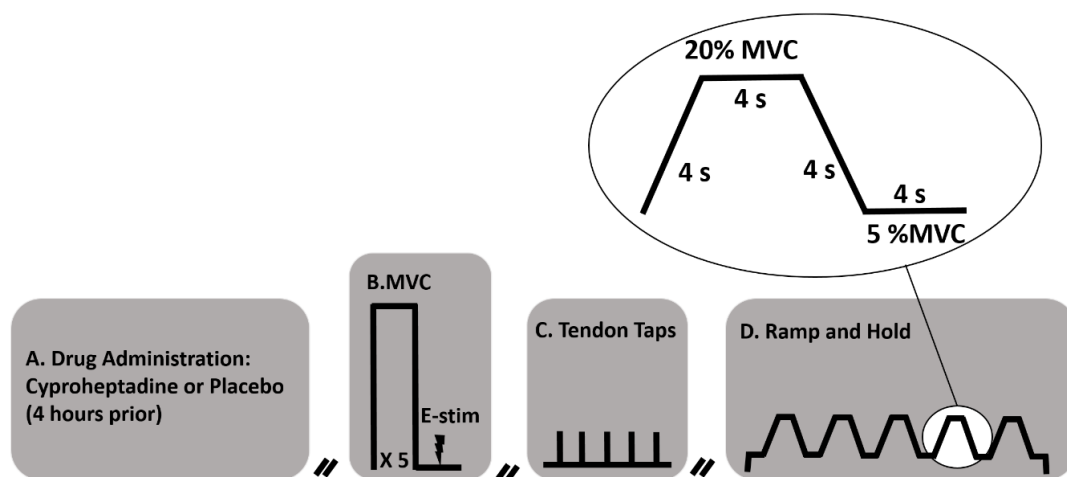


Figure 4.1. Experimental Protocol. A) In a double blind, cross-over design, either a 8 mg 5-HT₂ antagonist, cyproheptadine, or a placebo was administered at least 4 hours before beginning the protocol. B) Isometric maximum voluntary contractions (MVC) of the knee extensor muscles were performed. Immediately following complete relaxation of the knee extensor muscles, a maximum electrical stimulation was administered to the rectus femoris muscle to obtain a resting twitch torque amplitude. This was repeated about 5 times until 2 subsequent MVCs were within 10% of each other. C) 5 consecutive patellar tendon taps at 0.5 Hz were administered to elicit a reflex response. D) The “Ramp and Hold” protocol consisted of 5 subsequent trapezoidal contractions without complete relaxation. One trapezoid contraction consisted of a 4s increase to 20% MVC, holding for 4s, and then a controlled, relaxation back to 5% MVC and holding 4s.

4.2.9 Data Processing

Data processing was performed in Matlab R2017b (Mathworks, Natick, MA). Each variable was calculated for each contraction of the ramp and hold protocol and the mean was calculated over all contractions of the ramp and hold protocol.

The discharge rates of the inter-spike intervals (ISI) were calculated by excluding abnormally long (>250 ms, 4 Hz) or short (<20 ms, 50 Hz) ISI values (Negro et al. 2016). Abnormally long ISIs were excluded because we only wanted to consider motor units that were likely continuously contributing to force generation, as well as remove the ISI when the motor unit ceased to fire. The instantaneous firing rates of individual motor units were calculated as the inverse of the inter-spike interval (Hz, PPS, $\frac{1}{ISI}$). The motor unit action potential timings were time-locked with the torque trace (Figure 4.2). The firing instances for each motor unit were filtered with a unit area Hanning window of 1-s duration. The mean firing rates were determined as the average firing rates during the 4s hold phase of the ramp and hold protocol. Therefore, the mean motor unit firing rate for each participant was determined for the entire ramp and hold protocol. Motor unit contraction rate was calculated as the slope of the increasing instantaneous firing rate of each individual motor unit during the rising phase of the ramp and hold contraction. Likewise, the relaxation rate of each individual motor unit was calculated as the slope of the instantaneous firing rate during the controlled, voluntary relaxation phase of the ramp and hold contraction. The motor unit recruitment threshold was calculated as the %MVC when it began firing, and the motor unit de-recruitment threshold was calculated as the %MVC when it ceased firing.

The torque values were determined for the MVC, resting twitch torque, tendon tap torque, and rate of relaxation during the voluntary relaxation phase of the ramp and hold protocols. The mean value for the five contractions was calculated for each condition (control/stroke and placebo/cyproheptadine).

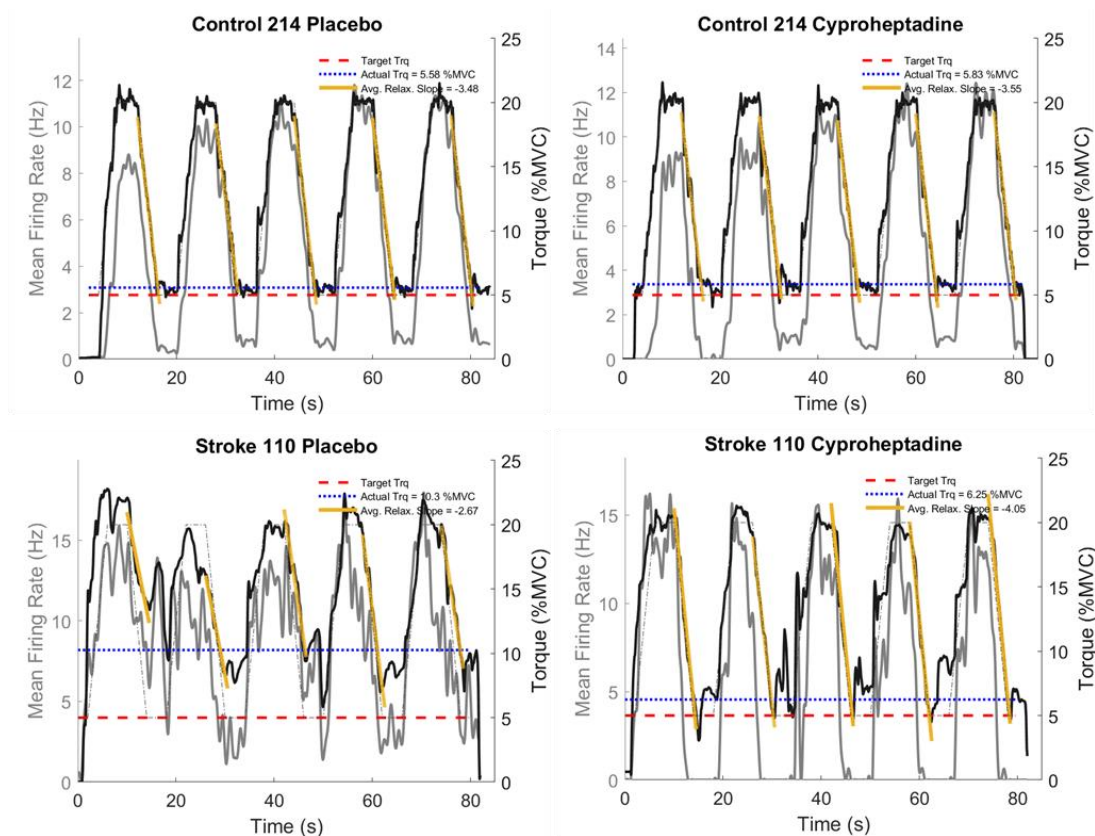


Figure 4.2. Single Participant Data. The filtered motor unit firing rate (gray trace, left axis) and the corresponding torque trace normalized to %MVC (black trace, right axis). The yellow line is the slope of the torque during the relaxation phase, the dashed blue line is the mean torque value during the 5% hold phase, and the dashed red line is the target 5% hold phase. The blue line approaching closer to the red line would suggest greater controlled relaxation, and the more elongated yellow line indicates a faster decrease in torque during the relaxation phase. Note the greater torque relaxation (yellow trace) during the relaxation phase and the average 5% hold torque value (blue trace) after cyproheptadine administration for the individual with stroke, indicating a greater rate of torque relaxation as well as a closer torque value to the 5% hold target torque (red trace). There is little change for the control participant.

4.2.10 Paired Motor Unit Analysis (ΔF)

Because intracellular recordings from human motor neurons is not possible, a technique using paired motor units (referred to as paired motor unit analysis or ΔF) has been used to estimate PIC magnitude in humans (Gorassini et al. 2002a; b; Gorassini et al. 2004; Mottram et al. 2009; Vandenberk and Kalmar 2014). This method compares firing rates at recruitment and de-recruitment to estimate intrinsic excitability of the motoneurons. The paradigm (Figure 4.3) requires a pair of motor unit firing rates: 1) an earlier recruited, lower threshold (reporter) unit and 2) a later recruited, higher threshold (test) unit. The reporter unit is used to help control for firing rate changes due to changes in excitatory synaptic inputs to the motoneuron. The difference in firing rate (ΔF) of the reporter unit from when the test unit is recruited to when it is de-recruited is thought to reflect the magnitude of the PIC contribution to the total excitatory drive of the test unit.

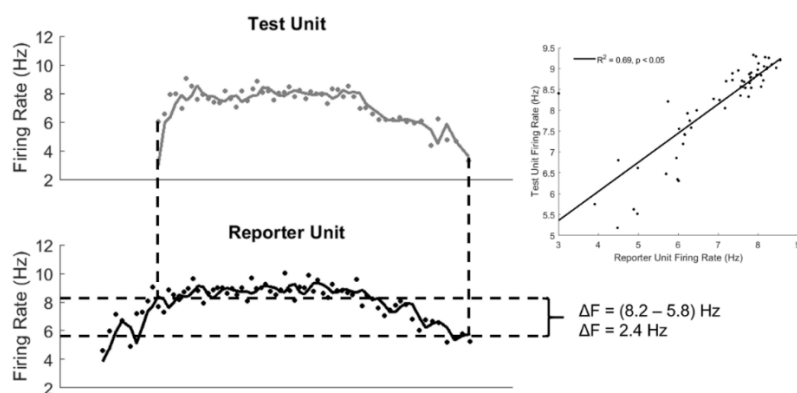


Figure 4.3. Paired Motor Unit Technique (ΔF). The firing rates and the filtered trace of two separate motor units, a lower threshold reporter unit (bottom) and a higher threshold test unit (top), are presented with the respective rate-rate plot (right). ΔF is calculated as the difference in the filtered firing rate of the reporter unit from when the test unit is recruited to when the test unit is de-recruited, an estimate of PIC contribution in humans.

The ΔF value provides a metric to the hysteresis in firing behavior caused by PICs (Figure 4.4). A more positive ΔF has been found to be consistent with larger PICs (Powers et al. 2008). The ΔF calculation was performed for all pairs of motor units at each individual contraction of the ramp and hold protocol under key assumptions supported by animal and human studies.

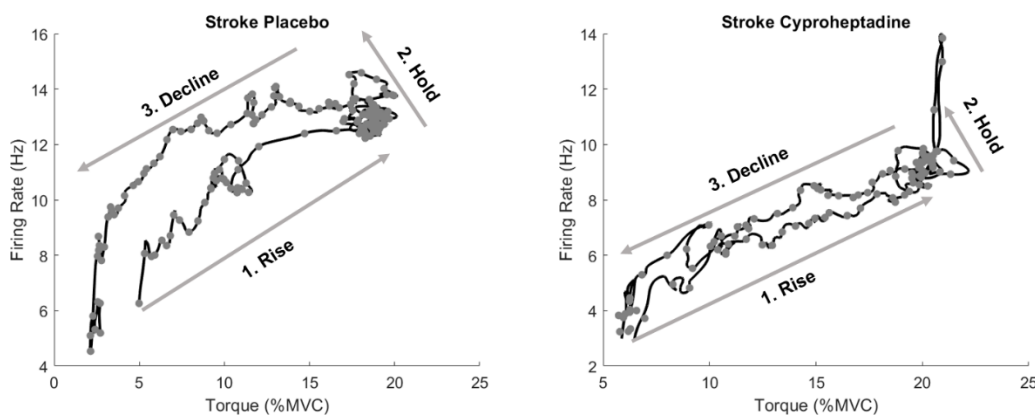


Figure 4.4. Hysteresis of motor unit firing rates. Single participant data representing hysteresis of motor unit firing rates between stroke cyproheptadine (right) and stroke placebo (left) individuals. The firing rate is plotted against the torque trace. The labels represent the different portions of the ramp and hold contraction. Note the decreased hysteresis after cyproheptadine administration.

There are four key assumptions described in previous studies (Gorassini et al. 2002a; Gorassini et al. 2004) but are briefly summarized here: 1) Due to its dendritic origin, motoneuron PICs are activated just before or at recruitment in an all-or-nothing manner. The PIC provides a depolarizing current that helps sustain motoneuron firing. 2) The firing rate smoothly varies with synaptic input and can be used to estimate input to the cell. 3) The reference and test motor units process synaptic inputs similarly. 4) Because of the assumed common drive to the pair of motor units, the reporter motor unit provides an estimate of synaptic drive to the test unit. Specific inclusion/exclusion

criteria for the motor unit pairs were derived from suggested recommendations established in previous studies (Gorassini et al. 2002a; Stephenson and Maluf 2011) to meet the primary assumptions of the paired motor unit recordings.

Adhering to the criteria intends to increase the validity of ΔF 's estimation of the PIC contribution to inputs to the test motor unit. 1) A regression analysis of the rate-rate plot of the pair was constructed and the F-test must be significant ($p < 0.05$) with $r^2 \geq 0.5$; 2) The test unit must be recruited at least 1s after the reporter unit was recruited. If the criteria were met, the ΔF measure was included in the analysis.

4.2.11 Statistical Analysis

Statistical tests were performed using IBM SPSS Statistics 24 (IBM, Armonk, NY). Data are reported as the mean \pm standard deviation. Differences in the dependent variables from repeated contractions were statistically compared using a multifactorial ANOVA [main factors: 1) group (control and stroke), and 2) drug (placebo and cyproheptadine); interaction: group*drug]. Within each ramp and hold protocol, the multifactorial ANOVA statistically compared the effects of drug and participant on the mean of the five contractions for paired motor unit recordings (ΔF) and motor unit behavior: 1) firing rate, 2) firing rate slope during the rising phase of the ramp and hold protocol, 3) firing rate slope during the decline phase of the ramp and hold protocol, and 4) recruitment and 5) de-recruitment threshold. A repeated measures ANOVA (main factors: 1) group: stroke and control; 2) drug: placebo and cyproheptadine) was used to statistically compare the 1) MVCs, 2) mean resting twitch torques, 3) mean tendon tap torque and 4) mean torque relaxation rates. A Bonferroni correction was used for post

hoc comparisons of the dependent variables. The following post hoc comparisons were made: stroke cyproheptadine to stroke placebo, stroke cyproheptadine to control cyproheptadine, stroke placebo to control placebo, and control cyproheptadine to control placebo. The α level was set at 0.05.

4.3 RESULTS

4.3.1 Torque Measurements: MVC, Resting Twitch, Tendon Tap, and Relaxation Rate

A main effect of group was observed for maximum voluntary contractions as the control groups generated a significantly greater amount of torque compared to the stroke groups, $F(1,18) = 12.093$, $p = 0.003$ (Control: 125.47 ± 55.25 Nm; Stroke: 56.19 ± 29.85 Nm). A main effect of drug was also observed as cyproheptadine administration decreased the torque generation, $F(1,18) = 5.832$, $p = 0.027$ (Placebo: 95.13 ± 58.85 Nm; Cyproheptadine: 86.45 ± 54.50 Nm). There was no group*drug interaction effect, $F(1,18) = 1.696$, $p = 0.209$. In summary, cyproheptadine administration lowered the MVC torque generation, and control participants generated significantly greater MVC torque compared to participants with stroke.

A main effect of group was observed for resting twitch torque as the control groups generated a significantly greater amount of torque compared to the stroke groups, $F(1,18) = 9.472$, $p = 0.006$ (Control: 45.20 ± 17.87 Nm; Stroke: 25.91 ± 10.69 Nm). There was no main effect of drug, $F(1,18) = 0.017$, $p = 0.898$ (Placebo: 35.60 ± 19.89 Nm; Cyproheptadine: 35.28 ± 15.59 Nm), and no group*drug interaction effect, $F(1,18) = 1.107$, $p = 0.307$. In summary, resting twitch torque was significantly greater for

controls compared to participants with stroke regardless of placebo for cyproheptadine administration.

A main effect of group was observed for mean tendon tap torque generation as the stroke group generated a significantly greater amount of torque compared to the control group, $F(1,18) = 8.477$, $p = 0.009$ (Control: 4.83 ± 4.93 Nm; Stroke: 12.35 ± 7.83 Nm). A main effect of drug was also observed as cyproheptadine administration decreased the tendon tap torque generation, $F(1,18) = 5.650$, $p = 0.029$ (Placebo: 10.41 ± 8.48 Nm; Cyproheptadine: 7.25 ± 5.95 Nm). There was no group*drug interaction effect, $F(1,18) = 0.172$, $p = 0.684$. In summary, cyproheptadine administration lowered the tendon tap torque generation, and individuals with stroke generated significantly greater tendon tap torque compared to the control participants.

A main group*drug interaction effect was observed for torque rate of relaxation during the relaxation phase of the ramp and hold protocol as cyproheptadine significantly increased relaxation rate (more negative) for the stroke group but not the control group, $F(1,18) = 6.444$, $p = 0.021$ (SC: -3.47 ± 0.31 %MVC/s; SP: -2.85 ± 0.25 %MVC/s; CC: -3.49 ± 0.44 %MVC/s; CP: -3.44 ± 0.37 %MVC/s). Post hoc analysis showed that cyproheptadine administration significantly increased relaxation rates for participants with stroke ($p = 0.004$) but not for controls ($p = 0.901$). There was also a main effect of drug as the cyproheptadine administration increased rate of relaxation, $F(1,18) = 5.596$, $p = 0.029$ (Placebo: -3.17 ± 0.42 %MVC/s; Cyproheptadine: -3.47 ± 0.40 %MVC/s). There was also a main effect of group, $F(1,18) = 7.557$, $p = 0.013$ (Control: -3.48 ± 0.37 %MVC/s; Stroke: -3.06 ± 0.73 %MVC/s). In summary, cyproheptadine administration

increased the rate of relaxation rate for the participants with stroke but there was no difference between placebo and cyproheptadine conditions for the controls.

4.3.2 Paired Motor Unit Recordings (ΔF)

A total number of 1,058 pairs were accepted for analysis and divided up as follows: Stroke placebo: 97 pairs; stroke cyproheptadine: 99 pairs; control placebo: 523 pairs; control cyproheptadine: 339 pairs. During the ramp and hold protocol a group*drug interaction effect occurred, $F(1,1054) = 4.315$, $p = 0.038$, for the paired motor unit recordings as cyproheptadine administration decreased mean ΔF values for the stroke group but not the control group (Figure 4.5). Pairwise comparisons showed the ΔF value for the stroke placebo group to be significantly greater than the stroke cyproheptadine ($p = 0.007$) and the control placebo ($p = 0.019$) groups. There was no difference in drug administration for the control group ($p = 0.946$). There was also a main effect of drug, $F(1, 1054) = 4.644$, $p = 0.031$, as cyproheptadine administration decreased the ΔF values (Placebo: 1.99 ± 3.39 Hz; Cyproheptadine: 1.78 ± 3.89 Hz). There was no main effect of group, $F(1, 1054) = 2.922$, $p = 0.088$ (Control: 1.81 ± 3.62 Hz; Stroke: 2.29 ± 3.53 Hz). In summary, mean ΔF throughout the ramp and hold protocol was greatest in the stroke placebo group but subsided after cyproheptadine administration; however, there was no drug-related difference in ΔF for the control group.

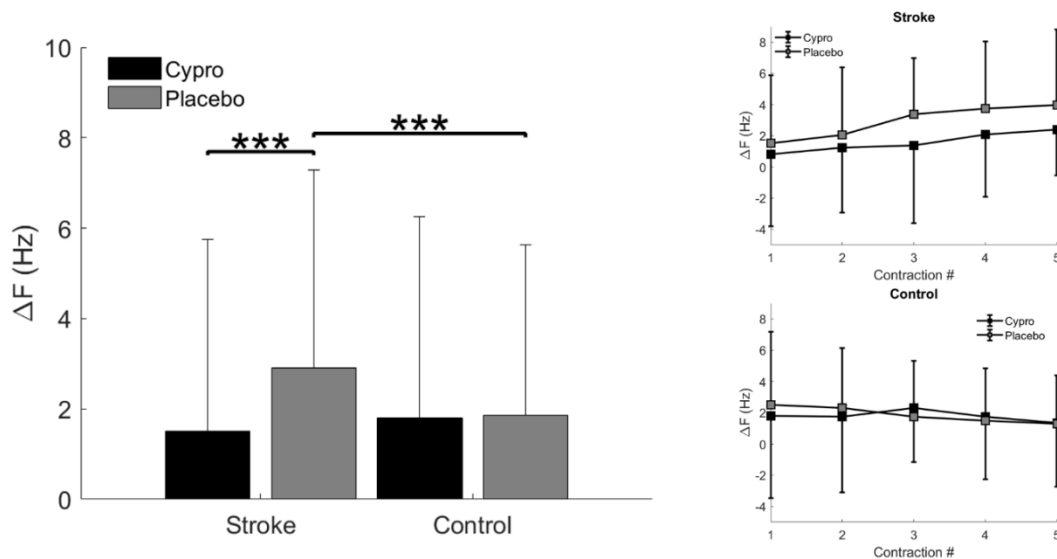


Figure 4.5. Paired Motor Unit Recording (ΔF). Mean ΔF for the entire ramp and hold protocol (left) and for each contraction of the protocol (right) for stroke (top) and control (bottom). Cyproheptadine administration significantly decreased ΔF values for the stroke group but not the control groups.

4.3.3 Mean Motor Unit Firing Rate

A total number of 278 motor unit firing were accepted for analysis and divided up as follows: Stroke placebo: 45 motor units; stroke cyproheptadine: 52 motor units; control placebo: 99 motor units; control cyproheptadine: 82 motor units. There was a main effect of group for mean motor unit firing rates, $F(1,274) = 12.630$, $p < 0.001$, as the control group had a higher motor unit firing rate compared to the stroke group (Control: 12.85 ± 4.53 Hz; Stroke: 10.93 ± 3.67 Hz). There was no main effect of drug, $F(1,274) = 0.063$, $p = 0.803$ (Placebo: 12.28 ± 4.22 Hz; Cyproheptadine: 12.08 ± 4.49 Hz), or group*drug interaction effect, $F(1,274) = 0.248$, $p = 0.619$. In summary, the magnitude of the firing rates was greater for the control groups compared to the stroke groups regardless of drug taken.

4.3.4 Recruitment Threshold

There was no main effect of group, $F(1,274) = 2.144$, $p = 0.144$, for recruitment threshold during the ramp and hold protocol as the mean recruitment threshold was not different between control and stroke groups (Control: 11.29 ± 3.52 %MVC; Stroke: 12.06 ± 5.07 %MVC). There was also no main effect of drug (Placebo: 11.52 ± 4.10 %MVC; Cyproheptadine: 11.59 ± 4.15 %MVC), $F(1,274) = 0.026$, $p = 0.872$, and no group*drug interaction effect, $F(1,274) = 0.129$, $p = 0.720$. The results for recruitment threshold showed that recruitment threshold did not differ between group or drug.

4.3.5 Derecruitment Threshold

There was a main effect of drug, $F(1,274) = 4.341$, $p = 0.038$, observed for motor unit de-recruitment threshold during the ramp and hold protocol as the cyproheptadine significantly raised the de-recruitment threshold compared to the placebo (Placebo: 9.91 ± 3.95 %MVC; Cyproheptadine: 10.63 ± 4.12 %MVC). No main effect of group, $F(1,274) = 1.188$, $p = 0.277$, was observed (Control: 10.43 ± 3.61 %MVC; Stroke: 9.92 ± 4.82 %MVC), but there was a near significant group*drug interaction effect, $F(1,274) = 3.832$, $p = 0.051$. In summary, motor units were de-recruited at a higher normalized torque level after cyproheptadine administration regardless of group.

4.3.6 Slope of Motor Unit Firing Rates During Muscle Contraction

No main effect of group, $F(1,274) = 0.307$, $p = 0.580$, on motor unit firing rate slope during the rising phase of the ramp and hold protocol was observed as firing rates increased similarly between control and stroke groups (Control: 3.73 ± 1.16 Hz/s; Stroke:

3.82 ± 1.34 Hz/s). There was also no main effect of drug, $F(1,274) = 0.296$, $p = 0.587$, as the contraction rates between drug administration were not different (Placebo: 3.69 ± 1.22 Hz/s; Cyproheptadine: 3.83 ± 1.24 Hz/s). There was also no group*contraction interaction effect, $F(1,274) = 0.898$, $p = 0.344$. Overall, the slope of the motor unit firing rates during the rising phase of the ramp and hold protocol were similar between groups regardless of placebo or cyproheptadine administration.

4.3.7 Slope of Motor Unit Firing Rates During Muscle Relaxation

A group*drug interaction effect was observed, $F(1,274) = 4.812$, $p = 0.029$, for motor unit firing rate slope during the decline phase of the ramp and hold protocol as cyproheptadine administration decreased firing rates a greater rate (more negative) for the stroke group but not the control group (Figure 4.6). The decrease in firing rates was significantly slower for the stroke placebo group compared to the stroke cyproheptadine ($p = 0.001$) and control placebo ($p < 0.001$) groups. There was no difference in drug administration between the control groups ($p = 0.404$). A main effect of group, $F(1,274) = 10.417$, $p = 0.001$, (Control: -3.03 ± 1.20 Hz/s; Stroke: -2.57 ± 1.33 Hz/s) and a main effect of drug, $F(1,274) = 10.123$, $p = 0.002$, (Placebo: -2.70 ± 1.28 Hz/s; Cyproheptadine: -3.05 ± 1.23 Hz/s) was also detected. These results showed that cyproheptadine increased motor unit firing rate slopes (more negative slope) during the controlled relaxation rate of the ramp and hold protocol for the stroke group but not the control group.

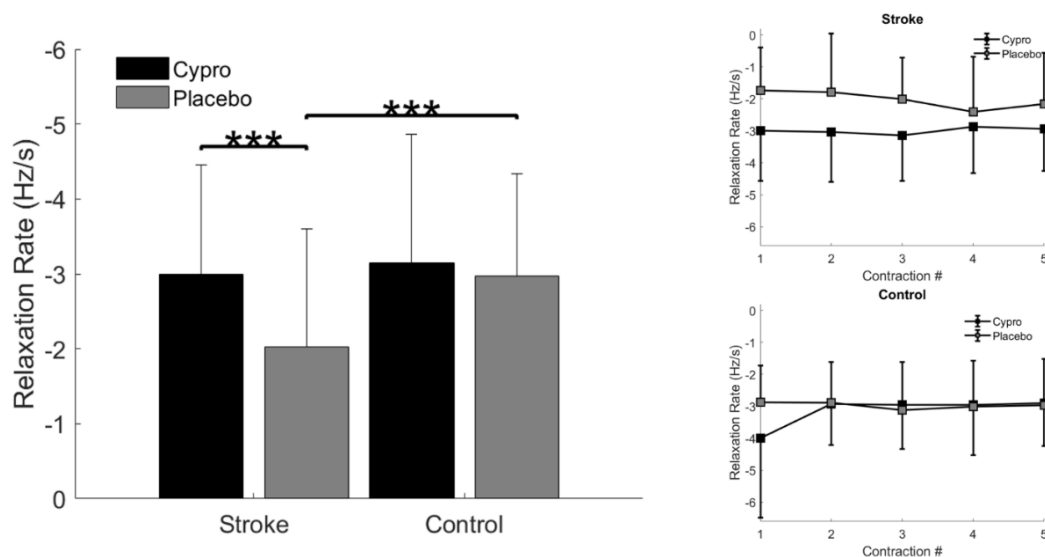


Figure 4.6. Motor Unit Relaxation Rate. Cyproheptadine administration to the stroke group significantly increased motor unit relaxation rate ($p < 0.001$).

4.4 DISCUSSION

In the present study, repeated isometric contractions of the knee extensor muscles in participants with chronic stroke induced motor unit firing behavior consistent with enhanced persistent inward currents (PICs), but this behavior subsided with the administration of a 5-HT receptor antagonist, cyproheptadine. Here, in chronic stroke, we provide evidence for dysregulated PICs resulting in prolonged motor unit firing during volition relaxation. The main findings to support augmented PIC activation in chronic stroke were 1) increased ΔF of paired motor unit recordings within the stroke placebo condition, 2) a decreased motor unit relaxation rate in the stroke placebo condition, and 3) the stroke cyproheptadine condition reduced ΔF and increased motor unit relaxation rate compared to the stroke placebo condition. Additionally, there were no effects on resting twitch properties but there was a reduction in tendon tap torque response for the stroke survivors in response to the serotonin antagonist. Taken together, the data are

consistent with stroke-related changes in the intrinsic electrical properties of the motoneuron interfering with volitional relaxation and not muscle contractile properties.

4.4.1 Validity of PIC Estimation Using ΔF via High Density Surface EMG

Calculating the PIC amplitude using the firing rate of the reference motor unit to estimate contributions to the test motor unit required assumptions that were validated by previous animal and human studies. The legitimacy of the paired motor unit measure is supported from animal studies where the cellular recordings of the PIC magnitude parallel ΔF (Bennett et al. 2001; Powers et al. 2008); nevertheless, as suggested in a modeling study, positive ΔF values can arise due to other nonlinear properties such as spike-threshold accommodation or spike-frequency adaptation (Revill and Fuglevand 2011). The counter-clockwise firing rate hysteresis that was observed in this study (Figure 4.4) has been attributed to PIC activation, while clockwise hysteresis has reflected spike frequency adaptation (Powers and Heckman 2015). This would have led to a lower firing rate on the decline phase of the contraction, which was not the case in this study. Revill and Fuglevand (2011) also explain that spike accommodation could result in a higher ΔF if the recruitment threshold of the test unit increased without changing the de-recruitment threshold. This would lead to a positive ΔF value. As Powers and Heckman (2015) show in their simulation study, spike threshold has little effect of recruitment threshold but does cause earlier de-recruitment. The stroke placebo group in this study de-recruit motor units at a lower threshold compared to recruitment. Though other factors may contribute to the discharge hysteresis, it appears that the differences in PIC magnitude primarily contribute to the ΔF values in this study.

4.4.2 Evidence for Enhanced PICs in the Chronic Stroke Population using Paired Motor Unit Recordings (ΔF)

In this study, all four of the groups (SC, SP, CC, CP) had mean ΔF values greater than zero; however, the stroke placebo group had a significantly higher ΔF value compared to the other three groups. Positive ΔF values associated with PIC amplitude have been shown and validated in paired motor unit recordings in animal models, such as the chronic spinal rat (Bennett et al. 2001) and the decerebrate cat (Powers et al. 2008). Consistent with the animal models, positive ΔF values were found in healthy human motor units and average ~ 4 Hz with gradually increasing force and no plateau (hold) phase (triangular target force) (Gorassini et al. 2002a; Mottram et al. 2009; Stephenson and Maluf 2011; Vandenberg and Kalmar 2014). The ΔF values in this study were lower with a total average for all groups together of 1.91 Hz and the stroke placebo group with an average of 2.91 Hz; however, a previous study using a protocol with a similar ramp and hold target torque as our protocol (5-10s to peak, 10s hold) found that mean ΔF values ranged between 2-3 Hz (Vandenberg and Kalmar 2014), similar to the findings in this study. It was also found in the spinal cord injury group, another spastic population, that ΔF values were 1.8 ± 1.0 Hz when the reporter unit was firing at < 8 Hz at test unit recruitment (Gorassini et al. 2004). Because the motor unit firing behavior demonstrated noticeable hysteresis with respect to the normalized torque produced (see figures 4.2 and 4.4 for single participant examples), especially in the stroke placebo group, it appears that motor unit firing rates during the voluntary contractions was not maintained solely by synaptic drive but was facilitated by activation of PICs in motoneurons.

Contrary to our findings, previous studies have not shown differing magnitudes of the ΔF values between stroke survivors and neurologically intact controls (Mottram et al.

2014; Mottram et al. 2009). A possible explanation for this difference is the discrepancy in experimental protocols and procedures: 1) In the current study, ΔF was evaluated in the lower extremity (vastus lateralis) rather than the upper extremity (biceps brachii) muscles; 2) The current study acquired multiple pairs (greater N) of motor units for each participant and trial via decomposition of multi-channel electrode arrays, while the previous studies utilized intra-muscular recordings to assess one pair of motor units per participant per trial; 3) Five consecutive ramp contractions with a plateau phase were used in this study compared to triangular ramp contractions (no plateau phase), separated by ~ 30 s, in the previous studies. Substantial variability of ΔF may occur within the same participant under similar conditions between trials (Stephenson and Maluf 2011); however, the reliability and value of this technique can be improved by averaging across multiple contractions and using multichannel arrays that allow for simultaneous recordings of multiple motor units (Powers and Heckman 2015; Udina et al. 2010). Simulations showed that under these conditions significant differences could be detected across conditions with differences in ΔF at < 1 Hz (Powers and Heckman 2015). Previously, it was suggested that ΔF of > 4.8 Hz would be needed to detect a statistical difference because of the between trial variation (Stephenson and Maluf 2011). This study applied both averaging over multiple contractions and utilized multiple pairs of motor units through the decomposition of HDsEMG, accounting for significantly greater ΔF values for the stroke placebo group.

PICs have been shown to “warm-up” with repetitive activation in the motoneurons of the decerebrate cat (Bennett et al. 1998; Bennett et al. 2001). A statistical difference in ΔF may not have been observed had the protocol only required one ramp

and hold contraction. Increasing ΔF with contractions for the stroke placebo group and not the other conditions may be due to the inability to inhibit the PIC response or inhibit neuromodulatory drive. Results from the study suggest that motoneuron PICs during voluntary muscle activation after a stroke may be affected by repetitive contractions and the inability to inhibit PICs.

The greater ΔF values found in the stroke placebo group compared to the other groups suggest dysregulated PICs from increased monoaminergic drive to the alpha motoneurons. Amplitude of the PICs is believed to be proportional to the monoaminergic input from the brainstem (Heckmann et al. 2005). To explain the difference in ΔF magnitude between groups, seemingly caused by differences in PICs, monoaminergic drive from the brainstem may be increased in the individuals with stroke. It has been suggested that following the loss of corticofugal projections after a stroke, similar to the decerebrate cat, inhibitory input from the corticobulbar pathways to the reticular formation is lost (Hounsgaard et al. 1988). Disinhibition of the excitatory neuromodulatory drive from the reticular formation to the spinal cord is thought to be the case following stroke in humans (Dewald et al. 1999; Kline et al. 2007; Matsuyama et al. 2004; McPherson et al. 2008; Sukal et al. 2007). It is feasible that enhanced motoneuron PICs after a stroke, and reflected in the higher ΔF values of the stroke placebo group, may be caused by disinhibition to monoaminergic brainstem input to the spinal cord previously suppressed through lost corticofugal projections.

4.4.3 Cyproheptadine Decreased ΔF Values and Increased Motor Unit Relaxation Rates

The significantly greater (more negative) motor unit relaxation rate during the decline phase of the trapezoidal contractions after cyproheptadine administration compared to the stroke placebo group supports our hypothesis. In a previous study, a similar response was observed in the finger flexor EMG of individuals with stroke during a grip and relax trial, in that relaxation time was significantly reduced after administration of cyproheptadine compared to placebo (Seo et al. 2011). This study is novel in that it observes lower extremity activity consistent with PIC behavior directly through a large number of individual motor units. The higher ΔF values observed in the stroke placebo group decreased following the administration of the 5-HT receptor antagonist, cyproheptadine. The lower motor unit relaxation rate observed in the stroke placebo group is possibly due to the same mechanism that caused the greater ΔF values. It is logical that the stroke placebo motor units are unable to cease firing, creating enhanced hysteresis and a slower relaxation rate; furthermore, the contraction rate of the motor units are not statistically different and further exemplify the greater hysteresis of the stroke placebo group. Both ΔF and relaxation rates changed after administration of cyproheptadine in a way that is consistent with suppression of PICs.

4.4.4 Cyproheptadine Reduced Motor Unit Gain

The data supports our hypothesis that cyproheptadine inhibits the gain at the motoneuron. After consecutive taps to the patellar tendon, the cyproheptadine group experienced lower torque production compared to the placebo group. This is consistent with the other results in this study because cyproheptadine, a 5HT receptor antagonist,

suppresses serotonin's effect on PICs in the motoneurons. The finding is consistent with a previous study on chronic spinal cord injury individuals in which cyproheptadine suppressed gain of the tendon tap reflex with differing 5-HT medications (Wei et al. 2014). Although the action of cyproheptadine affecting relaxation rate and ΔF could possibly be due to changes outside the spinal cord, the tendon tap reflex is too brief to be affected by changes in descending drive; furthermore, cyproheptadine does not appear to affect the muscle contractile properties as there was no statistical difference between drugs for the resting twitch torque. This provides further evidence that the action of cyproheptadine is occurring within the spinal cord and suppressing PICs in the motoneurons of the chronic stroke group.

4.4.5 Implications for Motor Performance

The results of this study showed that lower extremity relaxation time could be reduced but with a reduction in maximum strength. This may be especially useful during dynamic tasks as the monoaminergic effects may be different for different joint angles (Hyngstrom et al. 2007). A main benefit of cyproheptadine administration is that it has been shown to reduce spasticity and increase function (Barbeau et al. 1982; Nance 1994). The reduced spasticity may improve the ability to control relaxation of muscles and better perform activities of daily living. Evidence of this was observed in the spinal cord injury population in which cyproheptadine administration decreased tonic EMG activity and improved gait kinematics and walking speeds (Wainberg et al. 1986; 1990). The tradeoff of cyproheptadine administration could be a reduction in maximal strength. This result is contrary to previous studies (Seo et al. 2011; Wei et al. 2014), but considering the effects

that cyproheptadine has on reducing motor output gain, it makes sense that the MVC would be affected. This study warrants further investigation into the effects of a serotonin receptor antagonist on dynamic and functional tasks for individuals with stroke.

4.4.6 Conclusion

This study investigated the intrinsic excitability of the motoneuron in individuals with stroke by quantifying the sensitivity to the neuromodulator serotonin. A serotonin receptor antagonist showed to reduce prolonged motor unit firing and increase voluntary relaxation rates for participants with stroke. Based on the estimated PIC contributions, the lower ΔF values after cyproheptadine administration suggests that the greater reductions in motor unit firing rates were due to decreased PIC contributions. The results of this study suggest greater PIC contributions to motor unit firing rates for individuals with stroke, and a possible clinical application for a serotonin reuptake inhibitor for activities that require controlled relaxation.

CHAPTER 5: CONCLUSION

5.1 Brief Summary

The scope of this dissertation was to define post-stroke changes to central mechanisms that contribute to impaired motoneuron firing behavior. As the motoneuron is the last site of signal integration for supraspinal and spinal inputs that control force output, understanding the intrinsic excitability of the motoneuron and the inputs it receives is crucial to our understanding of motor impairment in the chronic stroke population. In the first aim (chapter 2), the results showed that central mechanisms remained the dominant factor (over peripheral factors) in deficient torque generation after intermittent, fatiguing exercise, because the muscle contractile properties were minimally affected despite a significantly decreased magnitude in post-contraction blood flow. The increased central fatigue was evident in the lack of motor unit modulation, a decreased EMG RMS response, and a significant decrease in the voluntary activation measurement compared to the control group. It is possible that decreased perfusion activated group III/IV afferents known to inhibit motoneuron outputs as motor unit firing rates decreased with a lower blood flow response. The second aim (chapter 3) further investigated the effects of ischemic conditions on motoneuron output. The results indicated that, after a stroke, motor unit firing rates decreased to a greater extent compared to control motor units at low force levels. It is likely that the ischemic condition from the total blood flow occlusion activated group III/IV afferents, contributing to decreased motor unit firing rates. Finally, in the third aim (chapter 4), the post-stroke intrinsic excitability of the motoneuron was investigated by quantifying its sensitivity to the neuromodulator

serotonin. The results showed that a serotonin receptor antagonist, cyproheptadine, lowered the ΔF value, indicating a decrease in estimated PIC contribution, and increased the slope (more negative) of the motor unit firing rates during the controlled relaxation of the quadriceps muscle. Collectively, the results from these studies suggests that, along with the compromised input from the motor cortex, inhibitory afferent input and the intrinsic properties of the motoneuron play a role in impaired motor control after a stroke.

5.2 Influence of hyper-excitability afferent inputs and enhanced intrinsic excitability on motoneuron output post-stroke

In a somewhat paradoxical message, these studies showed increased inhibitory afferent input to the motoneuron but increased intrinsic excitability of the motoneuron. Because PIC amplitude is highly sensitive to inhibition from sensory inputs (Heckman et al. 2004; Hyngstrom et al. 2007; Kuo et al. 2003), one might expect the increased inhibition from the group III/IV afferents to reduce the enhanced PICs. Ischemic conditions may explain the reason for the contradiction. As we observed from the results in chapter 2, the participants with stroke that had lower blood flow changes also had greater decreases in motor unit firing rates. We speculated that the lower blood flow response caused greater accumulation of metabolites that activated the group III/IV pathways known to inhibit motoneuron firing rates (Amann et al. 2008; Taylor et al. 2016). It is also possible that these afferent pathways are hyper-excitability after a stroke (Hidler and Schmit 2004; Li 2017). Because of this, we quantified how ischemic conditions affect motor unit firing behavior by completely occluding blood flow through the femoral artery (chapter 3). The ischemic conditions intended to activate the group III/IV afferents. From the results, we concluded that the greater decreases in motor unit

firing rates for the stroke group compared to the control group was due to increased excitability of the inhibitory group III/IV afferents. These two studies provided evidence that ischemic conditions were partially responsible for the reductions in motor unit firing rates; however, chapter 4, studying the intrinsic excitability of the motoneurons, involved no blood flow occlusion (other than the occlusion from the intramuscular pressure) and a much shorter bout of exercise. The prolonged firing behavior and increased ΔF values showed that the subsequent contractions appeared to provide enough time for PIC contributions to the motoneurons without significant contributions from inhibitory afferent inputs. From this we can speculate that the prolonged firing was not inhibited because the muscle was not exposed to ischemic conditions that activate the group III/IV afferents. This may provide important insight to motoneuron behavior because it emphasizes that subcortical contributions to the motoneuron are task dependent.

5.3 Interconnection of the Reticular System, Group III/IV Pathways, and Motor Unit Firing Behavior After Stroke

In chapter 2 we saw that changes in blood flow correlated with motor unit firing rate modulation in the stroke group. We also observed in chapter 3 that group III/IV pathways may be hyperexcitable after a stroke, accounting for greater reductions in motor unit firing rates; however, increased activity of group III/IV pathways also increases blood flow (Amann et al. 2011). One might expect that if group III/IV pathways are hyperactive during the fatigue protocol, that we would also observe an increase in blood flow with the decrease in motor unit firing rates. It is likely that disruptions to a common drive from the premotor and motor cortex to the reticular system and the corticospinal tract is responsible for the lower blood flow response and congruent decrease in motor

unit firing rates. The increased ΔF values and inability to reduce torque during relaxation described in chapter 4 suggests a loss of cortical inhibition to the reticular system. As a loss of corticospinal drive after a stroke is expected (Jang et al. 2017; Peters et al. 2017), we also expect to see losses in motor unit firing rates and modulation. We also expect greater output from the reticular system to have implications on autonomic control of blood flow. The decreased post-contraction blood flow through the femoral artery in this study may indicate increased autonomic drive, possibly caused by a disinhibited reticular drive providing an excessive sympathetic outflow. This would also explain why even though group III/IV pathways are hyperexcitable we only see decreases in motor unit firing rates and not increases in blood flow, as we might expect. Also, group III/IV pathways and their impact on increasing blood flow has been attenuated via their interactions with the brainstem and the pressor response (Sheriff et al. 1990), decreasing the post-contraction blood flow. With the increase in reticular drive because of loss cortical inhibition, it is possible that an increased pressor response attenuates the impact of group III/IV pathways on increasing blood flow. In summary, the loss of common drive from the motor cortex to the corticospinal tract and reticular system likely has systemic consequences: 1) Increases in reticular drive attenuates group III/IV impact on blood flow, increases monoaminergic drive to the motoneuron pool, and increases sympathetic drive that decreases post-contraction blood flow; 2) Decreases in activation of the corticospinal tract decreases motor unit firing rates and modulation. The culmination of these studies indicates that the loss of common drive to the reticular system and corticospinal tract from the stroke likely had an impact on these systems.

5.4 Potential new insights into motor unit firing behavior and motor control after a stroke

Central mechanisms include intrinsic excitability of the motoneuron and afferent inputs, and these studies show why it is important to consider subcortical contributions to impaired motor control after a stroke. Previous studies mainly focused on a compromised corticospinal tract because of damage to the motor cortex from the stroke lesion (Bowden et al. 2014; Horstman et al. 2008; Jones 2017; Knorr et al. 2011; Newham and Hsiao 2001). This dissertation demonstrates impaired motor unit firing behavior after stroke but extends previous findings (Chou et al. 2013; Gemperline et al. 1995; Hu et al. 2016; 2015; Hu et al. 2006; McManus et al. 2017; Mottram et al. 2014; Mottram et al. 2009; Mottram et al. 2010) by demonstrating that neuromodulatory and inhibitory afferent input contributes to force generating impairments during muscle contractions. We showed that individuals with the largest reductions in motor unit firing rates also experienced greater ischemic conditions. This is important for motor control because it emphasizes that adequate perfusion may affect inhibition to the motoneuron pool. This may be important for motor tasks that involve fatiguing contractions, such as long walks. When ischemia is not a factor during muscle contractions, such as alternating contraction-relaxation activity, prolonged motor unit firing rates may be detrimental to the relaxation phase of motor tasks. Cyproheptadine showed to reduce delays during relaxation and may have clinical implications for increasing motor control after a stroke. Many activities of daily living involve submaximal force regulation and understanding the mechanisms of impaired force regulation is important for targeting rehabilitation strategies.

5.5 Future Investigations

The methods of these studies involved isometric contractions, in part, because the EMG decomposition algorithm has been limited to isometric contractions. Isometric contractions are important for studying force production after a stroke because changes in the length of the muscle can activate hyperactive group Ia afferents (Sangani et al. 2007); however, the identification of motor unit discharge patterns acquired from surface EMG signals during dynamic contractions would be beneficial to future studies and should be addressed. Dynamic contractions are important to investigate because they better describe functional movements. More research is required to understand the role of muscle perfusion during dynamic contractions; furthermore, this may have an impact on afferent input to the motoneuron pool. This may be especially critical for PIC contribution within the motoneurons as PIC amplitude has been shown to vary with changes in joint angle due to sensory inhibition (Hynstrom et al. 2007). If similar results can be reproduced during the dynamic contractions, it would confirm the importance subcortical contributions to the motoneuron pool and would contribute to patient-specific rehabilitation.

BIBLIOGRAPHY

- Allen GM, Gandevia SC, and McKenzie DK.** Reliability of measurements of muscle strength and voluntary activation using twitch interpolation. *Muscle Nerve* 18: 593-600, 1995.
- Amann M.** Significance of Group III and IV muscle afferents for the endurance exercising human. *Clin Exp Pharmacol Physiol* 39: 831-835, 2012.
- Amann M, Blain GM, Proctor LT, Sebranek JJ, Pegelow DF, and Dempsey JA.** Implications of group III and IV muscle afferents for high-intensity endurance exercise performance in humans. *J Physiol* 589: 5299-5309, 2011.
- Amann M, Proctor LT, Sebranek JJ, Eldridge MW, Pegelow DF, and Dempsey JA.** Somatosensory feedback from the limbs exerts inhibitory influences on central neural drive during whole body endurance exercise. *J Appl Physiol (1985)* 105: 1714-1724, 2008.
- Amann M, and Secher NH.** Point: Afferent feedback from fatigued locomotor muscles is an important determinant of endurance exercise performance. *J Appl Physiol (1985)* 108: 452-454; discussion 457; author reply 470, 2010.
- Amann M, Venturelli M, Ives SJ, Morgan DE, Gmelch B, Witman MA, Jonathan Groot H, Walter Wray D, Stehlik J, and Richardson RS.** Group III/IV muscle afferents impair limb blood in patients with chronic heart failure. *Int J Cardiol* 174: 368-375, 2014.
- Aston-Jones G, Rajkowski J, and Cohen J.** Locus coeruleus and regulation of behavioral flexibility and attention. *Prog Brain Res* 126: 165-182, 2000.
- Barbeau H, Richards CL, and Bédard PJ.** Action of cyproheptadine in spastic paraparetic patients. *J Neurol Neurosurg Psychiatry* 45: 923-926, 1982.
- Barnes WS.** The relationship between maximum isometric strength and intramuscular circulatory occlusion. *Ergonomics* 23: 351-357, 1980.
- Bennett DJ, Hultborn H, Fedirchuk B, and Gorassini M.** Short-term plasticity in hindlimb motoneurons of decerebrate cats. *J Neurophysiol* 80: 2038-2045, 1998.
- Bennett DJ, Li Y, Harvey PJ, and Gorassini M.** Evidence for plateau potentials in tail motoneurons of awake chronic spinal rats with spasticity. *J Neurophysiol* 86: 1972-1982, 2001.
- Bigland-Ritchie B, Johansson R, Lippold OC, Smith S, and Woods JJ.** Changes in motoneurone firing rates during sustained maximal voluntary contractions. *J Physiol* 340: 335-346, 1983.

Bigland-Ritchie B, and Woods JJ. Changes in muscle contractile properties and neural control during human muscular fatigue. *Muscle Nerve* 7: 691-699, 1984.

Billinger SA, Coughenour E, Mackay-Lyons MJ, and Ivey FM. Reduced cardiorespiratory fitness after stroke: biological consequences and exercise-induced adaptations. *Stroke Res Treat* 2012: 959120, 2012.

Billinger SA, Gajewski BJ, Guo LX, and Kluding PM. Single limb exercise induces femoral artery remodeling and improves blood flow in the hemiparetic leg poststroke. *Stroke* 40: 3086-3090, 2009.

Blennerhassett JM, Carey LM, and Matyas TA. Clinical measures of handgrip limitation relate to impaired pinch grip force control after stroke. *J Hand Ther* 21: 245-252; quiz 253, 2008.

Blok JH, Stegeman DF, and van Oosterom A. Three-layer volume conductor model and software package for applications in surface electromyography. *Ann Biomed Eng* 30: 566-577, 2002.

Bowden JL, Taylor JL, and McNulty PA. Voluntary Activation is Reduced in Both the More- and Less-Affected Upper Limbs after Unilateral Stroke. *Front Neurol* 5: 239, 2014.

Brownstone RM, and Chopek JW. Reticulospinal Systems for Tuning Motor Commands. *Front Neural Circuits* 12: 30, 2018.

Buford JA, and Davidson AG. Movement-related and preparatory activity in the reticulospinal system of the monkey. *Exp Brain Res* 159: 284-300, 2004.

Chae J, Quinn A, El-Hayek K, Santing J, Berezovski R, and Harley M. Delay in initiation and termination of tibialis anterior contraction in lower-limb hemiparesis: relationship to lower-limb motor impairment and mobility. *Arch Phys Med Rehabil* 87: 1230-1234, 2006.

Chae J, Yang G, Park BK, and Labatia I. Delay in initiation and termination of muscle contraction, motor impairment, and physical disability in upper limb hemiparesis. *Muscle Nerve* 25: 568-575, 2002.

Chang SH, Francisco GE, Zhou P, Rymer WZ, and Li S. Spasticity, weakness, force variability, and sustained spontaneous motor unit discharges of resting spastic-paretic biceps brachii muscles in chronic stroke. *Muscle Nerve* 48: 85-92, 2013.

Chen G, and Patten C. Joint moment work during the stance-to-swing transition in hemiparetic subjects. *J Biomech* 41: 877-883, 2008.

- Chou LW, Palmer JA, Binder-Macleod S, and Knight CA.** Motor unit rate coding is severely impaired during forceful and fast muscular contractions in individuals post stroke. *J Neurophysiol* 109: 2947-2954, 2013.
- De Deyne PG, Hafer-Macko CE, Ivey FM, Ryan AS, and Macko RF.** Muscle molecular phenotype after stroke is associated with gait speed. *Muscle Nerve* 30: 209-215, 2004.
- De Luca CJ.** Myoelectrical manifestations of localized muscular fatigue in humans. *Crit Rev Biomed Eng* 11: 251-279, 1984.
- De Luca CJ, and Contessa P.** Biomechanical benefits of the Onion-Skin motor unit control scheme. *J Biomech* 48: 195-203, 2015.
- De Luca CJ, and Contessa P.** Hierarchical control of motor units in voluntary contractions. *J Neurophysiol* 107: 178-195, 2012.
- De Luca CJ, and Hostage EC.** Relationship between firing rate and recruitment threshold of motoneurons in voluntary isometric contractions. *J Neurophysiol* 104: 1034-1046, 2010.
- De Luca CJ, LeFever RS, McCue MP, and Xenakis AP.** Control scheme governing concurrently active human motor units during voluntary contractions. *J Physiol* 329: 129-142, 1982.
- Dean CM, Richards CL, and Malouin F.** Walking speed over 10 metres overestimates locomotor capacity after stroke. *Clin Rehabil* 15: 415-421, 2001.
- Delvaux V, Alagona G, Gérard P, De Pasqua V, Pennisi G, and de Noordhout AM.** Post-stroke reorganization of hand motor area: a 1-year prospective follow-up with focal transcranial magnetic stimulation. *Clin Neurophysiol* 114: 1217-1225, 2003.
- Dewald JP, Beer RF, Given JD, McGuire JR, and Rymer WZ.** Reorganization of flexion reflexes in the upper extremity of hemiparetic subjects. *Muscle Nerve* 22: 1209-1221, 1999.
- Durand MJ, Murphy SA, Schaefer KK, Hunter SK, Schmit BD, Gutterman DD, and Hyingstrom AS.** Impaired Hyperemic Response to Exercise Post Stroke. *PLoS One* 10: e0144023, 2015.
- Dütsch M, Burger M, Dörfler C, Schwab S, and Hilz MJ.** Cardiovascular autonomic function in poststroke patients. *Neurology* 69: 2249-2255, 2007.
- Enoka RM, and Duchateau J.** Muscle fatigue: what, why and how it influences muscle function. *J Physiol* 586: 11-23, 2008.

- Enoka RM, and Duchateau J.** Rate Coding and the Control of Muscle Force. *Cold Spring Harb Perspect Med* 2017.
- Enoka RM, and Stuart DG.** Neurobiology of muscle fatigue. *J Appl Physiol* 72: 1631-1648, 1992.
- Farina D, and Negro F.** Common synaptic input to motor neurons, motor unit synchronization, and force control. *Exerc Sport Sci Rev* 43: 23-33, 2015.
- Farina D, Negro F, Gazzoni M, and Enoka RM.** Detecting the unique representation of motor-unit action potentials in the surface electromyogram. *J Neurophysiol* 100: 1223-1233, 2008a.
- Farina D, Yoshida K, Stieglitz T, and Koch KP.** Multichannel thin-film electrode for intramuscular electromyographic recordings. *J Appl Physiol (1985)* 104: 821-827, 2008b.
- Fimland MS, Moen PM, Hill T, Gjellesvik TI, Tørhaug T, Helgerud J, and Hoff J.** Neuromuscular performance of paretic versus non-paretic plantar flexors after stroke. *Eur J Appl Physiol* 111: 3041-3049, 2011.
- Fitts R.** In: *Advanced Exercise Physiology* Lippincott Williams & Wilkins, 2011a.
- Fitts R.** The muscular system: fatigue processes. In: *Advanced Exercise Physiology* Lippincott Williams & Wilkins, 2011b.
- Foltys H, Krings T, Meister IG, Sparing R, Boroojerdi B, Thron A, and Topper R.** Motor representation in patients rapidly recovering after stroke: a functional magnetic resonance imaging and transcranial magnetic stimulation study. *Clin Neurophysiol* 114: 2404-2415, 2003a.
- Foltys H, Krings T, Meister IG, Sparing R, Boroojerdi B, Thron A, and Töpper R.** Motor representation in patients rapidly recovering after stroke: a functional magnetic resonance imaging and transcranial magnetic stimulation study. *Clin Neurophysiol* 114: 2404-2415, 2003b.
- Fuglevand AJ, and Keen DA.** Re-evaluation of muscle wisdom in the human adductor pollicis using physiological rates of stimulation. *J Physiol* 549: 865-875, 2003.
- Gallina A, Merletti R, and Gazzoni M.** Uneven spatial distribution of surface EMG: what does it mean? *Eur J Appl Physiol* 113: 887-894, 2013.
- Gandevia SC.** Spinal and supraspinal factors in human muscle fatigue. *Physiol Rev* 81: 1725-1789, 2001.

Gandevia SC, Allen GM, Butler JE, and Taylor JL. Supraspinal factors in human muscle fatigue: evidence for suboptimal output from the motor cortex. *J Physiol* 490 (Pt 2): 529-536, 1996.

Garland SJ, Enoka RM, Serrano LP, and Robinson GA. Behavior of motor units in human biceps brachii during a submaximal fatiguing contraction. *J Appl Physiol (1985)* 76: 2411-2419, 1994.

Gemperline JJ, Allen S, Walk D, and Rymer WZ. Characteristics of motor unit discharge in subjects with hemiparesis. *Muscle Nerve* 18: 1101-1114, 1995.

Gorassini M, Yang JF, Siu M, and Bennett DJ. Intrinsic activation of human motoneurons: possible contribution to motor unit excitation. *J Neurophysiol* 87: 1850-1858, 2002a.

Gorassini M, Yang JF, Siu M, and Bennett DJ. Intrinsic activation of human motoneurons: reduction of motor unit recruitment thresholds by repeated contractions. *J Neurophysiol* 87: 1859-1866, 2002b.

Gorassini MA, Knash ME, Harvey PJ, Bennett DJ, and Yang JF. Role of motoneurons in the generation of muscle spasms after spinal cord injury. *Brain* 127: 2247-2258, 2004.

Hafer-Macko CE, Ryan AS, Ivey FM, and Macko RF. Skeletal muscle changes after hemiparetic stroke and potential beneficial effects of exercise intervention strategies. *J Rehabil Res Dev* 45: 261-272, 2008.

Heckman C, and Enoka R. Physiology of the motor neuron and the motor unit. In: *Clinical Neurophysiology of Motor Neuron Diseases: Handbook of Clinical Neurophysiology*. Amsterdam: Elsevier, 2004.

Heckman CJ, and Enoka RM. Motor unit. *Compr Physiol* 2: 2629-2682, 2012.

Heckman CJ, Hynstrom AS, and Johnson MD. Active properties of motoneurone dendrites: diffuse descending neuromodulation, focused local inhibition. *J Physiol* 586: 1225-1231, 2008.

Heckman CJ, Kuo JJ, and Johnson MD. Synaptic integration in motoneurons with hyper-excitable dendrites. *Can J Physiol Pharmacol* 82: 549-555, 2004.

Heckman CJ, Lee RH, and Brownstone RM. Hyperexcitable dendrites in motoneurons and their neuromodulatory control during motor behavior. *Trends Neurosci* 26: 688-695, 2003.

- Heckman CJ, Mottram C, Quinlan K, Theiss R, and Schuster J.** Motoneuron excitability: the importance of neuromodulatory inputs. *Clin Neurophysiol* 120: 2040-2054, 2009.
- Heckmann CJ, Gorassini MA, and Bennett DJ.** Persistent inward currents in motoneuron dendrites: implications for motor output. *Muscle Nerve* 31: 135-156, 2005.
- HENNEMAN E.** Relation between size of neurons and their susceptibility to discharge. *Science* 126: 1345-1347, 1957.
- Herbert RD, and Gandevia SC.** Twitch interpolation in human muscles: mechanisms and implications for measurement of voluntary activation. *J Neurophysiol* 82: 2271-2283, 1999.
- Herbert WJ, Powell K, and Buford JA.** Evidence for a role of the reticulospinal system in recovery of skilled reaching after cortical stroke: initial results from a model of ischemic cortical injury. *Exp Brain Res* 233: 3231-3251, 2015.
- Hidler JM, and Schmit BD.** Evidence for force-feedback inhibition in chronic stroke. *IEEE Trans Neural Syst Rehabil Eng* 12: 166-176, 2004.
- Hoffmann G, Conrad MO, Qiu D, and Kamper DG.** Contributions of voluntary activation deficits to hand weakness after stroke. *Top Stroke Rehabil* 23: 384-392, 2016.
- Holobar A, Minetto MA, Botter A, Negro F, and Farina D.** Experimental analysis of accuracy in the identification of motor unit spike trains from high-density surface EMG. *IEEE Trans Neural Syst Rehabil Eng* 18: 221-229, 2010.
- Holobar A, and Zazul D.** Multichannel Blind Source Separation Using Convolution Kernel Compensation. *IEEE Transactions on Signal Processing* 55: 4487-4496, 2007.
- Honeycutt CF, and Perreault EJ.** Planning of ballistic movement following stroke: insights from the startle reflex. *PLoS One* 7: e43097, 2012.
- Hornby TG, Tysseling-Mattiace VM, Benz EN, and Schmit BD.** Contribution of muscle afferents to prolonged flexion withdrawal reflexes in human spinal cord injury. *J Neurophysiol* 92: 3375-3384, 2004.
- Horstman AM, Beltman MJ, Gerrits KH, Koppe P, Janssen TW, Elich P, and de Haan A.** Intrinsic muscle strength and voluntary activation of both lower limbs and functional performance after stroke. *Clin Physiol Funct Imaging* 28: 251-261, 2008.
- Houngaard J, Hultborn H, Jespersen B, and Kiehn O.** Bistability of alpha-motoneurons in the decerebrate cat and in the acute spinal cat after intravenous 5-hydroxytryptophan. *J Physiol* 405: 345-367, 1988.

Hu X, Suresh AK, Rymer WZ, and Suresh NL. Altered motor unit discharge patterns in paretic muscles of stroke survivors assessed using surface electromyography. *J Neural Eng* 13: 046025, 2016.

Hu X, Suresh AK, Rymer WZ, and Suresh NL. Assessing altered motor unit recruitment patterns in paretic muscles of stroke survivors using surface electromyography. *J Neural Eng* 12: 066001, 2015.

Hu XL, Tong KY, and Hung LK. Firing properties of motor units during fatigue in subjects after stroke. *J Electromyogr Kinesiol* 16: 469-476, 2006.

Hunter SK. Performance Fatigability: Mechanisms and Task Specificity. *Cold Spring Harb Perspect Med* 8: 2018.

Hunter SK, Griffith EE, Schlachter KM, and Kufahl TD. Sex differences in time to task failure and blood flow for an intermittent isometric fatiguing contraction. *Muscle Nerve* 39: 42-53, 2009.

Hynstrom AS, Johnson MD, Miller JF, and Heckman CJ. Intrinsic electrical properties of spinal motoneurons vary with joint angle. *Nat Neurosci* 10: 363-369, 2007.

Hynstrom AS, Onushko T, Heitz RP, Rutkowski A, Hunter SK, and Schmit BD. Stroke-related changes in neuromuscular fatigue of the hip flexors and functional implications. *Am J Phys Med Rehabil* 91: 33-42, 2012.

Hyvärinen A. Fast and robust fixed-point algorithms for independent component analysis. *IEEE Trans Neural Netw* 10: 626-634, 1999.

Iosa M, Morone G, Fusco A, Pratesi L, Bragoni M, Coiro P, Multari M, Venturiero V, De Angelis D, and Paolucci S. Effects of walking endurance reduction on gait stability in patients with stroke. *Stroke Res Treat* 2012: 810415, 2012.

Ivey FM, Gardner AW, Dobrovolny CL, and Macko RF. Unilateral impairment of leg blood flow in chronic stroke patients. *Cerebrovasc Dis* 18: 283-289, 2004.

Jacobs BL, and Fornal CA. Activity of serotonergic neurons in behaving animals. *Neuropsychopharmacology* 21: 9S-15S, 1999.

Jacobs BL, and Fornal CA. Serotonin and motor activity. *Curr Opin Neurobiol* 7: 820-825, 1997.

Jacobs BL, Martín-Cora FJ, and Fornal CA. Activity of medullary serotonergic neurons in freely moving animals. *Brain Res Brain Res Rev* 40: 45-52, 2002.

- Jang SH, Kim DH, Kim SH, and Seo JP.** The relation between the motor evoked potential and diffusion tensor tractography for the corticospinal tract in chronic hemiparetic patients with cerebral infarct. *Somatosens Mot Res* 34: 134-138, 2017.
- Jones TA.** Motor compensation and its effects on neural reorganization after stroke. *Nat Rev Neurosci* 18: 267-280, 2017.
- Jonkers I, Delp S, and Patten C.** Capacity to increase walking speed is limited by impaired hip and ankle power generation in lower functioning persons post-stroke. *Gait Posture* 29: 129-137, 2009.
- Kaufman MP, Longhurst JC, Rybicki KJ, Wallach JH, and Mitchell JH.** Effects of static muscular contraction on impulse activity of groups III and IV afferents in cats. *J Appl Physiol Respir Environ Exerc Physiol* 55: 105-112, 1983.
- Kent-Braun JA, Fitts RH, and Christie A.** Skeletal muscle fatigue. *Compr Physiol* 2: 997-1044, 2012.
- Kim JK, Sala-Mercado JA, Hammond RL, Rodriguez J, Scislo TJ, and O'Leary DS.** Attenuated arterial baroreflex buffering of muscle metaboreflex in heart failure. *Am J Physiol Heart Circ Physiol* 289: H2416-2423, 2005.
- Klass M, Baudry S, and Duchateau J.** Voluntary activation during maximal contraction with advancing age: a brief review. *European journal of applied physiology* 100: 543-551, 2007.
- Klein CS, Brooks D, Richardson D, McIlroy WE, and Bayley MT.** Voluntary activation failure contributes more to plantar flexor weakness than antagonist coactivation and muscle atrophy in chronic stroke survivors. *J Appl Physiol (1985)* 109: 1337-1346, 2010.
- Kline TL, Schmit BD, and Kamper DG.** Exaggerated interlimb neural coupling following stroke. *Brain* 130: 159-169, 2007.
- Knorr S, Ivanova TD, Doherty TJ, Campbell JA, and Garland SJ.** The origins of neuromuscular fatigue post-stroke. *Exp Brain Res* 214: 303-315, 2011.
- Kouzi I, Trachani E, Anagnostou E, Rapidi CA, Ellul J, Sakellaropoulos GC, and Chroni E.** Motor unit number estimation and quantitative needle electromyography in stroke patients. *J Electromyogr Kinesiol* 24: 910-916, 2014.
- Kuhnen HR, Rybar MM, Onushko T, Doyel RE, Hunter SK, Schmit BD, and Hynstrom AS.** Stroke-related effects on maximal dynamic hip flexor fatigability and functional implications. *Muscle Nerve* 51: 446-448, 2015.

Kuo JJ, Lee RH, Johnson MD, Heckman HM, and Heckman CJ. Active dendritic integration of inhibitory synaptic inputs in vivo. *J Neurophysiol* 90: 3617-3624, 2003.

Kupa EJ, Roy SH, Kandarian SC, and De Luca CJ. Effects of muscle fiber type and size on EMG median frequency and conduction velocity. *J Appl Physiol (1985)* 79: 23-32, 1995.

Landin S, Hagenfeldt L, Saltin B, and Wahren J. Muscle metabolism during exercise in hemiparetic patients. *Clin Sci Mol Med* 53: 257-269, 1977.

Lee RH, and Heckman CJ. Adjustable amplification of synaptic input in the dendrites of spinal motoneurons in vivo. *J Neurosci* 20: 6734-6740, 2000.

Lee RH, and Heckman CJ. Bistability in spinal motoneurons in vivo: systematic variations in rhythmic firing patterns. *J Neurophysiol* 80: 572-582, 1998.

Lewek MD, Hornby TG, Dhaher YY, and Schmit BD. Prolonged quadriceps activity following imposed hip extension: a neurophysiological mechanism for stiff-knee gait? *J Neurophysiol* 98: 3153-3162, 2007.

Lewek MD, Schmit BD, Hornby TG, and Dhaher YY. Hip joint position modulates volitional knee extensor muscle activity after stroke. *Muscle Nerve* 34: 767-774, 2006.

Li S. Spasticity, Motor Recovery, and Neural Plasticity after Stroke. *Front Neurol* 8: 120, 2017.

Li X, Holobar A, Gazzoni M, Merletti R, Rymer WZ, and Zhou P. Examination of Post-stroke Alteration in Motor Unit Firing Behavior Using High Density Surface EMG Decomposition. *IEEE Trans Biomed Eng* 2014.

Lieber RL, and Fridén J. Functional and clinical significance of skeletal muscle architecture. *Muscle Nerve* 23: 1647-1666, 2000.

Lloyd-Jones D, Adams R, Carnethon M, De Simone G, Ferguson TB, Flegal K, Ford E, Furie K, Go A, Greenlund K, Haase N, Hailpern S, Ho M, Howard V, Kissela B, Kittner S, Lackland D, Lisabeth L, Marelli A, McDermott M, Meigs J, Mozaffarian D, Nichol G, O'Donnell C, Roger V, Rosamond W, Sacco R, Sorlie P, Stafford R, Steinberger J, Thom T, Wasserthiel-Smoller S, Wong N, Wylie-Rosett J, Hong Y, and Subcommittee AHASCaSS. Heart disease and stroke statistics--2009 update: a report from the American Heart Association Statistics Committee and Stroke Statistics Subcommittee. *Circulation* 119: 480-486, 2009.

Lodha N, Naik SK, Coombes SA, and Cauraugh JH. Force control and degree of motor impairments in chronic stroke. *Clin Neurophysiol* 121: 1952-1961, 2010.

- Lukács M, Vécsei L, and Beniczky S.** Large motor units are selectively affected following a stroke. *Clin Neurophysiol* 119: 2555-2558, 2008.
- Marsden CD, Meadows JC, and Merton PA.** "Muscular wisdom" that minimizes fatigue during prolonged effort in man: peak rates of motoneuron discharge and slowing of discharge during fatigue. *Adv Neurol* 39: 169-211, 1983.
- Martin PG, Weerakkody N, Gandevia SC, and Taylor JL.** Group III and IV muscle afferents differentially affect the motor cortex and motoneurons in humans. *J Physiol* 586: 1277-1289, 2008.
- Martinez-Valdes E, Falla D, Negro F, Mayer F, and Farina D.** Differential Motor Unit Changes after Endurance or High-Intensity Interval Training. *Med Sci Sports Exerc* 49: 1126-1136, 2017a.
- Martinez-Valdes E, Negro F, Laine CM, Falla D, Mayer F, and Farina D.** Tracking motor units longitudinally across experimental sessions with high-density surface electromyography. *J Physiol* 595: 1479-1496, 2017b.
- Matsuyama K, Mori F, Nakajima K, Drew T, Aoki M, and Mori S.** Locomotor role of the corticoreticular-reticulospinal-spinal interneuronal system. *Prog Brain Res* 143: 239-249, 2004.
- Matthews PBC.** *Mammalian Muscle Receptors and Their Central Actions*. London: Arnold, 1972.
- McComas AJ, Sica RE, Upton AR, and Aguilera N.** Functional changes in motoneurons of hemiparetic patients. *J Neurol Neurosurg Psychiatry* 36: 183-193, 1973.
- McManus L, Hu X, Rymer WZ, Suresh NL, and Lowery MM.** Motor Unit Activity during Fatiguing Isometric Muscle Contraction in Hemispheric Stroke Survivors. *Front Hum Neurosci* 11: 569, 2017.
- McNulty PA, Lin G, and Doust CG.** Single motor unit firing rate after stroke is higher on the less-affected side during stable low-level voluntary contractions. *Front Hum Neurosci* 8: 518, 2014.
- McPherson JG, Ellis MD, Harden RN, Carmona C, Drogos JM, Heckman CJ, and Dewald JPA.** Neuromodulatory Inputs to Motoneurons Contribute to the Loss of Independent Joint Control in Chronic Moderate to Severe Hemiparetic Stroke. *Front Neurol* 9: 470, 2018.
- McPherson JG, Ellis MD, Heckman CJ, and Dewald JP.** Evidence for increased activation of persistent inward currents in individuals with chronic hemiparetic stroke. *J Neurophysiol* 100: 3236-3243, 2008.

Merletti R, and Farina D. Analysis of intramuscular electromyogram signals. *Philos Trans A Math Phys Eng Sci* 367: 357-368, 2009.

Merletti R, Knaflitz M, and De Luca CJ. Myoelectric manifestations of fatigue in voluntary and electrically elicited contractions. *J Appl Physiol (1985)* 69: 1810-1820, 1990.

Miller LC, Thompson CK, Negro F, Heckman CJ, Farina D, and Dewald JP. High-density surface EMG decomposition allows for recording of motor unit discharge from proximal and distal flexion synergy muscles simultaneously in individuals with stroke. *Conf Proc IEEE Eng Med Biol Soc* 2014: 5340-5344, 2014.

Milner-Brown HS, Stein RB, and Yemm R. The orderly recruitment of human motor units during voluntary isometric contractions. *J Physiol* 230: 359-370, 1973.

Mottram CJ, Heckman CJ, Powers RK, Rymer WZ, and Suresh NL. Disturbances of motor unit rate modulation are prevalent in muscles of spastic-paretic stroke survivors. *J Neurophysiol* 111: 2017-2028, 2014.

Mottram CJ, Suresh NL, Heckman CJ, Gorassini MA, and Rymer WZ. Origins of abnormal excitability in biceps brachii motoneurons of spastic-paretic stroke survivors. *J Neurophysiol* 102: 2026-2038, 2009.

Mottram CJ, Wallace CL, Chikando CN, and Rymer WZ. Origins of spontaneous firing of motor units in the spastic-paretic biceps brachii muscle of stroke survivors. *J Neurophysiol* 104: 3168-3179, 2010.

Murase N, Duque J, Mazzocchio R, and Cohen LG. Influence of interhemispheric interactions on motor function in chronic stroke. *Ann Neurol* 55: 400-409, 2004.

Murphy SA, Berrios R, Nelson PA, Negro F, Farina D, Schmit B, and Hyngstrom A. Impaired regulation post-stroke of motor unit firing behavior during volitional relaxation of knee extensor torque assessed using high density surface EMG decomposition. *Conf Proc IEEE Eng Med Biol Soc* 2015: 4606-4609, 2015.

Nadeau S, Arsenault AB, Gravel D, and Bourbonnais D. Analysis of the clinical factors determining natural and maximal gait speeds in adults with a stroke. *Am J Phys Med Rehabil* 78: 123-130, 1999.

Nance PW. A comparison of clonidine, cyproheptadine and baclofen in spastic spinal cord injured patients. *J Am Paraplegia Soc* 17: 150-156, 1994.

Negro F, Muceli S, Castronovo AM, Holobar A, and Farina D. Multi-channel intramuscular and surface EMG decomposition by convolutive blind source separation. *J Neural Eng* 13: 026027, 2016.

Nette RW, Ie EH, Vletter WB, Krams R, Weimar W, and Zietse R. Norepinephrine-induced vasoconstriction results in decreased blood volume in dialysis patients. *Nephrol Dial Transplant* 21: 1305-1311, 2006.

Newham D, Davies J, and Mayston M. Voluntary force generation and activation in the knee muscles of stroke patients with mild spastic hemiparesis. *J Physiol* 483: 1995.

Newham DJ, and Hsiao SF. Knee muscle isometric strength, voluntary activation and antagonist co-contraction in the first six months after stroke. *Disabil Rehabil* 23: 379-386, 2001.

Peters HT, Dunning K, Belagaje S, Kissela BM, Ying J, Laine J, and Page SJ. Navigated Transcranial Magnetic Stimulation: A Biologically Based Assay of Lower Extremity Impairment and Gait Velocity. *Neural Plast* 2017: 6971206, 2017.

Pollock CL, Ivanova TD, Hunt MA, and Garland SJ. Motor unit recruitment and firing rate in medial gastrocnemius muscles during external perturbations in standing in humans. *J Neurophysiol* 112: 1678-1684, 2014.

Powers RK, and Heckman CJ. Contribution of intrinsic motoneuron properties to discharge hysteresis and its estimation based on paired motor unit recordings: a simulation study. *J Neurophysiol* 114: 184-198, 2015.

Powers RK, Nardelli P, and Cope TC. Estimation of the contribution of intrinsic currents to motoneuron firing based on paired motoneuron discharge records in the decerebrate cat. *J Neurophysiol* 100: 292-303, 2008.

Rekling JC, Funk GD, Bayliss DA, Dong XW, and Feldman JL. Synaptic control of motoneuronal excitability. *Physiol Rev* 80: 767-852, 2000.

Revill AL, and Fuglevand AJ. Effects of persistent inward currents, accommodation, and adaptation on motor unit behavior: a simulation study. *J Neurophysiol* 106: 1467-1479, 2011.

Riley NA, and Bilodeau M. Changes in upper limb joint torque patterns and EMG signals with fatigue following a stroke. *Disabil Rehabil* 24: 961-969, 2002.

Roeleveld K, Blok JH, Stegeman DF, and van Oosterom A. Volume conduction models for surface EMG; confrontation with measurements. *J Electromyogr Kinesiol* 7: 221-232, 1997.

Rybar M, Walker E, Kuhnen H, Ouellette D, Berrios R, Hunter SK, and Hynstrom AS. The stroke-related effects of hip flexion fatigue on over ground walking. *Gait and Posture* 39: 1103-1108, 2014a.

Rybar MM, Walker ER, Kuhnen HR, Ouellette DR, Berrios R, Hunter SK, and Hyingstrom AS. The stroke-related effects of hip flexion fatigue on over ground walking. *Gait & posture* 39: 1103-1108, 2014b.

Sadamoto T, Bonde-Petersen F, and Suzuki Y. Skeletal muscle tension, flow, pressure, and EMG during sustained isometric contractions in humans. *Eur J Appl Physiol Occup Physiol* 51: 395-408, 1983.

Sangani SG, Starsky AJ, McGuire JR, and Schmit BD. Multijoint reflex responses to constant-velocity volitional movements of the stroke elbow. *J Neurophysiol* 102: 1398-1410, 2009.

Sangani SG, Starsky AJ, McGuire JR, and Schmit BD. Multijoint reflexes of the stroke arm: neural coupling of the elbow and shoulder. *Muscle Nerve* 36: 694-703, 2007.

Sauvage C, Manto M, Adam A, Roark R, Jissendi P, and De Luca CJ. Ordered motor-unit firing behavior in acute cerebellar stroke. *J Neurophysiol* 96: 2769-2774, 2006.

Schmit BD, Benz EN, and Rymer WZ. Reflex mechanisms for motor impairment in spinal cord injury. *Adv Exp Med Biol* 508: 315-323, 2002.

Schmit BD, Hornby TG, Tysseling-Mattiace VM, and Benz EN. Absence of local sign withdrawal in chronic human spinal cord injury. *J Neurophysiol* 90: 3232-3241, 2003.

Schwarz LA, Miyamichi K, Gao XJ, Beier KT, Weissbourd B, DeLoach KE, Ren J, Ibanes S, Malenka RC, Kremer EJ, and Luo L. Viral-genetic tracing of the input-output organization of a central noradrenaline circuit. *Nature* 524: 88-92, 2015.

Schwerin S, Dewald JP, Haztl M, Jovanovich S, Nickeas M, and MacKinnon C. Ipsilateral versus contralateral cortical motor projections to a shoulder adductor in chronic hemiparetic stroke: implications for the expression of arm synergies. *Exp Brain Res* 185: 509-519, 2008.

Seo NJ, Fischer HW, Bogey RA, Rymer WZ, and Kamper DG. Effect of a serotonin antagonist on delay in grip muscle relaxation for persons with chronic hemiparetic stroke. *Clin Neurophysiol* 122: 796-802, 2011.

Sheriff DD, O'Leary DS, Scher AM, and Rowell LB. Baroreflex attenuates pressor response to graded muscle ischemia in exercising dogs. *Am J Physiol* 258: H305-310, 1990.

Sherk KA, Sherk VD, Anderson MA, Bemben DA, and Bemben MG. Lower limb neuromuscular function and blood flow characteristics in AFO-using survivors of stroke. *J Geriatr Phys Ther* 38: 56-61, 2015.

- Shield A, and Zhou S.** Assessing voluntary muscle activation with the twitch interpolation technique. *Sports medicine* 34: 253-267, 2004.
- Soo Hoo J, Paul T, Chae J, and Wilson RD.** Central hypersensitivity in chronic hemiplegic shoulder pain. *Am J Phys Med Rehabil* 92: 1-9; quiz 10-13, 2013.
- Stephenson JL, and Maluf KS.** Dependence of the paired motor unit analysis on motor unit discharge characteristics in the human tibialis anterior muscle. *J Neurosci Methods* 198: 84-92, 2011.
- Sukal TM, Ellis MD, and Dewald JP.** Shoulder abduction-induced reductions in reaching work area following hemiparetic stroke: neuroscientific implications. *Exp Brain Res* 183: 215-223, 2007.
- Svantesson UM, Sunnerhagen KS, Carlsson US, and Grimby G.** Development of fatigue during repeated eccentric-concentric muscle contractions of plantar flexors in patients with stroke. *Arch Phys Med Rehabil* 80: 1247-1252, 1999.
- Taylor JL, Amann M, Duchateau J, Meeusen R, and Rice CL.** Neural Contributions to Muscle Fatigue: From the Brain to the Muscle and Back Again. *Med Sci Sports Exerc* 48: 2294-2306, 2016.
- Tesch PA, Komi PV, Jacobs I, Karlsson J, and Viitasalo JT.** Influence of lactate accumulation of EMG frequency spectrum during repeated concentric contractions. *Acta Physiol Scand* 119: 61-67, 1983.
- Theiss RD, Hornby TG, Rymer WZ, and Schmit BD.** Riluzole decreases flexion withdrawal reflex but not voluntary ankle torque in human chronic spinal cord injury. *J Neurophysiol* 105: 2781-2790, 2011.
- Twitchell TE.** The restoration of motor function following hemiplegia in man. *Brain* 74: 443-480, 1951.
- Udina E, D'Amico J, Bergquist AJ, and Gorassini MA.** Amphetamine increases persistent inward currents in human motoneurons estimated from paired motor-unit activity. *J Neurophysiol* 103: 1295-1303, 2010.
- Vandenberk MS, and Kalmar JM.** An evaluation of paired motor unit estimates of persistent inward current in human motoneurons. *J Neurophysiol* 111: 1877-1884, 2014.
- Wainberg M, Barbeau H, and Gauthier S.** Quantitative assessment of the effect of cyproheptadine on spastic paretic gait: a preliminary study. *J Neurol* 233: 311-314, 1986.
- Wainberg M, Barbeau H, and Gauthier S.** The effects of cyproheptadine on locomotion and on spasticity in patients with spinal cord injuries. *J Neurol Neurosurg Psychiatry* 53: 754-763, 1990.

Walter JP, McGahan JP, and Lantz BM. Absolute flow measurements using pulsed Doppler US. Work in progress. *Radiology* 159: 545-548, 1986.

Wei K, Glaser JI, Deng L, Thompson CK, Stevenson IH, Wang Q, Hornby TG, Heckman CJ, and Kording KP. Serotonin affects movement gain control in the spinal cord. *J Neurosci* 34: 12690-12700, 2014.

Wu M, Hornby TG, Kahn JH, and Schmit BD. Flexor reflex responses triggered by imposed knee extension in chronic human spinal cord injury. *Exp Brain Res* 168: 566-576, 2006.

Xiong L, Leung HW, Chen XY, Leung WH, Soo OY, and Wong KS. Autonomic dysfunction in different subtypes of post-acute ischemic stroke. *J Neurol Sci* 337: 141-146, 2014.

Young JL, and Mayer RF. Physiological alterations of motor units in hemiplegia. *J Neurol Sci* 54: 401-412, 1982.